

**Uniwersytet Medyczny
Im. Karola Marcinkowskiego
w Poznaniu**

mgr Klaus Lücke

**Isolation of Fetus Cells from
Maternal Blood
Pre-clinical Study**

**PRACA NAUKOWA NA STOPIEŃ
DOKTORA NAUK BIOLOGICZNYCH**

PROMOTOR

Prof. dr hab. n. med. Grzegorz H. Bręborowicz
Katedra i Klinika Perinatologii I Ginekologii

POZNAŃ 2011

CONTENTS

1	Abbreviations	5
2	Introduction	8
2.1	Prenatal diagnostics	8
2.2	Fetal cells.....	10
2.3	Isolation techniques.....	13
2.4	The technology of the nanodetector.....	15
2.5	Nanotechnology	16
3	Aims of this work	19
4	Material	20
4.1	HLA-G antigen.....	20
4.2	Antibodies	20
	4.2.1 Human antibodies – phage display	21
	4.2.2 Purification of the antibody	21
	4.2.3 Structure of the used antibodies	21
4.3	Cell Lines	22
4.4	Animals.....	23
	4.4.1 Rats	23
	4.4.2 Overview: Studied groups	23
4.5	Animal study outline.....	25
5	Methods	28
5.1	Surface of the wire	28
	5.1.1 Nanostructure (horizontal approach).....	29
	5.1.2 Nanostructure (vertical approach)	33
5.2	Binding of the antibody to the surface of the wire.....	34
	5.2.1 Activation of the hydrogel and coupling of antibodies.....	35
5.3	Surface acoustic wave methodology.....	36
	5.3.1 Modification of the sensor chip surfaces and measurement in the microfluidic SAW sensor system	37
5.4	Flow Cytometry	37

5.5	Surface plasmon resonance (SPR)	38
5.6	Flow system	38
5.7	Visualization of cells	39
5.8	Safety testing including animal trials (EN ISO 10993)	40
5.8.1	Description of the device including any materials that will be in contact with tissues or body fluids	40
5.8.2	Relevant inspections.....	41
5.8.3	Cytotoxicity test.....	41
5.8.4	Acute systemic toxicity	43
5.8.5	Autopsy and organ weight.....	44
5.8.6	Hemocompatibility	45
5.9	Intended medical application of the nanodetector including any necessary storage and handling requirements.....	54
5.9.1	Sterilization and packaging	54
5.9.2	Application and usage	55
5.10	Statistical analysis	57
6	Results	58
6.1	Horizontal approach with nanoisland.....	58
6.1.1	Amount of antibodies bound to nanostructured and complete gold surfaces	58
6.1.2	Calculation of the number of antibodies per nanospot	59
6.2	Vertical approach with different hydrogels adsorbed onto gold surface.....	62
6.2.1	Hydrogels based on agarose and polyacrylic acid (PAA)	62
6.2.2	Hydrogels based on polyethylene imine (PEI) and polyacrylic acid (PAA)	63
6.2.3	Concentration of carboxyl groups	64
6.3	Preclinical <i>in vitro</i> testing.....	70
6.3.1	Flow cytometry with the antibody	70
6.3.2	Immunohistochemistry (IHC).....	71
6.3.3	Cell binding experiments in spiked blood on chips.....	72
6.3.4	Cell binding experiments in peripheral blood of pregnant women.....	73
6.4	Cytotoxicity tests	74
6.4.1	Cytotoxicity of the nanodetector with and without PEG.....	74

6.4.2	Investigation of the cytotoxicity of antibody solutions	76
6.4.3	Study of the cytotoxicity of the nanodetector with an elution test	77
6.5	Animal tests.....	78
6.6	Hemocompatibility test.....	90
6.6.1	Thrombosis.....	90
6.6.2	Coagulation.....	94
6.6.3	Specific coagulation factors	95
6.6.4	Hemolysis	96
6.7	Abrasion tests on the nanodetector	96
7	Discussion.....	97
7.1	Functionality of the nanodetector.....	97
7.2	Amount of antibody on the nanodetector	98
7.3	Device risk analysis and risk assessment (EN ISO 14971)	99
7.3.1	Introduction	99
7.3.2	Wire, gold and hydrogel.....	99
7.3.3	Application time.....	100
7.3.4	Safety	100
7.4	Evaluation of the potential effects which might originate from nanodetector-bound antibodies	100
7.4.1	The use of fully human antibodies is preferred to murine, humanized or chimeric antibodies	102
7.5	Therapeutic monoclonal antibodies	102
7.6	Risk analysis and assessment including a description of the risk graph..	104
7.7	Claims and intended performance of the device that are to be verified in a clinical study	105
7.8	Possible other applications.....	105
7.9	Can enough cells be caught ?.....	106
8	Conclusions	107
9	Summary.....	108
10	References	109
11	Acknowledgement.....	115

1 Abbreviations

AFM	Atomic force microscopy
ALAT	Alanine aminotransferase
ALARP	as low as reasonable possible
ALP	Alkaline phosphatase
ANCA	Anti-neutrophil cytoplasmic antibody
ASAT	Aspartate aminotransferase
AT	anucleated trophoblasts
Bil	Bilirubin
bp	Base pairs
BUN	Blood urine nitrogen
BW	Body weight
CCP	Cyclic citrullinated peptide
CD	Cluster of differentiation
CIP	Clinical investigation plan
CK	Cytokeratin
CMV	Cytomegalovirus
CRP	C-reactive protein
CT	Cytotrophoblasts
CVS	Chorionic villus sampling
DC	Density gradient centrifugation
Df	Dilution factor
DLE	Discoid lupus erythematosus
DNA	Deoxyribonucleic acid
EDC	(N-(3-Dimethylamino-propyl)-N'-ethylcarbodiimide hydrochloride)
EGF(-R)	Epidermal growth factor(-receptor)
ELISA	Enzyme-linked immunosorbent assay
EMA	European Medicines Agency
Ery	Erythrocytes
FACS	Fluorescence activated cell sorting
FDA	Food and Drug Administration
FISH	Fluorescence <i>in situ</i> - hybridization
FPA	Fibrinopeptide A
Glu	Glucose
HAMA	Human anti-mouse antibody

HGB	Hemoglobin
HLA	Human leukocyte antigen
HRP	Horse radish peroxidase
HTC	Hematocrit
TAT	Thrombin-antithrombin III complex
ICC	Immunocytochemistry
IDT	Interdigital transducers
INR	International Normalized Ratio
ket	Ketones
kDa	kilo Dalton
leu	Leukocytes
Ig	Immunoglobulin
IL	Interleukin
MACS	Magnetic activated cell sorting
MCH	Mean corpuscular hemoglobin
MCHC	Mean corpuscular hemoglobin concentration
MCV	Mean corpuscular volume
MPV	Mean platelet volume
MRI	Magnetic resonance imaging
MSAFP	Maternal serum alpha-fetoprotein
N/A	Not applicable
NHL	Non-Hodgkin lymphoma
NHS	N-Hydroxysuccinimide
nit	Nitrite
NK	Natural killer cells
NSL	Nanosphere lithography
NT	Nuchal translucency
NTC	No template control
NTD	Neural tube defect
PALS	Periarteriolar Lymphoid Sheaths
PBS	Phosphate buffered saline
PCR	Polymerase chain reaction
PCT	Platelet Hematocrit
PGD	Preimplantation genetic diagnostics
pl	Isoelectric point
PLT	Platelet count
ppm	parts per million

PPP	Platelet-poor plasma
PRP	Platelet-rich plasma
PRT	Plasma recalcification time
RA	Rheumatoid arthritis
RBC	Red blood cell
RDW	Red blood cell distribution width
RISH	RNA in situ-hybridization
RU	Resonance units
SAM	Self assembled monolayer
SCID	Severe combined immunodeficiency
SEM	Scanning electron microscopy
SG	Specific gravity
SOP	Standard operating procedure
SPR	Surface plasmon resonance
ST	Syncytiotrophoblast
SPR	Surface Plasmon resonance
TMB	Tetramethylbenzidin
TNF	Tumor necrosis factor
Ubg	Urobilinogen
UV	Ultra-violet
VNTR-PCR	Variable number of tandem repeats-PCR
WBC	White blood cell

2 Introduction

2.1 Prenatal diagnostics

At present there are a number of different methods which are applied to perform prenatal diagnostics according to the time of gestation and other factors. The most common methods used for prenatal diagnostics are amniocentesis, cordocentesis and chorionic villus sampling (CVS). The obtained fetal cells can be analysed for chromosomal aberrations.

Transabdominal amniocentesis is the most commonly used procedure to obtain fetal cells for cytogenetic analysis. During amniocentesis a sample of amniotic fluid is taken. The procedure is performed between weeks 15 to 18 of gestational age [1]. An accurate sample for analysis is provided in more than 99 % of the cases. Results are usually available within one to two weeks. Risks of this method include fetal loss, chorioamnionitis, fetal injury and maternal Rh sensitization, each of which is very uncommon. The highest risk is fetal loss at less than 0.5 %. The rate of miscarriages after 15 weeks of gestation varies and is most commonly quoted to be 1 % [2]. This risk increases in twin pregnancies up to 2.73 %. Early amniocentesis, before week 15 of gestation increases the risk of fetal loss to between 3 and 5 %. This also increases the risk of congenital foot deformities (mainly talipes equinovarus). A possible explanation for this could be the leakage of amniotic fluid after the procedure, with a subsequent reduction of the space and pressure within the amniotic sac. Early amniocentesis is not commonly used in prenatal genetic diagnosis, because of mentioned problems and first-trimester Chorionic villus sampling (CVS) has replaced it in everyday practice.

CVS has some disadvantages compared with amniocentesis. First, the procedure related pregnancy loss rate is somewhat higher than that of amniocentesis. Second, the incidence of limb deficiencies is greater in cases of CVS performed before the completed ninth week of pregnancy. Third, there is a 2 % false-mosaicism rate during the laboratory evaluation of the chorionic tissue [2]. The risks of CVS greatly depend on the time in pregnancy and on the procedure (transabdominal or transcervical) how it is carried out.

Evans and Wapner [3] conclude in comparison to [2], that the procedure induced miscarriage rate following mid trimester (16-20 weeks) amniocentesis in experienced hands appears to be 1/300. In addition to this, "early amniocentesis" (≤ 13 completed weeks) even with very experienced operators has a risk of fetal loss approaching 1/50 with a risk of *talipes equinovarus* between 1 and 2 %. For operators experienced in both first trimester CVS and mid-trimester amniocentesis the two procedures have comparable safety outcomes. For parents desiring a prenatal diagnosis before week 13 of gestation, CVS is currently the safest procedure.

Further methods for prenatal diagnoses include the sampling of fetal blood and preimplantation genetic diagnosis (PGD) [1]. Fetal blood sampling is applied only under special circumstances and carries a risk of spontaneous abortion of between 1 and 2 %, i.e. higher than amniocentesis or CVS. PGD is performed in cases where the family carries a known genetic disorder. In this procedure a single cell is taken from the early embryo and analysed using polymerase chain reaction (PCR).

Non-invasive prenatal diagnostic techniques include those using visualization techniques and maternal serum screening. Of the visualization techniques ultrasonography is most commonly used. With the sonography one can screen for fetal trisomy 21 by measuring the thickness of a fluid-filled space behind the fetal neck, otherwise known as the nuchal translucency (NT) measurement. In a study of 95.476 singleton pregnancies, combining the risk of maternal age with the NT measurement enabled detection of 268 (82.2%) of 326 with trisomy 21, and 253 (77.9%) of 325 with other chromosomal defects. The 5% of the study

population with the highest estimated risk included 77% of trisomy-21 cases [4]. In a different study, ultrasound detected an absence of the nasal bone in approximately 65 % of fetuses with trisomy 21 and in 1% of fetuses with a normal karyotype [5]. Combining absence of the nasal bone with first-trimester NT and screening of maternal serum free- β -human chorionic gonadotropin (hCG) and pregnancy-associated plasma protein-A (PAPP-A) resulted in the detection of 90 % of fetuses with Down syndrome with a false-positive rate of 5 % [5]. However, while these approaches are useful in screening for Down syndrome, they find limited application in diagnosing fetal aneuploidy.

Cordocentesis is a method to obtain a sample of fetal blood to assess fetal disorders, fetal infections, or isoimmunization or may be used for rapid fetal karyotyping. It also has been used to supply fetal treatment such as transfusions. Fetal loss or spontaneous abortion is reported in approximately 1% to 2% of cases, making the risk associated with this procedure higher than that with amniocentesis or CVS.[6]

Other less common techniques are MRI (magnetic resonance imaging) and fetal echocardiography. All these techniques are not strictly considered to be diagnostic. They only give a strong suggestion of possible fetal developmental problems that are indicative for further tests such as amniocentesis, cordocentesis or CVS.

Maternal serum screening gives another indicator for fetal diagnosis called maternal serum α -fetoprotein (MSAFP) which is elevated in approximately 90% of cases of anencephaly and in approximately 80% of cases of open spina bifida. Maternal serum markers indicative of the Down syndrome in the second trimester are MSAFP in combination with human chorionic gonadotropin and unconjugated estriol concentrations (these constitute the "triple screen" for fetal aneuploidy). Decreased concentrations of all 3 analytes may also be an indicator for fetal trisomy 18. MSAFP screening for the Down syndrome, however, only has a positive screening rate of approximately 5 % and a positive predictive value of approximately between 3 % and 5 % so that the great majority of those who have a positive screening result have a normal outcome [1].

Fetal RhD blood type in Rh-positive pregnant women can be reliably determined by analyzing maternal plasma. Furthermore, genetic diseases where the mother does not have the genetic alteration can be diagnosed by analyzing maternal plasma. However, plasma analysis is not meaningful about the health of the fetus and therefore cannot be used for prenatal diagnosis of maternally inherited genetic diseases and aneuploidies. This could only be done at the moment with amniocentesis or CVS.

In other investigation fetal DNA is in the centre of interest. They isolate and concentrate the fetal DNA circulating in the peripheral blood of the mother instead of fetal cells. Like in a recently published paper from Fan et al. [7] fetal DNA was statistically examined with shotgun sequencing or experimental digital PCR [8]. It is also shown, that pregnancies with Down syndrome fetuses exhibit 1.7 fold higher levels of cell-free fetal DNA in the circulation of the mother than in normal pregnancies [9]. Lo the pioneer for fetal DNA showed in a clinical trial that fetal trisomy 21 could be detected in high risk pregnancies with high sensitivity and specificity by a multiplexed sequencing technique of maternal plasma DNA [10]. The study compared a large number of trisomy 21 and unaffected pregnancies results against full karyotyping. This study reports the use of massively very expensive parallel genomic sequencing (so called next generation sequencing) for medical diagnostics and can only determine trisomy 21. But it seems still difficult to declare a sample positive for a chromosomal trisomy or monosomy based on statistical data. Therefore, it would be more recommendable to apply a quantitative real-time PCR or a FISH-analysis with whole fetal cells. In conclusion it appears to be necessary to isolate and analyse cells and not only free DNA. Alternative approaches use fetal cellular material circulating in the maternal blood for screening and evaluating the health of a fetus. The bases for such approaches are fetal cells released into the maternal circulation at the interface between mother and fetus in the uterus. These cells – trophoblasts or nucleated erythroid cells – survive for a limited time and are

then destroyed setting free fetal DNA. There are several reports in which the free fetal DNA was employed for the detection of a trisomy 21. The problem is that free and unprotected fetal DNA is broken down in the mother's blood to small fragments which are reliable sources for diagnostic purposes only in the case of a trisomy when statistical methods are used for analysis. The method described by Papageorgiou et al., e.g.,[11] is based on the methylated DNA immunoprecipitation (MeDiP) methodology in combination with real-time quantitative PCR (qPCR) to achieve fetal chromosome dosage assessment, this is compared to normal and trisomy fetal DNA. Its final statistical analysis can only be used for the detection of some trisomies, not for the detection of other fetal genetic defects. In addition these small fragments of fetal DNA are hidden and veiled by a tremendous amount of maternal DNA fragments also circulating in the blood.

It seems to be much more convenient and promising to capture the complete fetal cells with the entire genome of the fetus instead of searching for fetal DNA breakdown products in the blood. The cells may even contain several nuclei and they protect the fetal DNA from being broken down so that they represent the target of choice for fetal material isolation methods and they constitute the appropriate basis for comprehensive analyses of the genetic status of a fetus.

Since only a limited number of fetal cells circulate in maternal blood, procedures to enrich the cells and enable single cell analysis with high sensitivity are required, which is the focus of this work.

2.2 Fetal cells

There are three different fetal cell types floating in the maternal blood: fetal leukocytes, trophoblast cells and fetal erythroid/nucleated red blood cells. All these cells have advantages and disadvantages in relation to isolation, detection and the prenatal diagnostics.

Fetal leukocytes could be more easily enriched and are able to grow in culture, but they are very persistent in the maternal blood. Erythrocytes are only short-dated in the blood, but it is not easy to distinguish between fetal and maternal erythrocytes. Nucleated erythrocytes are abundant in first trimester fetal blood, during the yolk sac and liver phases of hematopoiesis. If fetomaternal transfusion is reflective of fetal blood, a 1000 to 1 red-cell-to-white-cell ratio is present. The advantage of trophoblasts over erythroblasts is the fact that they are of fetal origin only. It is possible for erythroblast cells to be of maternal origin, as they appear during physiological morphogenesis of erythrocytes.

Analyses of trophoblast cells have some advantages. First of all the trophoblast cell is involved in the implantation of the blastocyst. The trophoblasts cover the outer part of the blastocyst as an epithelial layer [12] and arrange the anchorage of the blastocyst with the endometrium [13]. The trophoblast cells surrounding the embryoblast infiltrate the endometrium and start to dissolve the decidual cells which release necessary nutrients for the proliferating trophoblasts. The outer trophoblastic layer is called syncytium consisting of syncytiotrophoblasts (ST). Cytotrophoblasts (CT) from the inner layer differentiate and move to the outer part as syncytiotrophoblasts. The syncytium breaks through the endometrium and enables a connection to the maternal capillaries. Parts of the syncytium are filled with blood for the maintenance of the placenta and the fetus.

During early pregnancy fetal cells circulate in maternal blood. Schmorl first observed fetal-maternal traffic of trophoblasts into maternal circulation in 1893 [14],[15]. Focusing the isolation of trophoblast cells from the maternal circulation during early pregnancy, however, different cell types have to be distinguished. These cells are syncytiotrophoblasts (STs), cytotrophoblasts (CTs) and anucleated trophoblasts (AT).

The frequency of trophoblast cells in maternal blood is enhanced in pregnancies complicated by pre-eclampsia. This includes the shedding of ST microvilli. CT or extravillous

trophoblasts are regularly found in maternal peripheral blood. Those originate from endovascular trophoblasts that migrate into the lumen of the spiral arteries to replace the endothelial cells during early pregnancy.

In the following two images the differentiation and aging of trophoblasts in discriminative stages is mapped. Figure 1 presents the trophoblastic pathway of differentiation. In the uterus the villous trophoblast stem cells (with dark nuclei) differentiate, fuse, and maintain the multinucleated ST. Within the ST, a second differentiation pathway takes place resulting in the accumulation of aged nuclei in syncytial knots (black arrows in villi on the lower left).

The extravillous trophoblast stem cells (with dark nuclei) are localized at the basement membrane of anchoring villi in the most proximal part of the cell columns. Their postproliferative daughter cells invade maternal tissues as interstitial trophoblasts, penetrating the endometrium and the first third of the myometrium (light grey arrow). A subset of the interstitial trophoblasts reaches the walls of the spiral arteries and becomes endovascular trophoblasts (dark grey arrow to the right) [12].

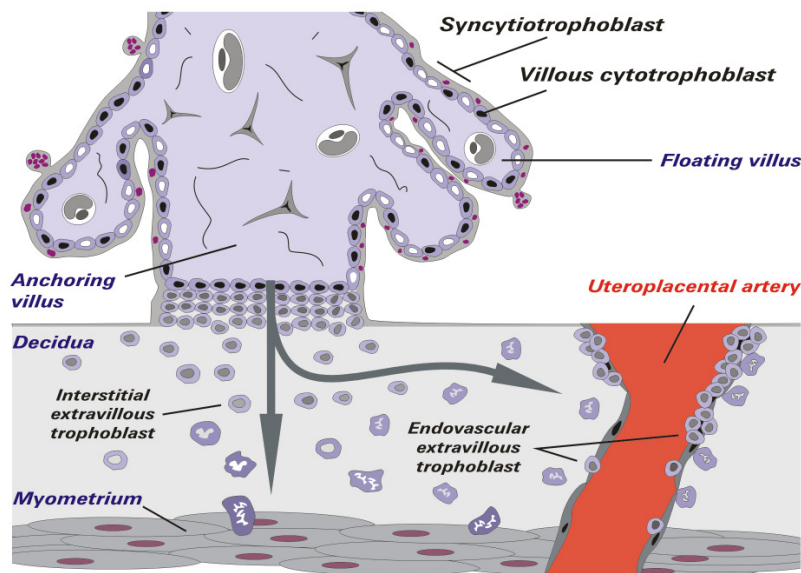


Figure 1 Schematic representation of villous and extravillous trophoblast [12]

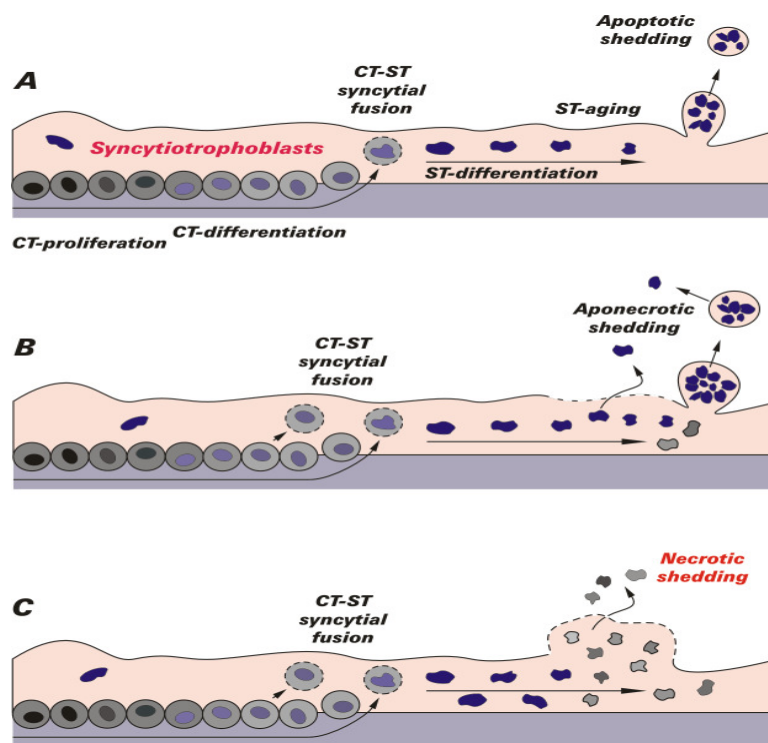


Figure 2 Modes of releasing syncytial material into the maternal circulation

Different steps of trophoblast-differentiation and the release of apoptotic syncytial knots are illustrated in Figure 2. In image A the normal apoptotic shedding is shown. The life cycle of a villous trophoblast comprises the following stages: CT-proliferation and differentiation, syncytial fusion of CT with the ST, further differentiation inside the ST and packing of old material into apoptotic syncytial knots. These corpuscular structures are surrounded by a sealed plasma membrane when they are extruded into maternal circulation and do not induce any inflammatory response of the mother. In part B the aponecrotic shedding is explained. Finalization of the apoptotic cascade may fail because of energetic or other problems. At these sites necrotic breakdown of the plasma membrane may take place. Thus, the already apoptotically cleaved material is released by necrosis (aponecrosis) and may induce inflammation. In part C the necrotic breakdown of syncytial sites is presented which releases cell-free trophoblast material into maternal circulation. Thus an inflammation is caused.

Because the ST fragments may be trapped in the capillary bed of the lungs as a result of their large size, and because the anucleate microvillous fragments are not useful for prenatal diagnosis, one has to focus on the isolation of extravillous CT circulating in maternal blood. Extravillous trophoblast invasion into maternal tissue is a process that starts at implantation, rises to a peak in the mid second trimester, and declines rapidly thereafter. Trophoblast cells vary in size from 20 to 200 μm and contain differing numbers of nuclei, depending on the trophoblast type.

The class I major histocompatibility complex (MHC-I) encodes the classical (class Ia) and nonclassical (class Ib) molecules. HLA-G is a class nonclassical Ib molecule and the genes show limited allelic variation compared with the class Ia genes. HLA-G has commanded centre stage among reproduction immunologists because its expression is restricted to extravillous trophoblasts [16]. It has not been convincingly demonstrated in any other fetal or normal adult tissue with the exception of fetal thymus where HLA-G is found in certain epithelial cells late in gestation and during the first year of life ([17], [18]). The expression of HLA-G by a cell, in this case a trophoblast cell, protected it from destruction by killers of the immune system, in this case NK cells [19]. The presence of HLA-G molecules is

able to suppress the cellular and humoral immune response being triggered by the classical HLA class I (HLA-A, B, C) or class II (HLA-DR, DQ, DP) molecules. HLA-G molecules [20]:

- (1) inhibit the proliferation and cytotoxic functions of T cells and natural killer (NK) cells [21]
- (2) drive T cells into an immunosuppressive profile or provoke the generation of regulatory T cells
- (3) induce the apoptosis of endothelial cells
- (4) inhibit the differentiation of antigen-presenting cells
- (5) alter the cytokine profile towards a Th2 polarization
- (6) up-regulate inhibitory receptors on all kinds of effectors cells.

As secreted/shed HLA-G (sHLA-G) and membrane-anchored molecules exhibit the same receptor specificity, both HLA-G and its soluble counterparts are potent regulator molecules for the innate and acquired cellular immune response. In line with its strong immune tolerogenic functionality, HLA-G is strongly expressed during pregnancy but an ectopic expression is also found in thymus, cornea, and erythroid cells as well as in blood cells [22] and in nonphysiological situations such as transplantation, cancer, infections, and autoimmunity [23].

Indeed, HLA-G was the first HLA class I molecule being identified on trophoblast cells. So far, no pregnancy in which all of the proteins derived from the HLA-G gene are absent has been reported. Thus, HLA-G seems largely to be responsible for the reprogramming of local maternal immune response towards protecting the fetus.

Concerning the tasks of HLA-G it was already mentioned that it has an anti-viral function between the maternal and fetal interface. HLA-G is expressed during the first month of pregnancy in certain cytotrophoblasts and seems responsible for a normal pregnancy without complications. Soluble HLA-G was also found in amniotic fluid and cord blood [24].

Trophoblasts are epithelial cells, which are shed into the maternal blood stream as early as the sixth week of gestation [25] [26], but unlike lymphoid and myeloid cells of fetal origin, they do not persist for years after delivery [27]. Detection of trophoblast cells were found to be optimal within the time window between 9 and 13 weeks [28]. A trend was seen by Knight et. al. [29] towards increasing Trophoblast levels with increasing gestational age. They did a comparison between pre-eclampsia and normal pregnant women and could see clear increase in trophoblasts in the case of pre-eclampsia. Their number regresses after delivery [30]. Trophoblasts do not persist after delivery.

2.3 Isolation techniques

To avoid the relatively complication-loaded invasive methods to obtain fetal cells, a method is needed to enrich fetal cells in sufficient numbers from peripheral blood of the mother. It is known that already from the 6th week of pregnancy fetal cells are in the maternal circulation. These include blood cells of the fetus (such as CD71 positive fetal erythroid progenitor cells) and fetal cells of placental origin (such as HLA-G positive trophoblasts). The cell number of these fetal cells in relation to the maternal cells is so small - 2 to 25 cells / ml maternal blood - that maternal blood is not readily suitable for molecular genetic studies. There are different techniques used for the sorting and the enrichment of fetal cells. The fluorescent-activated cell sorter (FACS) is one method for isolating cells from complex cell mixtures, the other one is the magnetic-activated cell separation system (MACS). Table 1 lists several works that have been tried to isolate trophoblasts from maternal blood. The method of enrichment is the biggest problem, as the subsequent investigations are able to identify or characterize individual cells.

Hawes et al. [31] used antibodies specific for ST to identify large multinucleated fragments of trophoblasts in maternal blood and used these cells for prenatal diagnosis of β -thalassemia. Mueller et al. [32] used the same antibodies to detect STs and subsequently applied the polymerase chain reaction (PCR).

By means of flow cytometry cell sorting, Cacheux et al. [33] identified extravillous CTs in a woman known to carry a fetus with a 47, XYY karyotype. Sbracia et al. [34] used HLA-G antibodies in flow cytometry cell sorting followed by PCR and correctly identified the fetal sex in 9 patients. Durrant et al. [35] identified CT cells with a monoclonal antibody and correctly predicted the fetal gender in 5 out of 6 male gestations, with no false-positive results in 7 female gestations.

According to Bianchi [27] in 90 samples of blood from women mainly in the second trimester of pregnancy a mean number of 19 male fetal cells were detected (1.2 cells per ml maternal blood). In contrast, in 109 samples (16 ml, maternal blood, 2nd trimester of pregnancy) the mean number of previous pregnancy fetal male cells obtained from female fetuses was 2 (0.1 cells per ml maternal blood are false positives). The cell number was determined using Y-chromosomal PCR without cell separation. For the detection of the fetal sex also the FISH-method was used.

One result of the identification of fetal cells in a maternal peripheral blood sample is shown in Figure 3, in which one single HLA-G positive cell was stained with a 7-amino-4-methylcoumarin-3-acetic acid labeled anti-HLA-G antibody (A) [36]. The same cells are visualized through the X-chromosomal specific signal (blue) in part B. HLA-G positive cells show a green staining for the Y-chromosome. In conclusion the analysis of the HLA-G positive cell revealed that the cell in the peripheral blood of the mother was of male fetal origin.

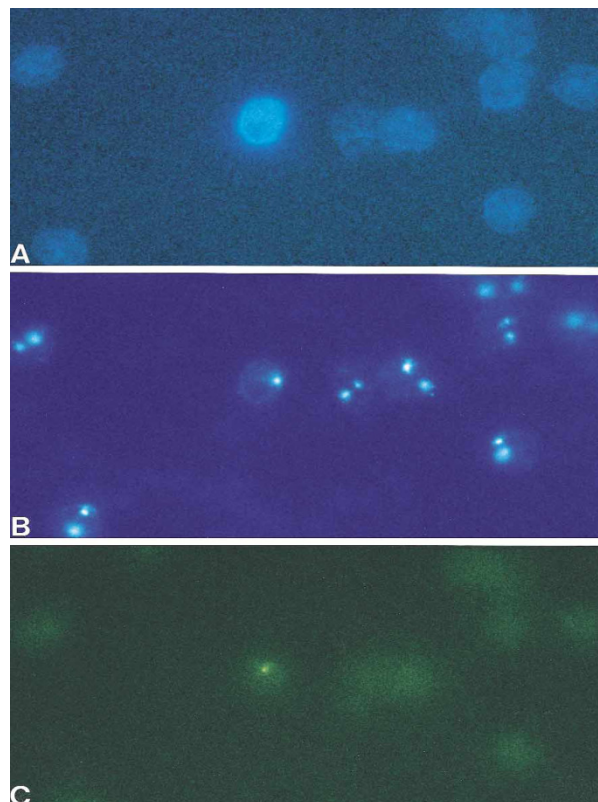


Figure 3 Immunostained maternal peripheral blood cells. HLA-G bearing cells detected in maternal peripheral blood of a pregnant woman with a male fetus after combined immunophenotyping

and fluorescence in situ hybridization [36]. A: Viewed with a triple filter visualizing blue 7-amino-4-methylcoumarin-3-acetic acid stained HLA-G. B: Single X chromosome-specific signal (blue dot) viewed with Spectrum Aqua filter visualizing Spectrum Aqua probe. C: Y-chromosome-specific signal (yellow-green dot).

Table 1 Overview of the characteristics of studies focused on the use of circulating trophoblasts for prenatal diagnosis (examples for positive cell selection taken from Oudejans, et al. [37]).

Study		Stage	Sample	Select.	Antibody	Method	Identification	Target
Author	Year	wks	(ml)	method				
Hawas [31]	1994	10-18	10-50	+	FDO	MACS	Morphology	
Durrant [35]	1996	10-14	15-20	+	340	MACS	PCR	Y
Lim [38]	1999	14-20	25	+ and -	CD45/ 340	MACS	FISH	XY
Hviid [39]	1999	1 st trim	20	+ and -	CD45/ LK26	DC + MACS	VNTR-PCR	TH01
Schueler [40]	2001	6-14	30-40	+	Cocktail	MACS	ICC + RISH /+ FISH	Cockt.+ XY
Lim [41]	2001	9-35	20	+ and -	CD45/ 340	MACS	FISH	XY
Koumantaki [42]	2001	8-12	16-18	+ and -	multiple	DC/ MACS	VNTR-PCR	Multi.
Van Wijk [36]	2001	8-18	25-30			DC	FISH	XY
Vona [43]	2002	11-12	5			ISET + MD	PCR VNTR-PCR ICC	XY Multi. CK
Guetta [44]	2005	17-20	20	+	MEM-G/9	DC + MACS	PCR	XY
Zhang [45]	2008	35-40	6			DC	ICC, PCR	HLA-G, Y

DC, density gradient centrifugation; ICC, immunocytochemistry; MACS, magnetic activated cell sorting; RISH, RNA in situ - hybridization; VNTR-PCR, variable number of tandem repeats-PCR; + positive selection; - negative selection.

2.4 The technology of the nanodetector

The goal in this work is to isolate trophoblast cells by catching them *in vivo* in the vein of a pregnant woman. For isolating trophoblast cells the recognition of the HLA-G antigen by an antibody is essential. Various types of noncovalent interactions may contribute to antibody binding of antigen, including electrostatic forces, hydrogen bonds, van der Waals forces and hydrophobic interactions. A medical guide wire is used as a platform for developing a

medical device, which is making use of different technologies to bind specific antibodies on a novel nanodetector device. The main issue is generating biocompatible surfaces that enable new diagnostic devices for intracorporeal *in vivo* application.

Although it is generally possible to isolate fetal cells from maternal blood in a complex combination of magnetic separation and density gradient centrifugation practical, widely applicable and standardized methods for the enrichment of fetal cells from maternal blood are not available. Therefore, to secure a 100% prenatal diagnosis in clinical practice the invasive amniocentesis or CVS has to be used as before, with the associated risks to the fetus.

All the existing techniques are applied to blood samples *in-vitro*. In this work a new nanodetector will be introduced, which is based on a biofunctionalized wire and enables the capture of fetal cells (trophoblasts) from the maternal blood stream *in-vivo*. An antibody against a special surface marker antigen of fetal trophoblasts is covalently bound to a hydrogel. By targeting these specific antigens, trophoblasts can attach to the catheter. Trophoblasts are the target, because there are have known antigens on the cell surface and commercial antibodies exist are available.

The catheter is intended to be inserted into a peripheral vein of a pregnant woman for about 30 min and specifically captures fetal trophoblasts from the blood stream. Afterwards cytogenetic methods are applied for the detailed analysis of chromosomal aberrations (e. g. the Down syndrome). The device is intended to be used from the 10th week of pregnancy on.

Due to the fact that the amount of trophoblasts is extremely low, a routine blood sample is unable to offer the required sensitivity. Furthermore, it is generally regarded as desirable to avoid taking any more blood than absolutely necessary from pregnant women.

The nanodetector should be used in prenatal screening for pregnant women to determine if their fetus has a particular disorder, such as the Down syndrome. Clinical indications for a high risk of a fetus disorder are the age of the women as well as prenatal biochemical and biophysical tests, family history, physical examination and results from ultrasound examination.

For the intended use of the nanodetector in the arm vein a contact with the circulating blood is necessary over a period of less than 1 h. According to European Norm ISO 10993-1 Table 1 the following safety tests are therefore to be considered: Cytotoxicity test according to EN ISO 10993-5, Hemocompatibility test according to EN ISO 10993-4, Irritation test according to EN ISO 10993-10 or Intracutane reactivity according to EN ISO 10993-10, Sensibility tests according to EN ISO 10993-10 and Acute systemic toxicity according to EN ISO 10993-11. Special emphasis will be laid on the Acute systemic toxicity test with a large animal trial.

2.5 Nanotechnology

Nanotechnology offers new opportunities for the development of a new diagnostic devices for isolating rare cells. Nanotechnology is defined by small feature sizes, a clear definition does not exist. In general nanomaterials have structural features between isolated atoms and bulk materials in the range of about one to 100 nanometers, physical attributes substantially different from those displayed by either atoms or bulk materials [46]. This changes characteristic properties of nanoparticles [47] and because of the small feature sizes applications like electron tunneling are enabled. Surface modifications change the chemical characteristic for binding reactions, like antibodies [46].

Nanostructures [48], [49], [50] are applied:

- in medicine [51], [52], and diagnostics [53] e.g. as lab-on-a-chip applications, nanoparticles, or as quantum dots [54], [55],

- for drug delivery systems including microchips, microneedle-based transdermal therapeutic systems, and assembled systems, [56], [57], [58], or
- nano/micro devices are in development for both diagnosis and therapy (theragnosis) which can improve the personalized medicine [59].

In many biosensors, biological materials are applied to nanostructures or a plain gold surface covering a non-binding surface, like a medical wire, to generate a horizontal or a vertical nanostructure. In this work it should be analysed which surface is the most effective for isolating cells *in vivo*.

Two principal factors determine the properties of nanomaterials to differ significantly from other materials: increased relative surface area and quantum effects. These factors can change or enhance properties such as reactivity, strength, and electrical characteristics. As a particle decreases in size, a greater proportion of atoms are found at the surface compared to those inside. For example, a particle with a diameter of 30 nm has 5 % of its atoms on its surface, at 10 nm 20 % of its atoms, and at 3 nm 50 % of its atoms. Thus nanoparticles have a much greater surface area per mass unit compared to larger particles. As catalytic chemical reactions occur at surfaces, this means that a given mass of material in nanoparticulate form will be much more reactive than the same mass of material made up of larger particles. This can affect the optical, electrical and magnetic behaviour of materials, particularly as the structure or particle size approaches the smaller end of the nanoscale.[60]

An effective diagnostic nanodetector depends on at least two components: a specific target binding structure, the sensor, and the appropriate presentation of this sensor to the target. While sensors are readily available nowadays, the presentation of the sensor to the target limits nanodetector application and sensitivity. Two approaches were developed to present sufficient sensors to target molecules by first coupling to a large-area, two-dimensional highly ordered metallic nanostructures using nanosphere-lithography (NSL) and second by applying a vertical hydrogel to a gold surface. Self-assembly of the hexagonal closed-packed monolayer of latex spheres (LS) is a basis of NSL. This technique is used for the creation of masks for deposition of various materials, typically by evaporation or sputtering. It is known that NSL can be used to make honeycomb lattices of triangularly shaped islands on various substrates. Using LS with different diameters, one can change the spacing and size of the periodically arranged islands. By annealing the samples at a temperature of about 70 % of the melting point of the bulk material and adjusting the time of the thermal treatment, spherical particles can be obtained. Nanodots and nanorods can be obtained by multiple metal depositions at different deposition angles. A variety of complex morphologies, ranging from cup-like structures to rods and wires, are possible using this technique.[61] Applying this technique to a medical wire allows to produce diagnostic nanodetectors with large area, two-dimensional gold nanostructures of 50 to 100 nm size. A typical example of these structures is shown in Figure 4.

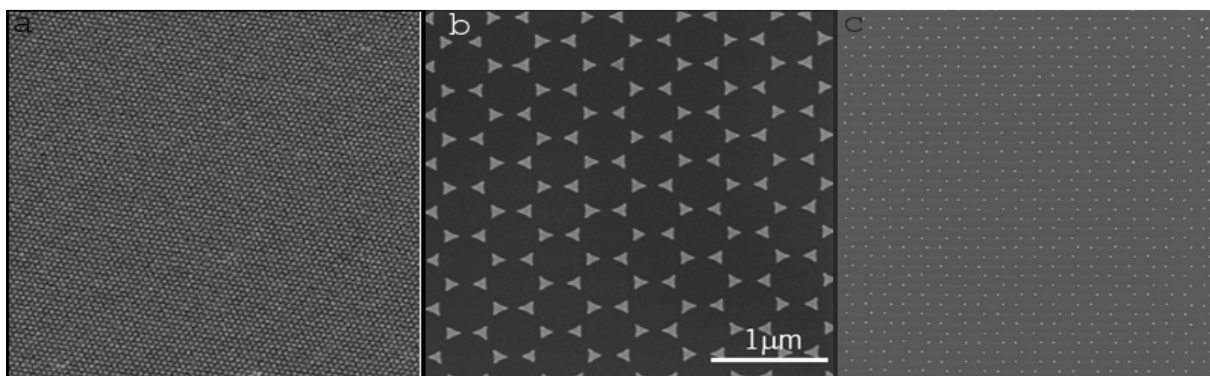


Figure 4 Typical atomic force microscopy images of a guide wire coating. a) Two-dimensional mask on a guide wire created by using latex particles with a diameter of 500 nm. b) Two-dimensional Au-triangle nanostructures. c) Samples presented in b) after annealing show spherical Au-nanoparticles with a diameter of 50 nm.

3 Aims of this work

The first goal of this study was to develop a nanodetector to isolate trophoblast cells to catch them *in vivo* in the peripheral blood stream in a pregnant woman. The second goal was the pre-clinical analysis for a clinical study with pregnant woman. In order to achieve the goal a common medical guide wire was used as a base for developing a nanodetector. Different technologies were applied to bind specific antibodies on the nanodetector against surface antigens of trophoblast cells which were targeted.

- Development of a nanodetector
 - a. finding out an optimized nanostructure surface (horizontal or vertical approach),
 - b. characterisation of the antibody specificity and avidity as well as determination of the antibody amount on the nanodetector surface,
- Proof of the functionality of the nanodetector to isolate trophoblast cells:
 - a. determination of nanodetector cell binding efficiency in *in vitro* settings,
 - b. evaluation of the ability to detect trophoblast cells in a peripheral blood stream of pregnant woman
- Assessment of the safety of the nanodetector for the clinical use in pregnant women:
 - a. determination of the nanodetector cytotoxicity,
 - b. evaluation of the risk for triggering thrombosis – hemocompatibility,
 - c. perform an animal trial to rule out an acute systemic toxicity,
 - d. evaluation of the immunogenicity of a nanodetector components.

4 Material

4.1 HLA-G antigen

Since HLA-G has been demonstrated to be expressed only in extravillous trophoblasts [16] and not in any other fetal or normal adult cells or tissues it was chosen as the prime target for antibodies. In this work a commercial available antibody and a F(ab) fragment, which were to be developed, for functionalizing the nanodetector. HLA-G is a nonclassical major histocompatibility complex class I (MHC-I) molecule consisting of 3 domains. MHC-I complexes are localized in plasma membranes and are involved in immunological defense and tolerance mechanisms differentiating between self and foreign molecules and cells. The overall structure of HLA-G is similar to that of other members of the MHC-I family - like HLA-A2, HLA-B44, HLA-C3 and HLA-E. They share a significant sequence similarity or even identity - HLA-G, e.g. 82 % with HLA-A2. [62]. In order to develop specific antibodies against HLA-G which do not cross-react with the other structurally related MHC-I molecules an amino acid sequence alignment was used to determine sequences unique for HLA-G and therefore suitable as potential antigens in the panning process of the development of recombinant human antibodies. Three such sequences were found. These sequences are located in the three different domains of HLA-G and they were the basis for synthesizing 4 peptides as antigens for the page display.

Alpha 1-Domain:

Peptide 1 :

E₆₁ E E T R N T K A H A Q T D R M N L Q T L R G₈₃

Alpha 2-Domain:

Peptide 2:

I₁₄₂ S K R K C E A A N V A E Q R R A Y L E G T₁₆₃

Peptide 3:

E₁₄₈ A A N V A E Q R R A Y L E G T C V E W L H R Y L E N₁₇₄

Alpha 3-Domain, ILT-2 binding site:

Peptide 4:

H₁₉₃ P V F D Y E A T L R C W A₂₀₆

4.2 Antibodies

Polyclonal antibodies are widely used as detection reagents in research and diagnostics but they are a batch-dependent limited resource and also contain antibodies with unknown specificity. A big milestone in antibody generation was the generation of monoclonal antibodies (mAbs) by hybridoma technology which is based on the fusion of antibody producing spleen cells from immunized mice or rats with immortal myeloma cells [63]. Although the development of the hybridoma technology was a landmark event in science, it still has a number of limitations. Developing hybridomas requires considerable time, expense and expertise, as well as specialized cell culture and animal facilities. As potential therapeutic agents mouse monoclonal antibodies are not suitable because they are

rejected by the human immune system. Exbio provides a mouse antibody called MEM-G/9 which reacts with native form of human HLA-G1 on the cell surface as well as with soluble HLA-G5 isoform in its beta2-microglobulin associated form.

To reduce the risk of immunogenicity today most of the novel therapeutic antibodies are of human origin or at least partially humanized. Many approaches to overcome these limitations of antibody production have been tried, such as to generate either chimeric antibodies or humanized antibodies or using mice that are genetically engineered to produce antibodies with human sequences or the recombinant human antibody technology – a fully *in vitro* method for developing highly specific and high-affinity antibodies.

4.2.1 Human antibodies – phage display

Today suitable recombinant human antibodies are identified with the help of very large libraries of antibody genes. These libraries typically contain human antibody gene sequences, as they were originally used to produce human antibodies for therapeutic purposes. In this work the Human Combinatorial Antibody Library (HuCAL®) technology of MorphoSys was used. The suitable antibodies that bind to a given antigen must be identified by selection rather than by screening. There are numbers of selection techniques like phage display, ribosome display and yeast display. Phage display is widespread and the most popular and best established system for selection over the last decade.

Phage display is based on the fusion of antibody fragments on a surface protein of the phage M13. In that way the antibody is presented on the surface and can be selected by “phage panning”, which is somewhat similar to solid-phase immunoassays [64]. In this process the antigen of interest is immobilized on microplate wells, on magnetic beads or on a column. The phages are then added. After washing to remove all non-specific materials, the bound phages are eluted and amplified by replication in new host cells. The selection procedure is repeated several times, resulting in a population that consists almost entirely of phages that express the desired antibodies. After the selection steps, the antibody genes are isolated and inserted into an expression vector.

4.2.2 Purification of the antibody

After transfection into new host cells and growing the cells, they were lysed and the antibody lysate was tested by ELISA for the presence of antigen-specific antibody material. This soluble antibody fragments produced by *Escherichia coli* are purified by one step affinity chromatography using the His-6-tag, which has been fused to the C-terminus of the antibody and is completed by the metal chelate Ni-NTA. To remove endotoxins from the antibody solution the antibodies were additionally purified with Endo-Trap® columns.

4.2.3 Structure of the used antibodies

The antibody used for the functionalization of the nanodetector is a murine IgG1 (see Figure 5) and a human F(ab). Therefore the antibody lacks completely the Fc part and consists only of the Fab-fragment (see Figure 6). Additionally, the antibody possesses two different tags: a His-Tag and a Cys-Tag. The Cys-Tag could be responsible for the dimerisation of two antibodies resulting in a Fab-Dimer.

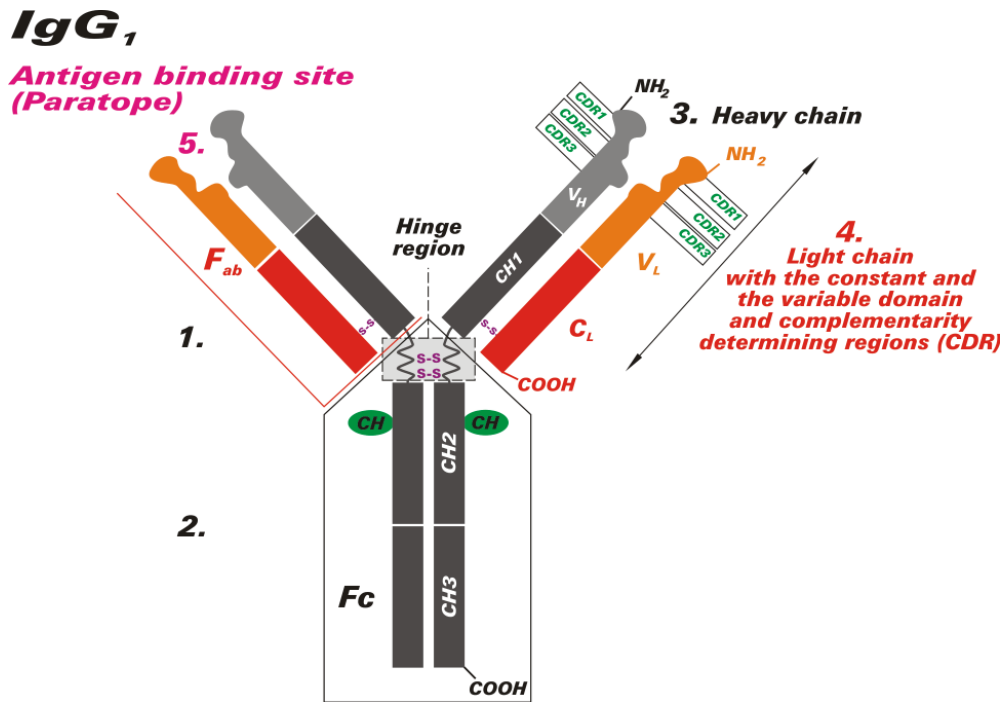


Figure 5 Schematic diagram of the basic symmetrical structure of immunoglobulins (antibodies) composed of two heavy and two light chains. 1. Fab fragment, 2. Fc part, 3. heavy chain (consisting of the variable region V_H with the hypervariable CDR regions, the constant regions CH1, CH2 and CH3 and the hinge region); 4. light chain (consisting of V_L and C_L regions), 5. antigen binding site.



Figure 6 Schematic drawing of the antibody format.

4.3 Cell Lines

Used cell lines:

Name	Description	source	Number
Jeg-3	human choriocarcinoma	DSMZ	ACC 463
K-562-HLA-G	Transfected cell line HLA-G	LMU Munich	
K-562 WT	Wild type	LMU Munich	
K-562 A2	Transfected cell line A2	LMU Munich	
SK-BR-3	adenocarcinoma, malignant	cell-lines-service	
MOLT-17	a T-cell lymphoblastic leukemia cell line	DSMZ	ACC 29

MG-63	Human osteoblastic cell line	ATCC	CRL-1427
NHDF-c adult	humane Fibroblasten	PromoCell	C-12302
Jar	human choriocarcinoma	DSMZ	ACC 462

4.4 Animals

4.4.1 Rats

Female Wistar rats, both pregnant and non-pregnant ones, were used in the trial. The trial was carried out in accordance with ISO 10993-2. The animals were bred at the Department of Toxicology, University of Medical Sciences, Poznan, Poland.

All the tested rats were four months old at the start of the study. The pregnant animals were 4 months \pm 20 days old at the end of the experiment.

The minimum number of animals included in each studied group was 5. The control groups of non-pregnant and pregnant rats consisted of 12 animals each.

All animals were kept under standardised husbandry at the Department of Toxicology. The rats were housed in Tecniplast (1291H001) stainless-steel cages, which were maintained at the temperature of $22\pm 2^{\circ}\text{C}$, and a relative humidity of $50\pm 10\%$. The 12/12 hours light/dark cycle was maintained throughout the study.

The animals were fed with standardised normal LABOFEED H (PN ISO 9001) produced by the Feeds and Concentrates Production Plant, Certificate of Quality System No 181/1/98, Kcynia, Poland. The animals were fed every day at the same time, in the morning with a 10 % surplus added to the amount consumed on the previous day. Water was available ad libitum.

To adapt the animals to the new environment, the rats were kept in husbandry for 3-5 days in groups of two to three animals before the start of the tests.

During the observation, no changes in the behaviour and motoricity of animals were observed. The condition of skin, mucosa and fur was not altered.

4.4.2 Overview: Studied groups

The animals were divided into several experimental groups [65].

Two negative control groups (Control, Pregnant-Control) without any surgical procedures were used. Another control group comprised animals in which the surgical procedures were performed in the same way as in the case of animals belonging to the experimental groups, however, the catheters were not introduced (Control/Catheter/Catheter Gold, Pregnant-Control/Catheter/Catheter Gold). In the case of rats from the other control groups, the catheters, which were not covered with an antibody were introduced (Catheter, Pregnant/Catheter, Catheter Gold, Pregnant/Catheter Gold).

The experimental groups (Table 2) of non-pregnant and pregnant animals were established in order to determine the systemic toxicity to small amounts of antibody, which the nanodetector is coated with. For this purpose, the antibody was injected into the peritoneal cavity in three different doses and autopsy was done at different times after administration of the antibody (Table 2).

Table 2 Outline of the animal trial

Group symbol	Group description	
	Non-pregnant rats	Pregnant rats
Control	Control group; autopsy;	Control group; autopsy
Catheter	Catheter introduction; autopsy after 30 min.	
Catheter Gold	Catheter gold introduction; autopsy after 30 min.	
Control/Catheter/ Catheter Gold	Control group; incision, preparation of carotid vein; autopsy after 30 min.	Control group; incision, preparation of carotid vein; autopsy after 30 min.
Catheter + Anti-HLA-G	Catheter covered with Anti-HLA-G introduction; autopsy after 30 min.;	Catheter covered with Anti-HLA-G introduction; autopsy after 30 min.
Catheter Gold + Anti-HLA-G	Catheter gold covered with Anti-HLA-G introduction; autopsy after 30 min.	Catheter gold covered with Anti-HLA-G introduction; autopsy after 30 min.
Anti-HLA-G 0.05 ng/2 hours	Antibody administration 0.05 ng/250 g; autopsy after 2 h;	Antibody administration 0.05 ng/250g; autopsy after 2 h
Anti-HLA-G 0.10 ng/2 hours	Antibody administration 0.10 ng/250 g; autopsy after 2 h	Antibody administration 0.10 ng/250 g; autopsy after 2 h
Anti-HLA-G 0.25 ng/2 hours	Antibody administration 0.25 ng/250 g; autopsy after 2 h	Antibody administration 0.25 ng/250 g; autopsy after 2 h
Anti-HLA-G 0.05 ng/24 hours	Antibody administration 0.05 ng/250 g; autopsy after 24 h	Antibody administration 0.05 ng/250 g;autopsy after 24 h
Anti-HLA-G 0.10 ng/24 hours	Antibody administration 0.10 ng/250 g; autopsy after 24 h	Antibody administration 0.10 ng/250 g; autopsy after 24 h
Anti-HLA-G 0.25 ng/24 hours	Antibody administration 0.25 ng/250 g; autopsy after 24 h	Antibody administration 0.25 ng/250 g; autopsy after 24 h
Anti-HLA-G 0.05 ng/6 or 3 weeks	Antibody administration 0.05 ng/250 g; autopsy after 6 weeks	Antibody administration 0.05 ng/250 g; autopsy after 3 weeks
Anti-HLA-G 0.10 ng/6 or 3 weeks	Antibody administration 0.10 ng/250 g; autopsy after 6 weeks	Antibody administration 0.10 ng/250 g; autopsy after 3 weeks
Anti-HLA-G 0.25 ng/6 or 3 weeks	Antibody administration 0.25 ng/250 g; autopsy after 6 weeks	Antibody administration 0.25 ng/250 g; autopsy after 3 weeks

The other experimental groups were established in order to test the systemic toxicity of the complete medical product or nanodetector. Catheters covered with the antibody with and without the special gold nanometer sized structure were introduced into a jugular vein for

a period of 30 minutes. After this time, the autopsy was performed. The used nanodetector contained about 1.5 ng of the antibody, with and without gold nanostructures.

The animal trial was performed in accordance with the guidelines provided in the Ministry of High Education Report from 1959, and the UNESCO Declaration of Animal Rights from 1978 (Paris).

An approval was released from the Local Committee of Bio-Ethics for Animal Experiments (Wielkopolska District) (agreement – 16/2007) on February 19th, 2007.

The pregnancy was induced in 4-month-old rats and the experiments were performed (or terminated) on day 20 of the pregnancy.

4.5 Animal study outline

The study groups A to R, i.e. PA to PR for pregnant animals (in alphabetical order, see table 4), were established in order to determine the systemic toxicity to small amounts of antibody which the nanodetector is coated with. For this purpose the antibody was injected into the peritoneum in three different doses/ study groups (0.05 ng, 0.1 ng and 0.25 ng). The antibody used is a mouse monoclonal antibody against human HLA-G. The reason behind using an antibody from a rodent in another rodent is the fact that the final product contains a fully human antibody to be inserted into humans, the results obtained should thus be comparable to the real situation. A rat antibody was not used as this is not available. In addition, three different time spans for observation were included in the trial (2 hours, 24 hours and 6 weeks i.e. 3 weeks for pregnant rats).

Control group: Control groups L and PL were performed as negative controls without insertion of the nanodetector but with performing the same minimal invasive procedure to be used before nanodetector insertion. Additional controls included nanodetectors without the special gold nanometer sized structuring (group R and PR) and nanodetectors without antibody coating (groups M and N). The nanodetector used contained about 1 ng of antibody, with and without gold nanostructures.

Study Groups – Antibody Injection: Groups B to K (respectively PB to PK for pregnant animals) were injected with increasing concentrations of the antibody into the peritoneum. The solutions of the anti HLA-G monoclonal antibody in concentrations of 0.05; 0.1 and 0.25 ng in 0.5 ml were prepared using 0.9 % NaCl. The finished dilution was injected into the peritoneum of the rats from selected groups. Afterwards, the rats were observed for different time spans (from 2 hours to 6 weeks). See Table 3.

Table 3 Outline of study groups for injection of the test substance (monoclonal mouse anti-human HLA-G antibody).

Time\ Concentration	0.05 ng	0.1 ng	0.25 ng
2 hours	B, PB	C, PC	D, PD
24 hours	E, PE	F, PF	G, PG
3 weeks	PH	PI	PK
6 weeks	H	I	K

For each group hematological tests and clinical biochemistry tests were performed. The urinalysis as well as the tests for gross pathology (analysis of different organs) were only done for certain study groups. Body weight and body weight changes were also recorded where applicable. The tests were performed in accordance with ISO 10993.

The different study groups with dates of experiments are listed in Table 4 (below)

Table 4 Outline of the animal trial including a description of the groups included in the study, the dates the experiments were performed, the numbering of animals included in each group and the numbering of documentation for each experiment.

GROUP		NUMBER	DATE / Number	
A	Control	1-20	20.03.2007	1-12
PA	Pregnant – Control	501-520	26.06.2007	501-512
B	Anti-HLA-G 0,05 ng/2 hours	61-80	4.05.2007	61-66
PB	Pregnant Anti-HLA-G 0,05 ng/2 hours	581-600	28.06.2007	581-586
C	Anti-HLA-G 0,10 ng/2 hours	81-100	4.05.2007	81-86
PC	Pregnant Anti-HLA-G 0,10 ng/2 hours	601-620	28.06.2007	601-606
D	Anti-HLA-G 0,25 ng/2 hours	101-120	4.05.2007	101-106
PD	Pregnant Anti-HLA-G 0,25 ng/2 hours	621-640	28.06 .2007	621 -626
E	Anti-HLA-G 0,05 ng/24 hours	181-200	10.05.2007 11.05.2007	181-186 section
PE	Pregnant Anti-HLA-G 0,05 ng/24 hours	641-660	28.06.2007 29.06.2007	641-646 section
F	Anti-HLA-G 0,10 ng/24 hours	201-220	10.05.2007 11.05.2007	201-206 section
PF	Pregnant Anti-HLA-G 0,10 ng/24 hours	661-680	28.06.2007 29.06.2007	661-666 section
G	Anti-HLA-G 0,25 ng/24 hours	221-240	10.05.2007 11.05.2007	221-226 section
PG	Pregnant Anti-HLA-G 0,25 ng/24 hours	681-700	28.06.2007 29.06.2007	681-686 section
H	Anti-HLA-G 0,05 ng/6 weeks	121-140	4.05.2007 21.06.2007	121-126 section
PH	Pregnant Anti-HLA-G 0,05 ng/3 weeks	701-720	20.06.2007 10.07.2007	701-706 section

I	Anti-HLA-G 0,10 ng/6 weeks	141-160	4.05.2007 21.06.2007	141-146 section
PI	Pregnant Anti-HLA-G 0,10 ng/3 weeks	721-740	20.06.2007 10.07.2007	721-726 section
K	Anti-HLA-G 0,25 ng/6 weeks	161-180	4.05.2007 21.06.2007	161-166 section
PK	Pregnant Anti-HLA-G 0,25 ng/3 weeks	741-760	20.06.2007 10.07.2007	741-746 section
L	Control/Catheter/ Catheter Gold	241-260	18.05.2007	241-246
PL	Pregnant Control/Catheter/ Catheter Gold	561-580	28.06.2007	561-566
M	Catheter	21-40	4.04.2007 26.04.2007 17.07.2007	21-23 24-25 26-31
N	Catheter Gold	41-60	4.04.2007 26.04.2007 17.07.2007	41-43 44-49 50-55
O	Catheter Gold + Anti-HLA-G	261-280	20.06.2007 21.06.2007	261-266 267
PO	Pregnant – Catheter Gold + Anti-HLA-G	521-540	27.06.2007	521-526
R	Catheter + Anti-HLA-G	281-300	21.06.2007	281-285
PR	Pregnant – Catheter + Anti-HLA-G	541-560	27.06.2007	541-546

5 Methods

5.1 Surface of the wire

In pre-clinical studies, nanodetectors were produced and assembled for use in minimal invasive diagnostic procedures by nanostructuring the surface of spring wires that are used in hospitals for patients. Modification of a nanostructured commercially available, health-board approved spring wire with biofunctional components is presented in Figure 7. Regarding the nanodetector device: to the gold-coated surface of the guide wire human antibodies to human cell surface target molecules are attached through a linker molecule. The tendency of proteins or cells to physically adsorb onto a substrate without specific receptor recognition is known as nonspecific adsorption. This type of contamination reduces the efficacy of nanodetector. Undesirable features are high background noise and “false positives” results. Poly(ethylene glycol) (PEG) and PEG based polymeric materials have been used for many biological applications because of PEG’s capacity to resist protein and cell adhesion, as well as its nontoxicity and its non-immunogenicity. This modification allows specific detection of circulating rare cells present in the blood stream of a pregnant woman (fetal cells).

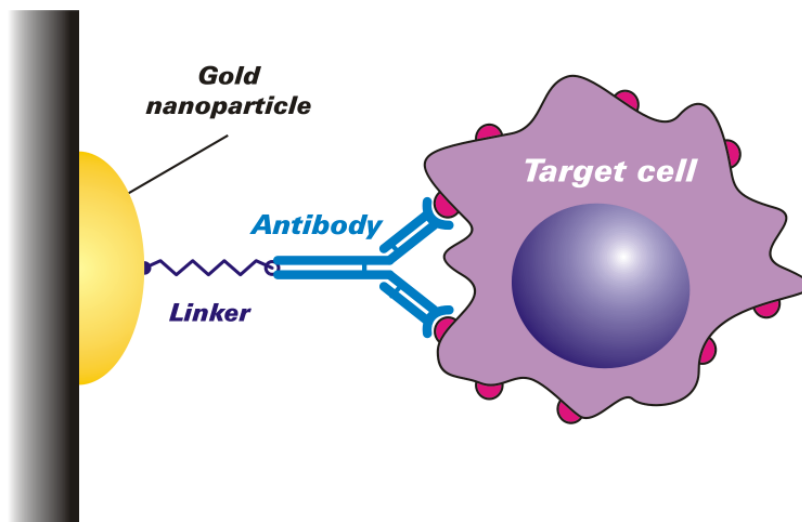


Figure 7 Detection of target cells (fetal cells, tumor cells) by binding to Au-modified nanoparticles, conjugated with target-cell-specific antibodies. Au-nanoparticles decorate the nanostructured surface of a guide wire. Antibodies are covalently bound to the gold nanoparticle by a linker-system. This technique is the first nano-sandwich approach for the production of an *in vivo*-nanodetector device.

Different methods of linker systems were tried to attach antibodies to the nanostructured gold surface.

The second approach is a nanodetector consisting of a wire which is covered with a hydrogel. Most commonly used surfaces in current nanobiotechnology applications are hydrophilic polymer or oligomer layers covalently attached to a substrate like gold due to the simplicity of the surface chemistry and the formation of ordered assemblies shown in Figure 8.

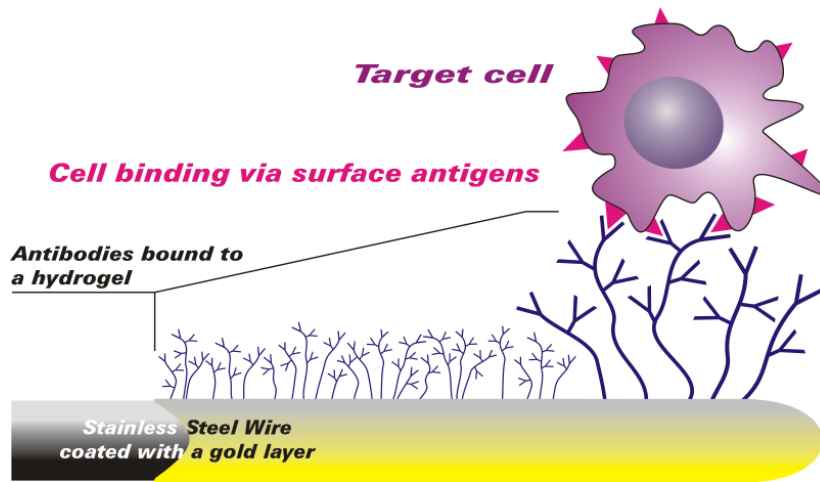


Figure 8 Nanodetector covered with hydrogel and antibodies

5.1.1 Nanostructure (horizontal approach)

As the basis of a covalent binding surface mostly gold nanoparticles are used. Despite the described advantages of the nanotechnology, fabrication of the surface modification is still a problem. Therefore, surface modifications in the nanostructure range are still investigated to address their sophisticated and challenging fabrication because little differences in size can make a difference in the performance. Györvary et al [66] build a closely packed monolayer of 4 nm amino-functionalized CdSe nanoparticles on a protein surface layer lattice. Heddle et al [67], captured and attached gold nanodots with a prepared protein surface. He was able to build gold nanodots onto the SiO₂ layer of a metal oxide semiconductor. Other techniques are sputtering [68]. These are different approaches to generate the similar patterns of defined nanostructured islands on a surface. For the horizontal nanostructured surfaces, small regions of gold are formed through deposition to another material. Self-assembled nanodots range from 10 to a few 100 nm in diameter. Nanosphere-lithography is an established method to generate with structured lithographic masks, nanoislands with dimensions exceeding 100 nm.

Nanoparticles or nanostructures can be modified by established surface chemistry protocols to functionalize the nanostructure or the small sized gold islands by adsorbing untagged antibodies. But the molecules are attached randomly. Alternatively, the antibodies can be bound via an interface of a self assembling monolayer (SAM), creating a surface bearing carboxylic end groups enabling subsequent coupling chemistries. Particle size characterization is important, because of the size similarity to antigen distances on cells. Nanoparticles are not detectable by normal optical microscopy, so electron microscopy or scanning electron microscopy have been used to obtain the information, but electron microscopy cannot recognize antibodies or PEG structures. Other techniques are evaluated by Hall et al. [69]. By too tight packing these antibodies to the nanostructure surface the risk of steric hindrance in binding the respective antigen is increased. This would prevent binding of antibodies to the respective antigen on the target cells. This effect can be reduced or avoided by the introduction of non-binding materials surrounding the islands of the nanostructure surfaces. In this work the nanosphere-lithography was used to generate small nano-islands.

5.1.1.1 Necessary steps for nanosphere lithography (NSL)

1. Preparation of a 2D-mask made from polystyrene particles with a mean diameter of 0.44 μm .

2. Coating of the wire surface with this mask.
3. Application of a gold coating by evaporation of titanium (for better surface contact) and gold.
4. Removal of the mask by various cleaning steps.
5. Structural characterization of the nanostructured wire surface by SEM.
6. Passivation against non-specific cell binding.
7. Sterilization of the nanodetector.

Step 1: Preparation of a 2D-mask made from polystyrene particles with a mean diameter of 0.44 μm .

This method is well known and already published by the group of Prof. Giersig [61, 70-72] A schematic diagram of this method is shown in Figure 9.

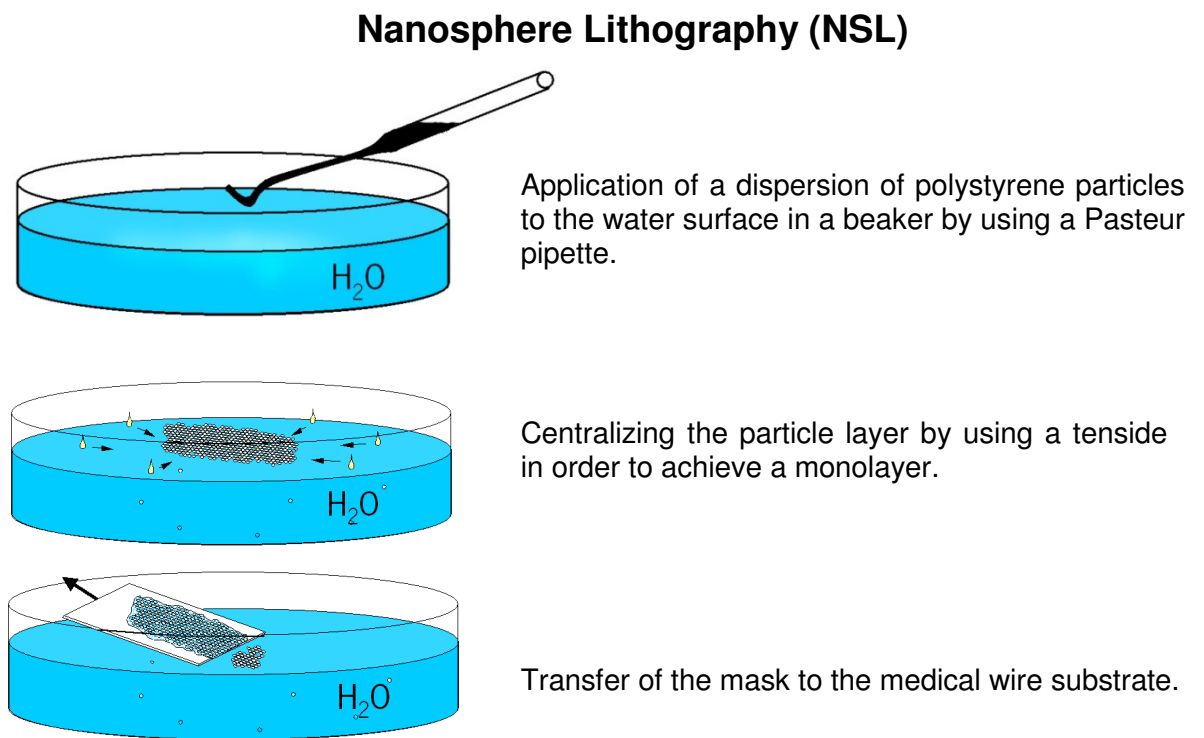


Figure 9 Schematic diagram of the preparation of a 2D-mask consisting of polystyrene particles

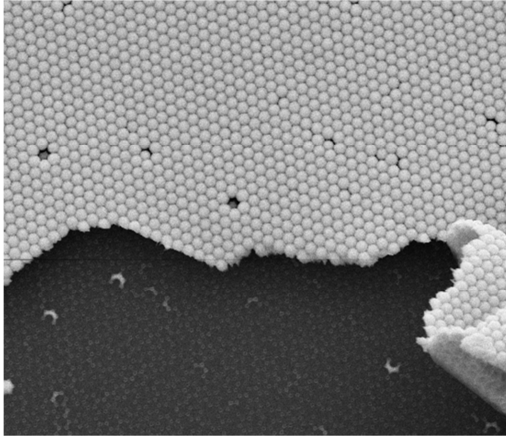


Figure 10 SEM Image of the 2D maske from latex Particel with 500 nm diameter The mask will cover 2 cm of the tip of wire

Step 2: Coating of the wire surface with this mask Figure 10.

The coating mask consists of polystyrene particles which applied to the tip of the wire see Figure 11

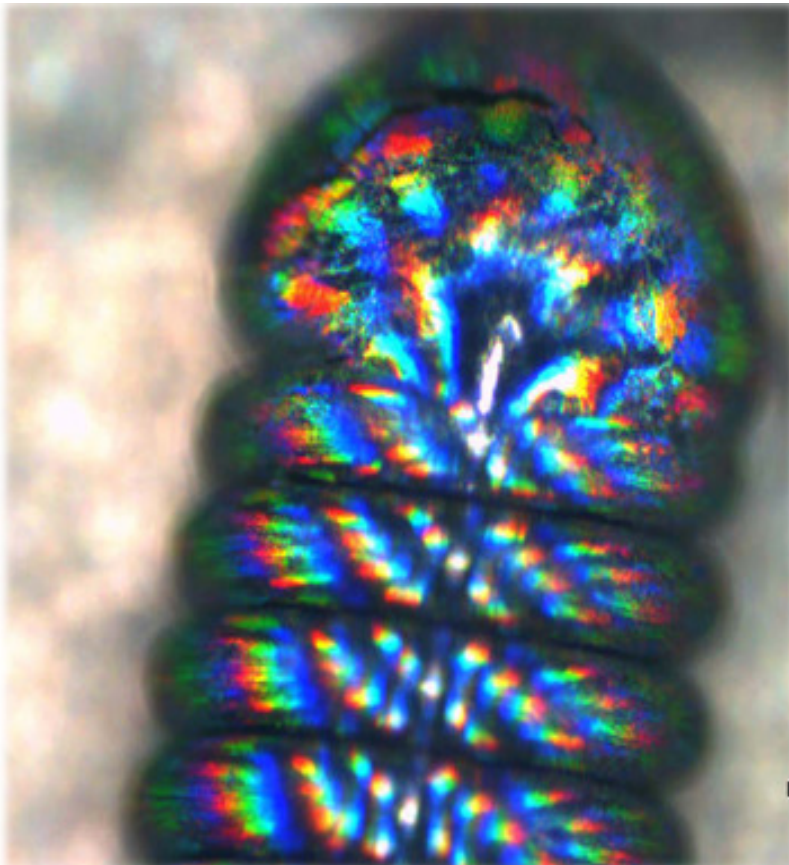


Figure 11 The image of a Seldinger wire wrapped with the mask under a light microscope showing the characteristic light refraction for the mask

Step 3: Application of the gold coating by evaporation of titanium (to encourage adhesion) and gold.

The next step is the coating with gold by evaporation. In order to encourage the adhesion of a gold layer on a substrate a layer of titanium is initially applied to the surface. After coating with titanium a layer of gold is applied by evaporation in the same evaporation chamber.

Step 4: Removal of the mask by various cleaning steps.

The removal of the mask is accomplished by using adhesive tape and several washing steps in an ultrasound bath.

Step 5: Structural characterization of the nanostructured wire surface by SEM.

On the medical wire an array of nanometer-sized gold islands has now been created. This array of gold islands is now analysed by SEM as seen in Figure 12.

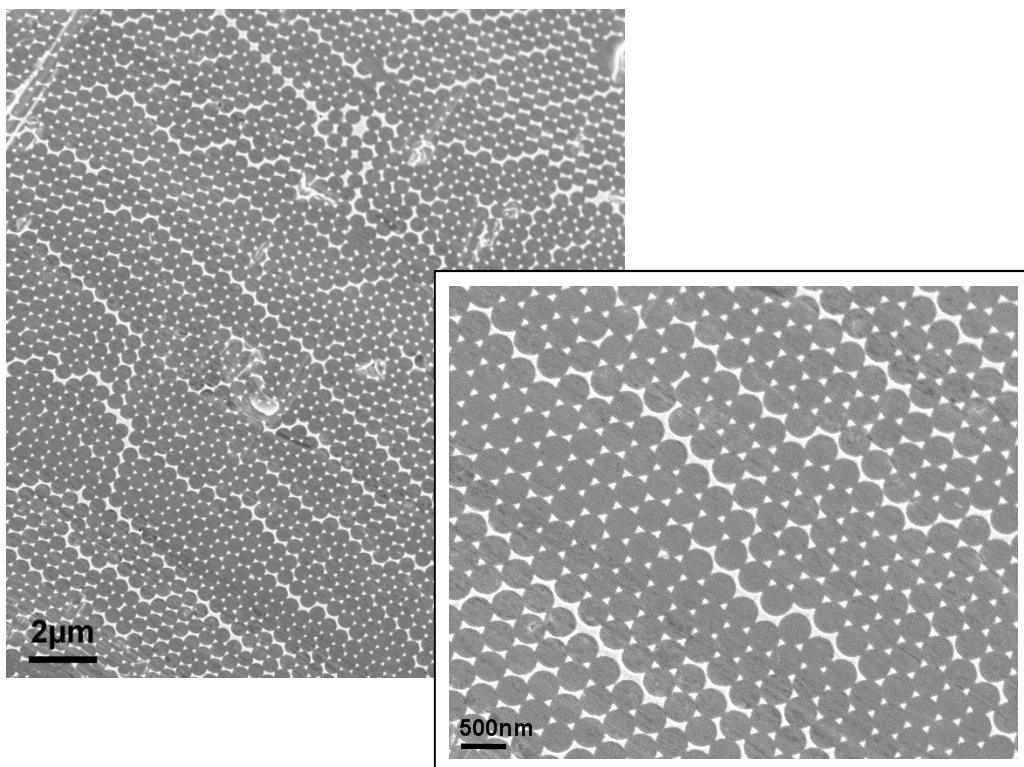


Figure 12 SEM images showing at different magnifications the arrays of gold islands produced by NSL.

Step 6: Passivation against non-specific cell binding

In order to avoid non-specific cell binding in the regions between the gold nanostructures, the medical wires are passivated by means of a PEG2000-Urea-silane solution (Figure 13). The passivation steps are as following:

- a. The nanostructured wires are chemically activated by immersing them into a 3:1 mixture of sulfuric acid (H_2SO_4) and hydrogen peroxide (H_2O_2), also called Piranha solution. The wires are then rinsed thoroughly with water and finally blown dry with nitrogen.

- b. Then the wires are placed inside a Schlenk flask filled with 10 ml of a dry solution of toluene.
- c. One drop of distilled, degassed triethylamine (Et₃N) is added to this solution.
- d. 10 mg of PEG2000-Urea-silane are dissolved in 5 ml of a dry solution of toluene employing a separate container. The solution is then added to the Schlenk flask.
- e. The Schlenk flask is sealed up and the nanostructured wires are kept in this passivation solution for 4-24 h at 80 °C.
- f. Afterwards, the wires are rinsed with ethyl acetate and then in methanol and finally dried in a stream of nitrogen.

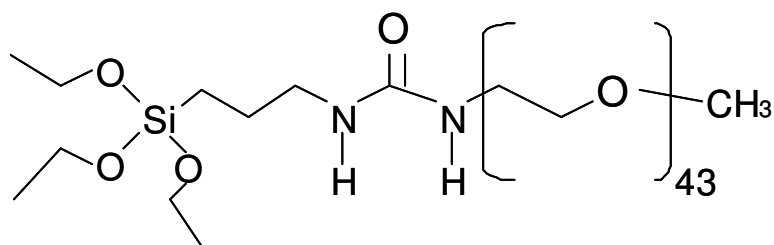


Figure 13 Chemical formula of the PEG2000-Urea-silane employed for the passivation

Step 7: Sterilization

The nanodetector is thoroughly cleaned and sterilized by steam before being transferred to a laminar flow hood to be coated with the antibody. All materials used during production of the nanodetector are cleaned and sterilized accordingly.

5.1.2 Nanostructure (vertical approach)

With galvanization techniques the first 2 cm of the medical wire were covered with a complete gold surface. The thickness of the gold surface is between 0,5 – 1 μm and the galvanization was done by a company (OTEK; Briselang).

There are two principal strategies to attach a polymer to a surface: grafting from and grafting onto. Grafting from means the in-situ polymerization from a surface, while grafting onto involves the covalent attachment of previously formed polymer chains to a substrate. Grafting from is believed to possess an inherent advantage: Theoretically, it is supposed to result in higher densities of polymer chains covering the surface. When the polymer chains are growing at the interface, only monomers of small to moderate size have to access the ends of the growing chains, a process which takes place with high diffusion rates and which does not imply steric hinderance. On the contrary, in the grafting onto scenario, entire polymer chains need to access a surface and react there. Diffusion of polymers is generally slower, and especially when some polymer chains are already attached, the access of further polymer chains to a reaction site on the surface will be sterically limited.

In 1990, Löfås and Johnsson [73] introduced a method to modify noble metal surfaces in an effective manner for biosensor applications. Hydrogel matrices composed of

polysaccharides (here: dextran) were utilised to immobilize biomolecules analogous to procedures in affinity chromatography. Noticing the importance of a barrier between the original noble metal surface and the hydrogel itself, they used a self assembled monolayer (SAM) of long-chain omega-functionalised alkyl thiols for primary surface functionalisation, because it forms a layer much less prone to defects than shorter chain variants (Figure 14). The combination of this dense SAM and the dextran covalently coupled to it is rather efficient and became the "standard" sensor surface for the surface plasmon resonance (SPR) based biosensor system commercialised by Biacore AB (Sweden).

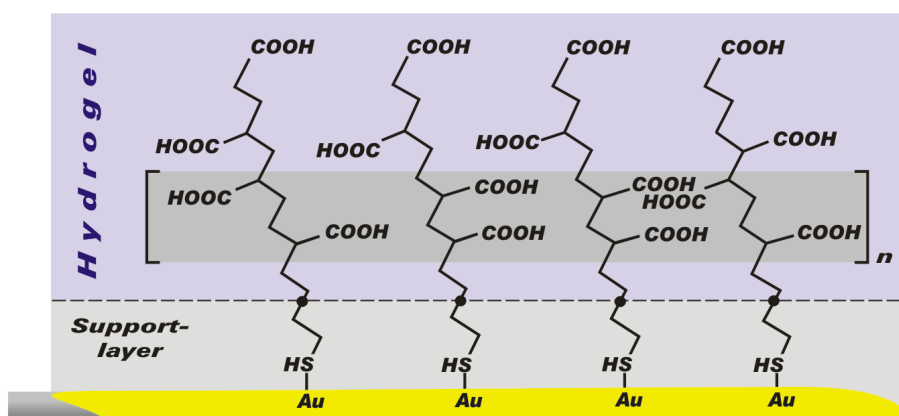


Figure 14 Structure of the hydrogel

Taking a closer look, one recognizes that a biocompatible surface suitable for biosensing is a complex system. Many parameters have the potential to influence the final performance of the biocompatible layer: chemical composition and morphology of the substrate, thickness, density and chemical composition of barrier and linker support layers, immobilization density, average molar mass and chemical composition as well as substitution pattern of the biocompatible polymer layer.

The surface of the wire was covered with different 3D-polymers and a hydrogel matrix made by XanTec GmbH, Germany. The Xantec Hydrogel consists of linear polycarboxylates and allows multilayer ligand immobilization, which leads to a significant signal amplification. They are employed for qualitative screening, concentration determinations, detection and kinetic analyses of low molecular weight compounds. As a rule of thumb, the smaller the analyte is, the thicker and denser the hydrogel structure should be.

The hydrogel C which was used, is available in four different thicknesses and porosities: C 30 M, C 80 M and C 200 D. The C type is based on a linear, synthetic polycarboxylate. Compared to branched dextrans, it is better defined, shows a higher signal to noise ratio, has improved diffusion properties (better curve fits) and a higher chemical stability. Beside the C matrix, an alternative polymer matrix with reduced negative charge density is available. This hydrogel, product code HC, is recommended for applications where non-specific interactions are critical. All derivatives of the C matrix are available with HC coatings, too. In this work a modified hydrogel HC was used.

5.2 Binding of the antibody to the surface of the wire

The binding of the antibody is mediated through the reaction with EDC/NHS. EDC (1-ethyl-3-[3-dimethylaminopropyl]carbodiimide) is a water soluble compound which is a carboxyl activating agent used for the coupling of primary amines to yield amide bonds. EDC is often used in combination with N-hydroxysuccinimide (NHS) or sulfo-NHS (SNHS) to increase coupling efficiency or create a stable amine-reactive product. EDC can also be used

to activate phosphate groups, which is used for example for the crosslinking of proteins. This feature has been used to crosslink isolated collagen fibres for manufacturing alternative biocompatible materials used in implant technology. Several studies showed that EDC/NHS treated collagen samples revealed *in vitro* and *in vivo* biocompatibility comparable to recently used industrial collagens [74-76].

On the nanodetector both EDC and NHS function as catalysts only. Following the reaction for coupling/immobilization of the anti-HLA-G antibody, EDC/NHS is removed thoroughly by several washing steps with water. Thus the total amount of EDC/NHS on the nanodetector is suggested to be zero.

5.2.1 Activation of the hydrogel and coupling of antibodies

5.2.1.1 Materials

- Hydrogel coated nanodetector, carboxylated
- Antibody solution: 5-100 µg/ml in coupling buffer after quick dialysis against the coupling buffer in order to remove excess salt.

One of the following coupling buffers:

- 2-20 mM sodium formiate, pH 3.0 – 4.0,
- or 2-20 mM sodium acetate, pH 4.0 – 5.5,
- or 1-10 mM sodium maleate, pH 5.5 – 7.0

are used depending on the pI of the antibody. The buffer pH should be 0.5 – 1 units below the pI of the antibody to ensure a positive net charge of the antibody which is required for electrostatic interaction with the negatively charged surface.

- Elution buffer: 2 M sodium chloride
- Blocking buffer: 1 M ethanolamine hydrochloride, pH 8.5
- Activation mix: 100 mM N-hydroxysulfosuccinimide (SNHS), in 50 mM 2-(N-morpholino) ethane sulfonic acid (MES) buffer, pH 5.3. Immediately before use 5 - 100 mM N-ethyl-N'-(dimethylaminopropyl)carbodiimide)hydrochloride (EDC-HCl) is added. The optimal EDC concentration depends on the coating and the ligand. A low EDC concentration (around 10 mM) is recommended for C and HC coatings and for the immobilization of larger ligands with abundant lysine residues.

All buffers are sterile filtered before use.

5.2.1.2 Protocol

Running buffer during immobilization should be double distilled water.

1. Mount a carboxylated nanodetector in a suitable test tube.
2. Elute contaminants from the surface for 5 min. with 2 M NaCl / 10 mM NaOH. To remove hydrophobically bound antibody from the tube, etc. The system might additionally be cleaned with an easily desorbable (avoid SDS) detergent solution followed by double distilled water.
3. Prepare the EDC/SNHS activation solution.
4. For a maximal activation level, incubate the nanodetector 3 - 15 min with the EDC/SNHS solution. If a lower level of immobilization is desired, choose a short activation time. Due to slight gas evolution, small bubbles might occur.
5. Wash quickly and fill in the antibody solution for 5 - 30 min. The immobilization yield can be increased by repeatedly applying the antibody solution.

6. Incubate the nanodetector for 10 min with water to complete the coupling reaction which proceeds slowly at low pH.
7. Quench remaining SNHS esters 15 min with blocking buffer.
8. Remove loosely physisorbed antibodies with regeneration solution.
9. Start binding experiments.

Antibodies used for the functionalization of the nanodetector have to fulfil certain defined quality criteria. The following quality of the antibodies is necessary for performing safety tests:

Definition of the quality criteria

- a) The antibody preparation has to be free from insoluble protein precipitates (preparation e.g. must not be opaque).
- b) There has to be a sufficient and defined level of functionality of the antibody. The functionality of an antibody will be determined by FACS- or BiaCore-analyses and will be compared with that of a standard antibody preparation.
- c) Criteria for purity of an antibody preparation:
 - Amount of F(ab)-antibody in the preparation: > 95 %.
 - Endotoxins: < 0.5 EU/ml in the antibody preparation

The antibody solution is sterilized by filtration immediately prior to use. On the sterile nanodetector the antibody is immobilized by thiol-gold interactions under sterile conditions.

The bio-functionalized sterile nanodetector is mounted to a diaphragm. This diaphragm fits to a glass with a lid which is filled with 4 ml sterile PBS. Afterwards it is placed together with the diaphragm on the glass and finally closed with the lid. The nanodetector with the glass is placed in the package bag and closed. All packaging components are sterilized by steam sterilization before assembly and the packaging takes place using aseptic techniques to ensure the sterility of the product.

5.3 Surface acoustic wave methodology

Surface acoustic wave (SAW) sensors and the surface plasmon resonance (SPR) technology enable the recording and the measurement of physical or chemical binding events from the liquid phase if one of the binding partners is attached to the surface of a sensor. These methods were used to estimate the amount of antibodies which can be fixed to the surface of a nanodetector. SAW sensors send out acoustic waves rolling over the surface of a piezoelectric crystal by converting electrical signals with an interdigital transducer (IDT) into polarized transversal waves. Their velocity is changed by any contact with a medium bound to the surface of the sensor. The sensor surface is in direct contact with the piezoelectric substrate to guarantee the precise measurement of specific molecular interactions. The acoustic wave is transmitted to a guiding layer and not directly to the substrate. The energy of the wave stays within this layer and not in the piezoelectric matrix. When passing the sensitive area, the waves are influenced by binding events on its surface. And after passing this area, the modulated wave is converted back into an electrical signal.

All incoming new wave signals are compared with the original input signal for frequency or phase changes which are then correlated to mass and viscosity alterations. In cooperation with SAW Instruments GmbH (Schwertberger Str. 16, D-53177 Bonn, Germany) antibodies were bound to a sensor [77]. This biosensor works in the frequency range of 25 to 500 MHz. Frequency increases or decreases are correlated with the penetration depth. SAW Instruments GmbH used the S-sens[®] K5 from Nanofilm, Germany with five separate sensor elements on one sensor chip operating with the Love-wave geometry. Instead of frequency shifts this device measures the delay-line geometry. It uses two fixed frequencies in the range between 130 and 170MHz. Mass differences are correlated to changes in the phase velocity inside the guiding layer of the sensor and can be determined on the basis of viscoelastic effects by using both phase shifts and amplitude shifts of the surface acoustic wave.

For the generation of love-wave sensor chips with nanoislands or a complete gold surface ST-cut quartz substrates and NSL were used [78]. Photolithography and ion beam etching were used to shape the inter-digital transducers and contact pads [79, 80]. The SiO₂ surface was processed with the wet-lithographic method, as described in chapter 5.1.1.1, for generating nanoparticles of defined interspaces and size (see Figure 9).

5.3.1 Modification of the sensor chip surfaces and measurement in the microfluidic SAW sensor system

On the gold sensor chip surface a self-assembling monolayer (SAM) of 11-mercapto-undecanoic acid molecules (Sigma-Aldrich) was generated and this modified chip was placed into a Sam[®] 5 read-out system and all subsequent binding experiments were performed within the microfluidic sensor system. Interactions of molecules on the chip surface which result in mass loading or mass changes are recorded by the sensor in real time as phase shift changes and amplitude modulations.

This makes it possible to accurately detect and discriminate mass from viscosity caused alterations. The samples were applied with an autosampler in a buffer stream at a flow rate 30 µl/min and at a constant temperature of 23°C. First the carboxyl groups of the 11-mercaptoundecanoic acid were activated using 200 mM N-(3-dimethylaminopropyl)-N-ethylcarbodiimide (EDC) and 50 mM N-hydroxysuccinimide (NHS). Antibodies were then coupled to the activated SAM by standard carbodiimide chemistry protocols [79]. Cell binding experiments were performed with PBS, pH 7.4. All surface modifications and the binding cycles were recorded. In the experiments with the SAW sensor system cells of the human chorioncarcinoma derived cell line JEG-3 (ECACC 92120308, American Type Culture Collection ATCC HTB 36, expressing HLA-G on their plasma membrane, were used and the mouse anti-HLA-G antibody (clone: MEM/G9, Batch - No 070207) or a human anti-HLA-G F(ab) fragment (both from AbD-SEROTEC, Munich, Germany) were coupled to the sensor chip surface in the cell binding experiments.

5.4 Flow Cytometry

Immunofluorescence is a technique whereby an antibody labeled with a fluorescent molecule (fluorescein or rhodamine or one of many other fluorescent dyes) is used to detect the presence of an antigen in or on a cell or tissue by the fluorescence emitted by the bound antibody.

The flow cytometry technique is used to identify and enumerate cells bearing a particular antigen. Cells in suspension are labeled with a fluorescent tag by either direct or indirect immunofluorescence. The cells are then analyzed in the flow cytometer.

In a flow cytometer, the cells exit a flow cell and are illuminated with a laser beam. The amount of laser light that is scattered by the cells as they pass through the laser beam can be measured giving information concerning the size of the cells. In addition, the laser can excite the fluorochrome on the cells and the fluorescent light emitted by the cells can be measured by one or more detectors.

The type of data that is obtained from the flow cytometer is usually analysed in the following way: In a one parameter histogram, increasing amount of fluorescence (e.g. green fluorescence) is plotted on the x axis and the number of cells exhibiting that amount of fluorescence is plotted on the y axis. The fraction of cells that are fluorescent can be determined by integrating the area under the curve. In a two parameter histogram, the x axis is one parameter (e.g. red fluorescence) and the y axis is the second parameter (e.g. green fluorescence). The number of cells is indicated by the contour and the intensity of the color.

5.5 Surface plasmon resonance (SPR)

SPR-based instruments use an optical method to measure the refractive index near (within ~300 nm) a sensor surface. In this work a BIAcore instrument was used for SPR measurements. In a BIAcore this surface forms the floor of a small flow cell, 20-60 nl in volume, through which an aqueous solution (henceforth called the running buffer) passes under continuous flow (1-100 $\mu\text{l}/\text{min}$). In order to detect an interaction one molecule (the ligand) is immobilised onto the sensor surface. Its binding partner (the analyte) is injected in aqueous solution (sample buffer) through the flow cell, also under continuous flow. As the analyte binds to the ligand the accumulation of protein on the surface results in an increase in the refractive index. This change in refractive index is measured in real time, and the result plotted as response or resonance units (RUs) versus time (a sensorgram). Importantly, a response (background response) will also be generated if there is a difference in the refractive indices of the running and the sample buffers. This background response must be subtracted from the sensorgram to obtain the actual binding response. The background response is recorded by injecting the analyte through a control or reference flow cell, which has no ligand or an irrelevant ligand immobilized to the sensor surface.

One RU represents the binding of approximately 1 pg protein/ mm^2 . In practice >50 pg/ mm^2 of analyte binding is needed. Because it is very difficult to immobilise a sufficiently high density of ligand onto a surface to achieve this level of analyte binding, BIAcore have developed sensor surfaces with a 100-200 nm thick carboxymethylated dextran matrix attached. By effectively adding a third dimension to the surface, much higher levels of ligand immobilization are possible. However, having very high levels of ligand has two important drawbacks. Firstly, with such a high ligand density the rate at which the surface binds the analyte may exceed the rate at which the analyte can be delivered to the surface (the latter is referred to as mass transport). In this situation, mass transport becomes the rate-limiting step. Consequently, the measured association rate constant (k_{on}) is slower than the true k_{on} . A second, related problem is, that following the dissociation of the analyte, it can rebind to the unoccupied ligand before diffusing out of the matrix and being washed from the flow cell. Consequently, the measured dissociation rate constant (apparent k_{off}) is slower than the true k_{off} . Although the dextran matrix may exaggerate these kinetic artifacts (mass transport limitations and re-binding) they can affect all surface-binding techniques.

The BIAcore is particularly well suited to evaluating the binding of recombinant proteins to natural ligands and mAbs.

5.6 Flow system

A flow system is an in vitro model to examine possible interactions between a flowing substance (e.g. blood) and a test item (e.g., medical wire). An in vitro-flow system was

developed, in which cell adhesion under flow conditions as they are found in a vein can be investigated. A flow rate of 0-38 ml/ min can be simulated, which also corresponds to the velocity of blood in the vein. With the flow system it is possible to observe the enrichment of cells on the nanodetector, because immobilized antibodies bind to cells in a suspension medium. Suspension medium can be PBS or blood. Culture cells can be spiked into the suspension medium. It is also possible to use peripheral blood from patients.

To avoid the destruction of cells by the peristaltic pump – and the release of unwanted proteins and other cellular components the blood passes in this system arrangement no longer through the pump see Figure 15.

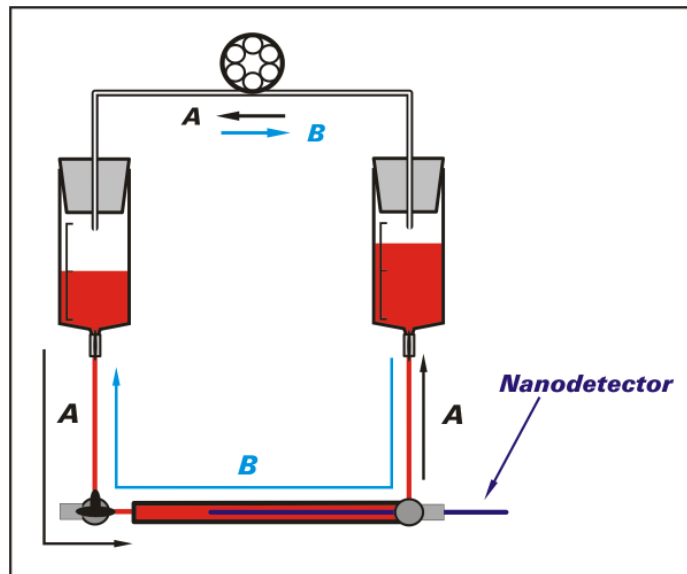


Figure 15 Schematic presentation of the flow system

5.7 Visualization of cells

Immunocytochemistry is a technique used to assess the presence of a specific protein or antigen in cells (cultured cells, cell suspensions) by a specific antibody, which binds to it, thereby allowing its visualization and examination under a microscope. Cells to be stained are attached to the nanodetector or chips to allow easy handling in subsequent procedures. In the *in vitro* tests for demonstrating the functionality of the nanodetector cells to be bound were prestained and spiked into the suspension medium.

To ensure free access of the antibody to its antigen, the cells must be fixed and permeabilized for accessing intracytoplasmic antigens. In general, fixation strengths and times are considerably shorter for cells than for the thicker, structurally complex tissue sections. For immunocytochemistry, sample preparation essentially entails fixing the target cells to the nanodetector. Perfect fixation would immobilize the antigens, while retaining authentic cellular and subcellular architecture and permitting unhindered access of antibodies to all cells and subcellular compartments. Wide ranges of fixatives are commonly used, and the correct choice of method will depend on the nature of the antigen being examined and on the properties of the antibody used. Fixation methods generally fall into two classes: organic solvents and cross-linking reagents. Organic solvents such as alcohols and acetone remove lipids and dehydrate the cells, while precipitating the proteins on the cellular architecture. Cross-linking reagents (such as paraformaldehyde) form intermolecular bridges, normally through free amino groups, thus creating a network of linked antigens. Cross-linkers preserve cell structure better than organic solvents, but may reduce the antigenicity of some

cell components, and require the addition of a permeabilization step, to allow access of the antibody to the specimen. Fixation with both methods may denature protein antigens, and for this reason, antibodies prepared against denatured proteins may be more useful for cell staining.

Immunohistochemistry or immunofluorescence are methods to localized antigens in tissue sections by the use of labeled antibody through antigen-antibody interactions that are visualized by a marker such as coupled enzyme for immunohistochemistry or fluorescent dye for immunofluorescences.

Tissue preparation is the cornerstone of immunohistochemistry. To ensure the preservation of tissue architecture and cell morphology, prompt and adequate fixation is essential. However, inappropriate or prolonged fixation may significantly diminish the antibody binding capability.

There is no one universal fixative that is ideal for the demonstration of all antigens. However, in general, many antigens can be successfully demonstrated in formalin-fixed paraffin-embedded tissue sections. The discovery and development of antigen retrieval techniques further enhanced the use of formalin as routine fixative for immunohistochemistry in many research laboratories.

Since its introduction, paraffin wax has remained the most widely used embedding medium for diagnostic histopathology in routine histological laboratories. Accordingly, the largest proportion of material for immunohistochemistry is formalin-fixed, paraffin-embedded. Certain cell antigens do not survive routine fixation and paraffin embedding. So the use of frozen sections still remains essential for the demonstration of many antigens. However, the disadvantage of frozen sections includes poor morphology, poor resolution at higher magnifications, special storage needed, limited retrospective studies and cutting difficulty over paraffin sections.

For light microscope analysis a fluorescence and labeling method has to be chosen:

Direct method is one step staining method, and involves a labeled antibody (i.e. fluorescence dye conjugated antiserum) reacting directly with the antigen in tissue sections. This technique utilizes only one antibody and the procedure is short and quick. However, it is insensitive due to little signal amplification and rarely used since the introduction of indirect method.

Indirect method involves an unlabeled primary antibody (first layer) which react with tissue antigen, and a labeled secondary antibody (second layer) react against primary antibody (The secondary antibody must be against the IgG of the animal species in which the primary antibody has been raised). This method is more sensitive due to signal amplification through several secondary antibody reactions with different antigenic sites on the primary antibody. In addition, it is also economy since one labeled second layer antibody can be used with many first layer antibodies (raised from the same animal species) to different antigens.

The secondary antibody can be labeled with a fluorescent dye such as FITC, rhodamine or Texas red, and this is called indirect immunofluorescence method. The second layer antibody may be also labeled with an enzyme such as peroxidase, alkaline phosphatase or glucose oxidase. After developing step using specific for an enzyme substrate, one can visualize in the light microscopy a presence and localization of an targeted by the primary antibody antigen. This is called indirect immunoenzymatic method.

5.8 Safety testing including animal trials (EN ISO 10993)

5.8.1 Description of the device including any materials that will be in contact with tissues or body fluids

The nanodetector consists of the following components:

1. Medical wire, certified medical product consisting of stainless steel 1.4310 with a diameter of 0.5 mm and a length of 300 mm and with rounded ends (Nr. 47006045, EPflex GmbH).
2. Gold coating of the wire tip: A 2 cm long stretch at the tip of the medical wire is coated by galvanisation or nanostructured with a 0.5 – 1 µm layer of gold (Au).
3. Hydrogel (Xantec) HC 200 M, consisting of a polycarboxylate with a thickness of 1 µm and a porosity of 200 m in the case of a plain gold surface, or in the nanostructured cases it is passivated with PEG2000-Urea-silane solution
4. Fully human Fab-antibody (MorphoSys) or murine MEM/G9 antibody targeted against the human HLA-G antigen; endotoxin value ≤ 0.5 EU/ml, purity ≥ 95 %.
5. Ethanolamine hydrochloride (Sigma, E6133) in water, pH 8.5; to block remaining carboxyl groups on the hydrogel.
6. IN Stopper (Sarstedt AG & Co., product no. 74.4312)
7. Closure combi (Sarstedt AG & Co., product no. 74.4311)

5.8.2 Relevant inspections

To assess the biocompatibility of the components mentioned in the preceding chapter the following tests are necessary: Cytotoxicity test according to EN ISO 10993-5, test for Acute systemic toxicity according to EN ISO 10944-11 and Hemocompatibility test based on EN ISO 10993-4. Further tests of the biocompatibility of the medical product are not considered.

5.8.3 Cytotoxicity test

The medical product comes into contact with cells from the organism during the application. To assess a possible effect of the product on cells the cytotoxicity test is performed. The appropriate test according to EN ISO 10993-5 was adapted to the conditions of the application of the nanodetector to improve its expressiveness.

Cell culture methods are good models to analyse the effect of unspecific toxicity. The goal of this *in vitro* test is the determination of any cytotoxicity potential of all single components used on the final product and of the complete product. Therefore, an elution test will be used. Different elution tests were performed with materials with direct contact to cells:

- Qualitative elution test: Microscopic analysis, change of morphology, adherence and cytolysis
- Quantitative elution test: Determination of the vitality and metabolic activity. Differently treated cells will be incubated with tetrazolium.

The standard test examines the effect of the product on murine fibroblasts. To improve the reliability of the test for the nanodetector, human fibroblasts were used as test subjects instead of murine cells. Human primary NHDF (C-12302) cells were directly treated with the eluate of the test catheter for 48 hours. Eluates of reference materials known to be

toxic (positive control) and non-toxic (negative control) were tested in parallel to the eluate of the test catheter.

The sample meets the requirements of the test if the response to the sample preparation is not greater than grade 2 (mildly reactive; see Table 5). The cell culture test system is suitable if the observed responses to the negative control preparation are of grade 0 (no reactivity) and to the positive control preparation at least grade 3 (moderate reactivity).

A total of three different tests were used to assess the cytotoxicity of the nanodetector in the *in vitro*-test. The following tests were performed with human fibroblasts:

- the cells were treated with high antibody concentrations
- the cells were treated with nanodetectors with and without PEG
- the cells were treated with eluates of the nanodetector

If the in parallel to the nanodetector tested reference materials have met the acceptance criteria of the negative and positive control, it can in principle be assumed to be an appropriate test design. The assessment of cultures and the evaluation of cytotoxicity were carried out in the following categories: morphology, adhesion and cell lysis of the tested fibroblasts.

Table 5 Reactivity Grades for the Elution Test

Grade	Reactivity	Conditions of all Cultures	% Vitality
0	None	Discrete intra-cytoplasmic granules; no cell lysis	95 – 100
1	Slight	Not more than 20 % of the cells are rounded, loosely attached, and without intracytoplasmic granules; occasionally lysed cells are present	80 – 95
2	Mild	Not more than 50 % of the cells are rounded and devoid of intracytoplasmic granules; no extensive cell lysis and empty areas between cells	50 – 80
3	Moderate	Not more than 70 % of the cell layers contain rounded cells or lysed cells	30 – 50
4	Severe	Nearly complete destruction of the cell layers	0 – 30

The sample of the test item meets the requirements of the study, when the reaction of the sample preparation has not exceeded a value of 2 (mild reactivity).

5.8.3.1 Morphological assessment of the human fibroblast cell line NHDF-c after incubation with the Fab nanodetector without hydrogel.

In this experiment, the cytotoxicity of the nanodetector is determined through assessment of the morphology of cells on the wires after 24 h of incubation of human fibroblast cell line NHDF-c. This test conforms to ISO standard 10993-5 for the biological evaluation of medical devices. A total of eight wires were examined with different coatings. In each case, four wires were passivated with PEG2000-Urea-silane and four others, which contained no PEG were used. Of these wires, two control wires with the antibody anti-human HLA-G F(ab) were, however, incubated in PBS.

Human fibroblasts (NHDF-c) were released with trypsin / EDTA from the culture flask, centrifuged at 220 x g for 7 minutes and concentrated to 200,000 cells per milliliter with FGM2 medium (fibroblast growth medium 2; PromoCell). The wires were sterile to a length of about 3-4 cm. They were cut and placed in a 6-well plate. Each 300 µL of cell suspension were seeded on the wires and then incubated for 24 hours in an incubator. After incubation, cells were stained with 10 microliters of the vital dye CFSE in PBS/0.1% BSA solution for 10 minutes in the incubator. The staining was stopped with cold PBS/10% FCS. The cells were gently washed with warm PBS and examined under the fluorescence microscope (Zeiss Axio Imager, green fluorescence).

5.8.4 Acute systemic toxicity

The purpose of this animal study was the evaluation of acute systemic toxicity for the nanodetector and its bound antibody. All relevant procedures were performed in accordance with ISO 10993. Due to the fact that the medical product is to be applied to pregnant women, the animal trials were performed in two steps. (see chapter 4.2)

5.8.4.1 Substances and devices

The anti-HLA-G antibody (BIOZOL, Germany, clone MEM-G/9) was used for injection into the peritoneal cavity of the test animals. The stock solution of the antibody was obtained at a concentration of 1 mg/ml in PBS with 15 mM sodium azide. The test substance was diluted to its final concentration (0.1 ng/ml; 0.2 ng/ml and 0.5 ng/ml) using 0.9 % NaCl.

The gold nanostructures nanodetector were coated with a monoclonal antibody against the human cell surface antigen HLA-G. The antibody coating was established up to a constant value of 1.5 ± 0.75 ng.

5.8.4.2 Laboratory test

For all rats from each group the following hematological tests, biochemical tests and urine analyses were performed in the Central Laboratory of the Gynaecology-Obstetrics University Hospital, Poznan, Poland – (The International Certification Network – Certificate IQNet and PCBC, Registration Number PL – 779/5/2007; PN-EN ISO 9001:2001; validity date: 23.09.2010; RIQAS – Certificate of Participation Immunoassay, Haematology, General Clinical Chemistry Programme):

- Body and organ weights were recorded.
- Biochemical tests included determinations of: interleukin 6 (IL-6), interleukin 10 (IL-10) and tumor necrosis factor (TNF-alpha).
- The following hematological tests were performed: hematocrit (HCT), hemoglobin (HGB), mean corpuscular hemoglobin (MCH), mean corpuscular hemoglobin concentration (MCHC), mean corpuscular volume (MCV), platelet hematocrit (PCT), platelet count (PLT), red blood cells (RBC), red blood cells distribution width (RDW), white blood cells (WBC).
- In selected animals the standard urine analysis was performed: bilirubin, glucose, ketone, nitrate, pH, protein, red blood cells, specific gravity, urobilinogen and white blood cells.
- The stock solution of the antibody was obtained at a concentration of 1 mg/ml in PBS with 15 mM of sodium azide. The test substance was diluted to its final concentration using 0.9 % NaCl.

5.8.4.3 Rational for dose selection

The dose is calculated in relation to the amount of antibodies, which covers the catheter and the weight of the rat. This is done purposely to test the reaction of the organism

to the antibody, which could be shed in a theoretical situation from the surface of the nanostructure of the catheter, according to ISO-10993-11, within the framework of the acute systemic toxicity test.

For this purpose, the antibody was injected in three different doses (0.05 ng, 0.1 ng and 0.25 ng). The actual amount of antibody on the nanodetector is around 1.5 ± 0.75 ng. The corresponding total dose in humans would be 15.31 ng, which is at least 10 times higher than that on the nanodetector (see Figure 16).

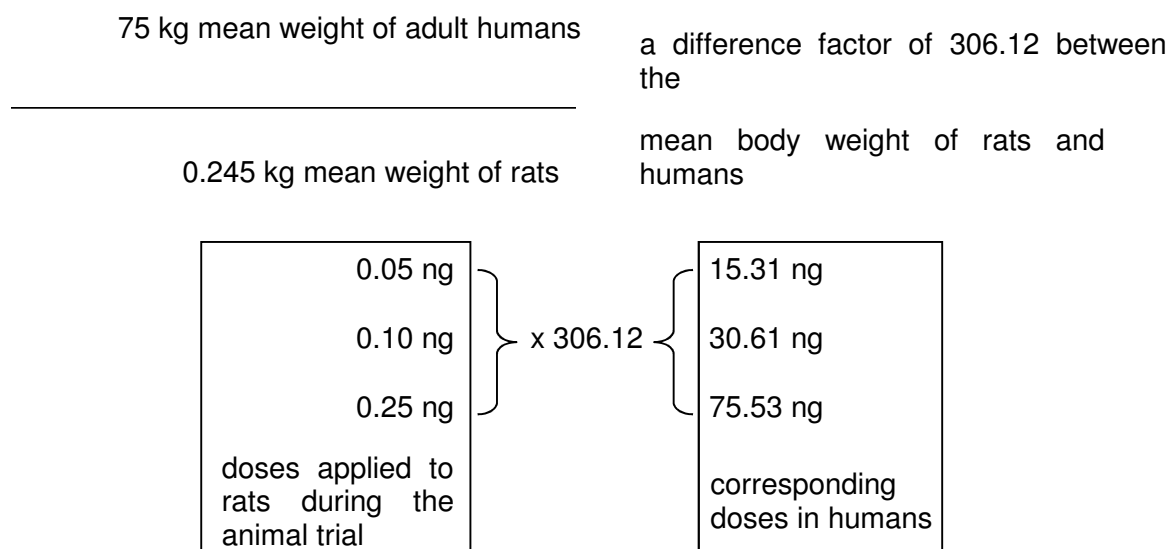


Figure 16 Calculation of the amount of antibodies for the compatibility test in rats based on the differences between the body weights.

5.8.5 Autopsy and organ weight

During the autopsy, selected organs (kidney, lung, liver, spleen) were collected, and after drying them in filter paper, they were weighed. Additionally, in the case of the pregnant rats the placentas and fetuses were weighed.

For all rats from each group the hematological tests, biochemical tests and urine analyses were performed. The whole blood was collected from the heart of the rat, causing the animal's death. Urine was taken out of the bladder.

The performed tests are listed in Table 6.

Table 6 The hematological and biochemical tests and urine analyses performed in studied rats.

Hematological test	Biochemical test	Urine analysis
Hematocrit	Interleukin 6	Bilirubin
Hemoglobin	Interleukin 10	Glucose
Mean corpuscular hemoglobin	Tumour necrosis factor alpha	Ketone
Mean corpuscular hemoglobin concentration		Nitrate
Mean corpuscular volume		pH
Platelet hematocrit		Protein
Platelet count		Red blood cells
Red blood cells		Specific gravity
Red blood cells distribution width		Urobilinogen
White blood cells		White blood cells

5.8.6 Hemocompatibility

Blood represents one of the most complex biochemical systems in living organism, and its various components play integral roles in several life functions, including the transport of oxygen, destruction of invading pathogens, and repair of damaged tissue. Because these functions are critical, medical devices that contact blood during routine use must be hemocompatible. That is, they must not adversely interact with any blood components so as to cause their inappropriate activation or even destruction.

Blood is composed of a multitude of cell types, ranging from simple oxygen-carrying erythrocytes to sophisticated antigen-specific lymphocytes. The various cells participate in a vast array of functions. Because of the range and criticality of these functions, any source of cytotoxicity to blood cells can cause significant harm. For example, hemolysis—a breakdown of red blood cells, which can be material mediated or result from mechanical damage—directly impairs the ability of the circulatory system to carry oxygen to body tissues. Likewise, adverse interactions with white blood cells can impair the body's ability to eliminate invading pathogens efficiently. Blood also contains several soluble multicomponent protein systems that systematically interact in various ways to perform critical functions. For example, the complement system participates in inflammatory reactions and facilitates removal of invading pathogens. The clotting cascade operates to initiate coagulation, thereby preventing excessive loss of fluid and facilitating tissue repair. Inhibition of either of these cascade systems can have significant adverse effects on the body.

The ISO 10993-4 provides general requirements for evaluating the interactions of medical devices with blood. It describes

- a. a classification of medical and dental devices that are intended for use in contact with blood, based on the intended use and duration of contact as defined in ISO 10993-1,
- b. the fundamental principles governing the evaluation of the interaction of devices with blood,
- c. the rationale for structured selection of tests according to specific categories, together with the principles and scientific basis of these tests.

Blood interactions can be classified into five categories based on the primary process or system being measured.

Table 7 shows examples of devices which contact circulating blood and the categories of testing appropriate to the device.

Table 7 Devices or device components with contact to circulating blood and the categories for appropriate testing – External communicating device.

Device examples	Test category				
	Thrombosis	Coagulation	Platelets	Haematology	Complement system
Atherectomy devices				x ^a	
Blood monitors	x			x ^a	
Blood storage and administration equipment, blood collection devices, extension sets		x	x	x ^a	
Extracorporeal membrane oxygenator systems, haemodialysis/haemofiltration equipment, percutaneous circulatory support devices	x	x	x	x	x
Catheters, guidewires, intravascular endoscopes, intravascular ultrasound, laser systems, retrograde coronary perfusion catheters,	x	x		x ^a	
Cell savers		x	x	x ^a	
Devices for absorption of specific substances from blood		x	x	x	x
Donor and therapeutic apheresis equipment		x	x	x	x

^a Haemolysis testing only.

The nanodetector is comparable to a guide wire, so it should be tested for thrombosis, coagulation and hemolysis.

The objective of this *in vitro* study was the assessment of the thrombosis, coagulation and haemolysis potential of the test item. A modified test method was developed as being described in the ISO Guideline 10993-4:2002 (E) (see Table 8) and according to the paper by Xu et al.[81]

Table 8 Test categories, evaluation method for the necessary hemotests

Test category	Evaluation method	Comments
Thrombosis	Percent occlusion	Same as a guide wire
	Flow reduction	Same as a guide wire
	Gravimetric analysis (thrombus mass)	Same as a guide wire
	Light microscopy (adhered platelets, leukocytes, aggregates, erythrocytes, fibrin, etc.)	See Thrombosis
	Pressure drop across device	Same as a guide wire
	Labelled antibodies to thrombotic components	done
	Scanning EM (platelet adhesion and aggregation, platelet and leukocyte morphology, fibrin)	See staining for fibrin, platelet adhesion
Coagulation	PTT (non activated)	See chapter coagulation
	Thrombin generation: Specific coagulation factor assays; FPA, D-dimer, F ₁₊₂ , TAT	See chapter specific coagulation factor
Platelets	Platelet count	Not required -
	Platelet	Not required -
	Template bleeding time	Not required
	Platelet function analysis	Not required
	PF-4, β -TG; thromboxane B2	Not required
	Platelet activation markers	Not required
	Platelet microparticles	Not required
	Gamma imaging of radiolabelled platelets, ¹¹¹ In-labelled platelets survival	Not required
Hematology	Leukocyte count with or without differentiation	Not required
	Leukocyte activation	Not required
	Hemolysis	See Hemolysis
	Reticulocyte count, activation-specific release products of peripheral blood cells (i.e. granulocytes)	Not required

To check the hemocompatibility of the product several tests were made:

- Thrombosis: Inspection under light and fluorescence microscope, Scanning SEM for platelets adhesion and aggregation, Staining for fibrin
- Coagulation: Plasma Recalcification Time (PRT), D-Dimer, PTT, Quick
- Hematology: hemolysis – flow system

5.8.6.1 Thrombosis

Antibody and hydrogel (Xantec) covered gold wires will be incubated in human blood for 30 min by employing a flow system. Gold covered stainless steel wires were also included for comparison. After the exposure to the blood all the samples were covered with a thin layer of gold and then characterized by the scanning electron microscopy (SEM) technique in order to find out if any adsorption of blood components took place during the incubation in blood. In the SEM technique an electron beam is scanning across a sample's surface. When the electrons strike the sample, a variety of signals is generated, and it is the detection of specific signals which produces an image or a sample's elemental composition. In the experiments the in-lens detector which collects the "secondary electrons" signal was employed. This is by far the most common type of image produced by SEMs. It is most useful for examining surface structures and gives the best resolution image of any of the scanning signals. The following SEM was used: SEM (Zeiss) LEO 32 microscope (magnification 800x 40x20). The adsorption of blood components on the surfaces of hydrogel (Xantec) covered gold wires will be followed by SEM. The samples will be incubated for 30 min with human blood employing a flow system.

5.8.6.1.1 Materials

- Nanodetector plain gold covered with a hydrogel (Xantec) and with the F(ab) AbD10521.3 antibody
- Gold wire
- Human EDTA-blood, (fresh < 4 hours)
- F(ab) antibody AbD10521.3, concentration 50 µg/ml in Na-acetate buffer (5 mM, pH 5)
- Ethanolamine-Hydrochloride (Sigma, Lot. 15331JH)
- N-hydroxy-succinimid (NHS) (Sigma-Aldrich)
- 1-Ethyl-3-(3-dimethylaminopropyl)carbodiimid (EDC) (Fluka)
- 2-(N-morpholino)ethanesulfonsäure (MES) (Sigma)
- Ultrapure water

5.8.6.1.2 Complete description of handling

- Gold wires are cleaned with acetone, ethanol and activated with oxygen plasma (150 W, 3 min).
- Hydrogel (Xantec) covered gold wires are immersed into pure H₂O for 15 min
- Activation step for the hydrogel (Xantec) on the nanodetector: EDC/NHS (100 mM NHS+0,5 EDC (w/v) in MES, pH 5.3)

- 1x wash with acetic acid, 100 %
- Incubation of all samples with F(ab) AbD10521.3, 1 h at room temperature
- 3x washing steps with pure H₂O
- Blocking step: 1 M ethanolamine, pH 8.5, 30 min at room temperature
- 3x washing steps with pure H₂O
- Incubation with blood, flow system, 30 min
- 3x washing steps with pure H₂O
- Following steps after washing are as follows:
 - Drying on air and storage at 4 °C over night
 - Evaporation of an gold layer (~10 nm) on the next day
 - Analysis of the wire's surface

5.8.6.1.3 Details of samples

# Sample	Test device	Description of the sample
1	Negative control	Hydrogel covered nanodetector + Fab
2	Test device 1	Hydrogel covered nanodetector + Fab + blood
3	Test device 2	Hydrogel covered nanodetector + Fab + blood
4	Positive control	Nanodetector + Fab + blood

5.8.6.1.4 Categories for the estimation of the amounts of organic human debris

The adsorption of blood components will be evaluated from the SEM images. The following main points are essential to the evaluation of the blood-component adsorption:

Analysis:

- Analysis of the complete area which is in contact with human blood during the application in a human vein (2,5 cm length); different areas will be analyzed
- The magnification is variable (from 100 – 800x)
- Documentation of images

Criteria:

- Organic human material (like carbon) will consist of dark spots or dark areas
- The golden EPflex wire with hydrogel consists of light grey areas
- The amounts of organic human debris are estimated according to the following categories (Figure 17):

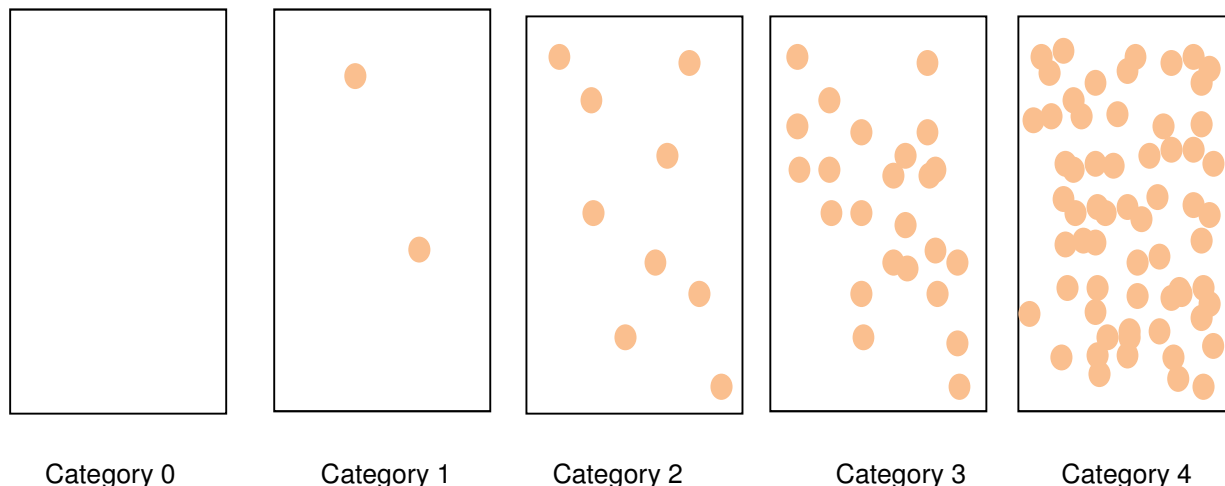


Figure 17 Categories of adhesion and aggregation : Category 0 – No adhesion; Category 1 – single, no bridging; Category 2 – multiple, no bridging points; Category 3 – multiple, single bridging points; Category 4 – multiple and many bridging points or confluent

The sample meets the requirement of the test if the adhesion to the sample is not greater than category 2.

5.8.6.2 Staining for fibrin

Coagulation is a complex process by which clots are formed. It is an important part of hemostasis (the cessation of blood loss from a damaged vessel), wherein a damaged blood vessel wall is covered by a platelet and fibrin - thrombus to stop bleeding and to begin repair of the damaged vessel. Disorders of coagulation can lead to an increased risk of bleeding (hemorrhage) or clotting (thrombosis). Coagulation begins instantly after an injury to the blood vessel where the endothelium was damaged and collagen from basement membranes is exposed. Platelets immediately form a plug at the site of injury; Proteins in the blood plasma, called *coagulation factors* or *clotting factors*, respond in a complex cascade to form fibrin strands, which strengthen the platelet plug. The goal is to check for fibrin strands.

To look for coagulation especially for fibrin the wires were stained after incubation in the flow system with blood with an anti-fibrin antibody. Subsequently the wires were stained with the secondary anti-mouse antibody. The fluorescence was measured under a fluorescence microscope. (Zeiss Microscope Axio Imager)

5.8.6.2.1 Materials

- 1,5 ml reaction tubes (VWR)
- Parafilm M (Brandt)
- Nanodetector plain gold covered with a hydrogel (Xantec) and with the F(ab) AbD10521.3 antibody
- Glas slides

- Anti-fibrin antibody (Santa Cruz)
- Donkey-anti-mouse-FITC-antibody (Jackson Immuno Research)

5.8.6.3 Platelet adhesion

Platelets play a central role in normal hemostasis. When circulating, they are membrane-bound smooth discs expressing a number of glycoprotein receptors of the integrin family on their surfaces. In case of hemostasis platelets will adhere and become activated, undergoing a shape change and releasing secretory granules. Within minutes the secreted products have recruited additional platelets to form a hemostatic plug; this is the process of primary hemostasis. The aim of the test is to look for platelet adhesion as a first step of hemostasis. Fresh blood from healthy human beings was mixed immediately with a 3.8% solution of sodium citrate at a dilution ratio of 9:1. The blood was centrifuged at 700 rpm and 8 °C for 10 min to obtain the platelet-rich plasma (PRP). The PRP was diluted in a 1:1 ratio. Then, 0.1 ml of the diluted PRP was introduced onto the FSWM. The FSWM was incubated at 37 °C for 30 min at static conditions. The adhered platelets were fixed. Under a microscope the platelet adhesion were analysed.

5.8.6.3.1 Materials

- Electronical Balance - Radwag WAA 60/C/01
- Centrifuge – Jouan
- Microscope – Olympus BX 41
- Pipettes – HTL (200 µl, 1000 µl)
- Glass tubes (300 µl)
- Pipettes- Corning (15 ml)
- Eppendorf pipettes (2 ml)
- Pasteur pipettes (5 ml)
- Glass slides for mounting a wire
- Parafilm
- Platelet-rich plasma (PRP) obtained from human blood
- 3,8 % solution of sodium citrate at a dilution ratio 9:1 used as an anti-coagulant
- PBS to dilute PRP in a 1:1 ratio and to wash the wire after incubation
- 2% aqueous solution of glutaraldehyde for fixing platelets
- Water to wash the wire and remove glutaraldehyde
- Ethanol to wash the wire

5.8.6.3.2 Complete description of handling

- 1) Mix fresh blood with a 3,8 % wt solution of sodium citrate at a dilution ratio of 9:1 (blood:sodium citrate solution).
- 2) Centrifugation of blood at 700 rpm and 8 °C for 10 min to obtain PRP.
- 3) Dilute PRP with PBS in a 1:1 (v/v) ratio.
- 4) Incubate wires in dilution of PRP in PBS for 30 min, at 37 °C under static conditions.
- 5) Wash wires 3x with PBS.
- 6) Fix adhered platelets with a 2,0 vol % aqueous solution of glutaraldehyde for 12 h at 4 °C.
- 7) Wash wires in succession with PBS, water and ethanol.
- 8) Dry wires on air.

9) Evaluate wires under microscope.

5.8.6.3.3 Samples and Control

Sample 1 – platelet-rich plasma diluted with PBS, ratio 1:1 (nanodetector)

Sample 2 - platelet-rich plasma diluted with PBS, ratio 1:1 (nanodetector)

Sample 3 – platelet-rich plasma diluted with PBS, ratio 1:1 (stainless steel)

Sample 4 – platelet-rich plasma diluted with PBS, ratio 1:1 (stainless steel)

Sample 5 – platelet-rich plasma diluted with PBS, ratio 1:1 (glass pipette)

Sample 6 - platelet-rich plasma diluted with PBS, ratio 1:1 (glass slide).

Glass pipettes and glass slides were used as controls.

5.8.6.4 Coagulation

5.8.6.4.1 Test of Plasma Recalcification Time

The plasma recalcification test is an ideal screening procedure by which to evaluate the total coagulation mechanism. It assesses all plasma coagulation factors except for factor IV (ionized calcium) and it is sensitive to quantitative and qualitative changes in platelets. The aim is to check whether clotting is occurring and in the range of 44 s (human norm). Fresh blood from healthy human beings was mixed immediately with 3.8 % solution of sodium citrate at a dilution ratio of 9:1. It was then centrifuged at 3000 rpm and 8 °C for 20 min to obtain the platelet-poor plasma (PPP). About 0.1 ml of the PPP was introduced onto the surface and incubated at 37 °C under static conditions for 10 min. The plasma solution was monitored for clotting by manual dipping the nanodetector hook. The clotting time was recorded at the first sign of fibrin formation on the hook.

5.8.6.4.2 Materials

Centrifuge – Radwag WAA 60/C/01

Microscope – Olympus BX41

Pipettes – HTL (200µl, 1000µl)

Glass tubes - Corning (15ml)

Glass slides to fix the wire.

Platelet-poor plasma (PPP) obtained from human blood (3.8% solution of sodium citrate at a dilution ratio of 9:1 used as an anti-coagulant)

0.025 M aqueous solution of CaCl₂ – Sigma-Aldrich.

Number of samples and repeats

n = 7 (7 different surface combinations for the F(ab) and MEM-G/9)

r = 2 for stainless steel/plastic and 3 for hydrogel/plastic

5.8.6.4.3 Samples and Control

Sample 1 – scratched glass / stainless steel, F(ab) and MEM-G/9

Sample 2 – plain glass / stainless steel, F(ab) and MEM-G/9

Sample 3 – plain glass / glass, F(ab) and MEM-G/9

Sample 4 – plastic / plastic, F(ab) and MEM-G/9

Sample 5 – plastic / stainless steel F(ab) and MEM-G/9

Sample 6 – plastic / nanodetector + PEG, F(ab) and MEM-G/9

Sample 7 – plastic / hydrogel, F(ab) and MEM-G/9

All combinations with glass incubated in PPP were used as controls.

5.8.6.4.4 Complete description of handling

- 1) Mix fresh blood with 3,8% solution of sodium citrate at a dilution ratio of 9:1 (blood:sodium citrate solution)
- 2) Centrifugation of blood at 3000 rpm and 8°C for 20min to obtain PPP
- 3) Incubate wires in PPP at 37°C for 10 min under static condition
- 4) Add the same amount of a 0.025 M aqueous solution of CaCl₂ (37°C)
- 5) Monitor plasma solution for clotting by manually touching and separating two wires covered with the same antibody
- 6) Detection of fibrin threads and recording the time of clotting at the first sign of fibrin formation.

5.8.6.5 Test for specific coagulation factors

Coagulation factor levels are determined, because low levels of the factors are associated with reduced clot formation and bleeding, or because high levels are sometimes associated with too much clot formation and thrombosis. To prove that there is no interaction of the medical product and the coagulation cascade we tested several coagulation factors. The INR is the ratio of a patient's prothrombin time to a normal (control) sample, raised to the power of the ISI value for the analytical system used.

Therefore, 5 ml of citrate blood are given into the flow system. The nanodetector was incubated in the flow system (with a peristaltic pump) for 30 min with a flow rate of 20 ml/min in blood (37 °C). Then, D-dimer, Quick, INR and PTT were determined. In addition, controls were analyzed (without nanodetector and without flow system).

5.8.6.5.1 Materials

- Blood of a healthy donor (blood with citrate, fresh < 4 h)
- Nanodetector
- Glowes (powder free, VWR International, Latex: Art.-Nr. 112-1525; Nitrile: Art.-Nr. 112-2372)

5.8.6.5.2 Samples and controls

sample1: Citrate-blood, without flow system and without nanodetector

sample 2: Citrate-blood, with flow system and with nanodetector

5.8.6.6 Test for hemolysis

The flow of blood through implants of non-physiological character is always accompanied by the release of free hemoglobin from erythrocytes into the plasma. This phenomenon seems not to be related to osmotic hemolysis, and is affected in a complex way by the fluid shear forces and the nature of material contacting the blood.[82, 83] 5 ml EDTA blood are added into the flow system. Additionally, a nanodetector coated with antibodies is put into the flow system. The blood was incubated for 30 minutes at 37 °C with a flow rate of 20 ml/min. Then all of the blood is collected for analysis of laboratory parameters.

5.8.6.6.1 Samples and controls

n = 3

repeats = 3

sample 1 EDTA-blood, without flow system and without nanodetector

sample 2 EDTA-blood, with flow system and without nanodetector

sample 3 EDTA-blood, with flow system and with nanodetector

5.9 Intended medical application of the nanodetector including any necessary storage and handling requirements

5.9.1 Sterilization and packaging

All components are sterilized by steam sterilization before the assembly and the packaging take place using aseptic techniques to ensure the product's sterility.

The bio-functionalized sterile nanodetector is mounted in a closure combi with an IN stopper. Thereby the functional part of the medical device is protected. Additionally, the closure combi is filled with sterile PBS. Both products are already used in other medical applications and are certified. The nanodetector with the closure combi and IN stopper is placed in the package bag and closed.

An example of a label attached to the final product is shown in Figure 18 . The first 8 digits of the lot number are the production date. Any used product or waste material should be disposed of in accordance with local requirements. The complete packaged nanodetector is shown in Figure 19.

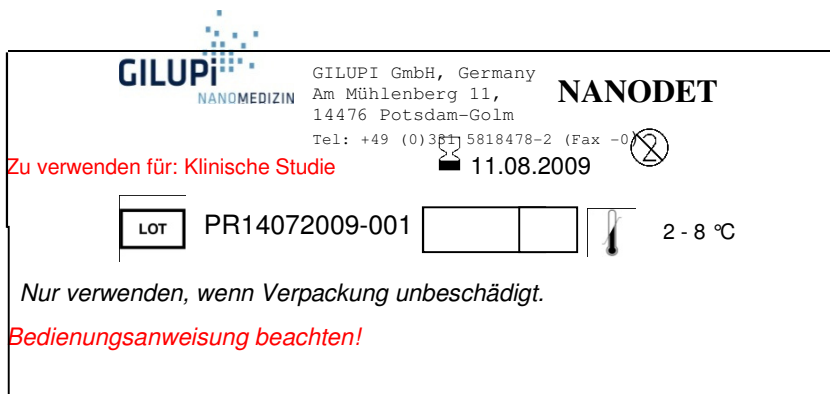


Figure 18 Label of the package



Figure 19 Package of the medical product.

Storage:

Refrigerated: 4 – 8 °C

Protect from direct light

The properly stored product should be used before the expiration date stated on the packaging.

5.9.2 Application and usage

The following materials need to be prepared before starting the procedure:

- 1x IN-Stopper (Sarstedt, already fixed on the wire),
- 1 x BD Venflon™ 18 GA 45 mm (BD 391453)
- Nanodetector (functionalized structured medical wire), see Figure 20.

a) 1 x BD Venflon™



b) Medical device (quantities 1)

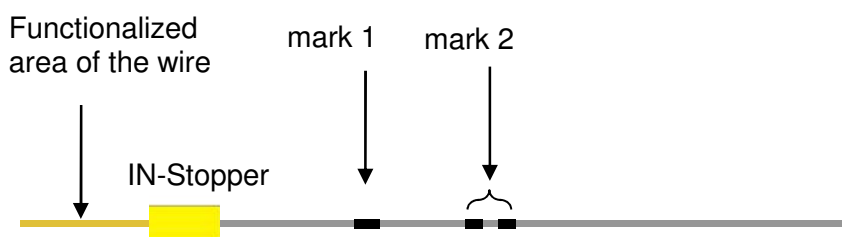


Figure 20 Material needed for the application of the medical wire.

In addition skin disinfection is needed in the area of puncture at the beginning of the procedure. A sterile wound dressing should be used to cover the site of puncture during the procedure. The area of puncture is cleaned and bandaged in the same way as for blood sampling.

The subject should be positioned in such a way that allows for the cubital joint (elbow) to remain stretched comfortably throughout the procedure. A sterile dressing is applied for the time of the procedure.

After disinfection of the puncture site and removal of the protective cap, a suitable vein should be punctured using the first 1 x BD Venflon™ 18 GA 45 mm (BD 391453) cannula and adhesive tape to fix the cannula to the skin. Before removing the steel needle the vein should be compressed at the tip of the catheter with the middle finger to prevent

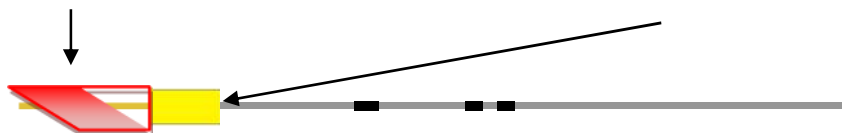
spillage of blood. At the same time the catheter hub should be stabilized with the index finger to prevent catheter displacement during needle removal. The needle should be removed by pulling it straight back and the needle should be disposed of immediately into sharps container.



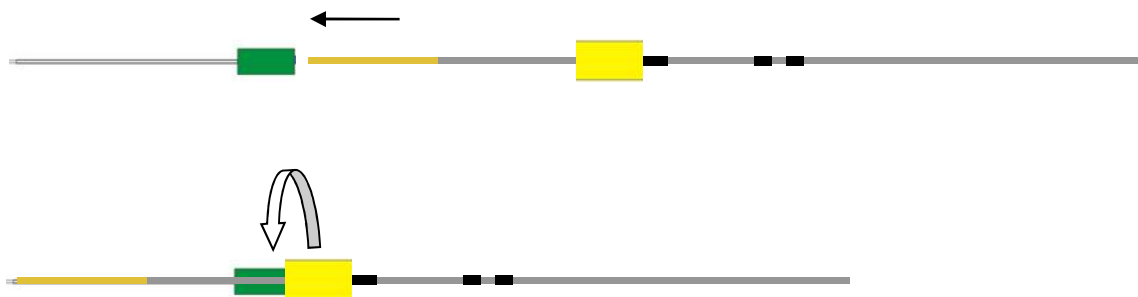
Unpacking the medical device:

- a) Secondary package (paper wrapping)
- b) Primary package

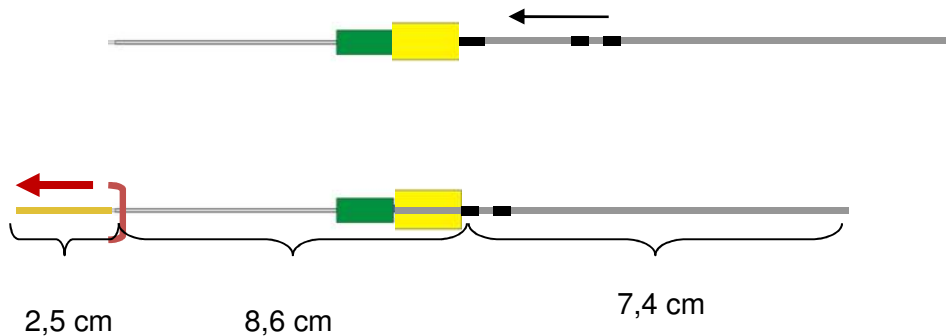
The red cap should be turned and removed.



The nanodetector should be carefully inserted into the cannula. The IN-Stopper is then screwed onto to the cannula.



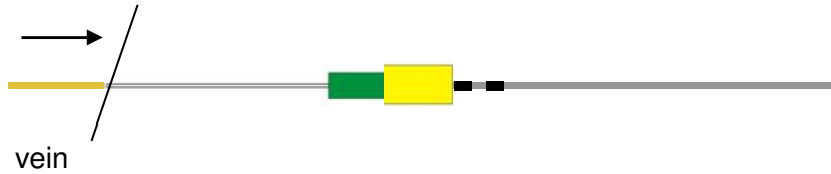
The nanodetector should be carefully pushed forward between the two bands of mark 2. Now the functionalized area is 2.5 cm deep in the vein. No force should be applied when inserting the wire into the vein.



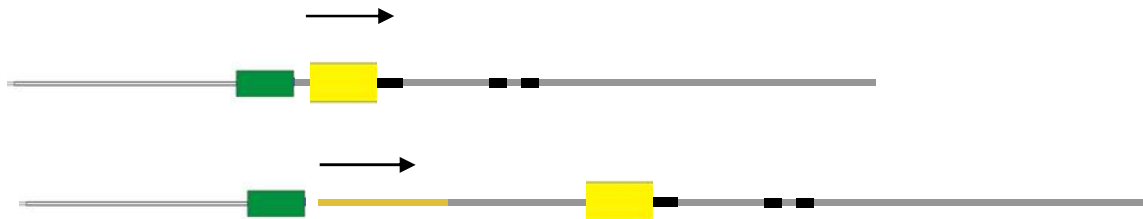
The wire should not be inserted farther than the 2nd band of mark 2. The nanodetector should be fixed with a bandage for 30 min.

After the application:

The wire should be pulled out from the vein carefully, but not further than the band of mark 1. Afterwards, the whole application system can be removed out of the vein. The handling was correct if the tip of the wire is protected by the Venflon cannula.



The IN stopper (Sarstedt AG & Co., product no. 74.4312) has to be turned and removed from the Venflon cannula.

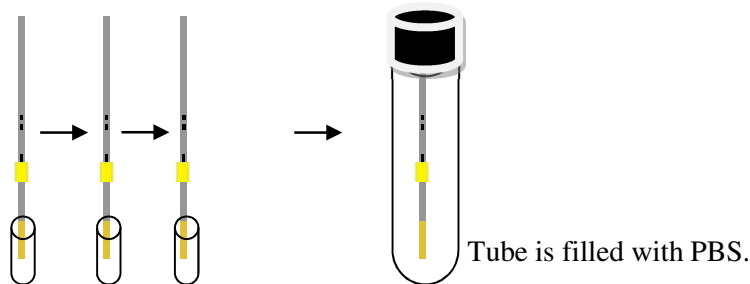


The needle is immediately disposed into sharps container.

Preparation for analysis

The wire is washed 3 x in PBS (consecutively using three different tubes and dipping the wire carefully into each solution two times, tubes 1, 2 and 3 with 2 ml PBS)

The nanodetector is transferred into the lab transport package (with PBS) and the lab transport package is closed. The tip should not touch the walls of the vessel (reaction tube).



The nanodetector should be transported to the investigating laboratory in a straight tube and on ice or at 4 °C.

5.10 Statistical analysis

The mean value and standard deviation were calculated for evaluated parameters. The differences in the distributions of the tested variables were evaluated by means of an analysis of variance (ANOVA). The mean values were compared applying the variance analysis and the Tukey post-hoc test.

6 Results

6.1 Horizontal approach with nanoisland

Different nanostructured Sam[®] 5 chips loaded with selective antibodies were introduced to increase the sensitivity for isolating vital cells. Size and shape of the nanoislands are determined by the diameter of polystyrene beads. Tested were polystyrene beads with a diameter from 200 to 2000 nm (GILUPI Patent). Evaporated Gold was precipitated by shadow nanosphere lithography [71]. Polystyrene beads with a diameter of 440 nm in hexagonal arrangement on SiO₂ surfaces of Sam[®] 5 chips were selected. The properties of the nanosphere lithography mask used to generate nanoislands resulted in triangular shaped spots (Figure 21). This was confirmed by AFM and SEM characterization. The nanopots were functionalized with antibodies.

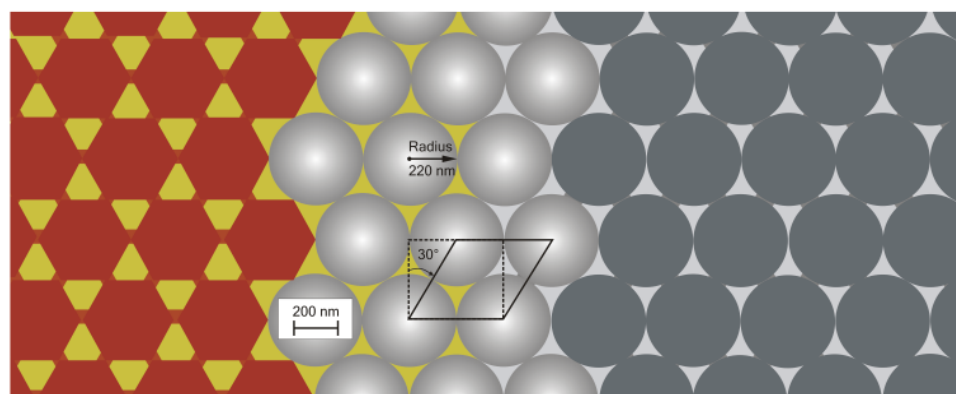


Figure 21 Schematic presentation of an AFM (left) and a SEM image (right) of the SiO₂ chip surface sputtered with nanopots. The drawn nanoparticles indicate their size and packing pattern. The area of one nanoisland is roughly 20,000 nm².

6.1.1 Amount of antibodies bound to nanostructured and complete gold surfaces

For comparison antibodies were coupled to Sam[®] 5 chips with a gold nanostructure or a complete gold surface.

Concluding from a variety of measurements, the nanoisland surface is saturated at an antibody concentration ≥ 500 ng/ml ($\Delta \varphi \sim 2.8^\circ$). By applying a SAM interface, the amount of antibody could be increased. (Table 9).

Table 9 Evaluation of phase shifts by antibody binding to Sam[®] 5 chips with nanostructures and with a complete gold surface, and with or without a SAM of 11-mercaptopundecanoic acid. The coverage was evaluated using the sensitivity factor and an assumed antibody size of 150 kDa.

Surface	SAM	Phase $\Delta\phi$	Coverage (ng/mm ²)
Nanostructure Islands	without	2.9±0.8	5.6±1.5
Nanostructure Islands	with	3.8±0.4	7.5±0.8
complete Gold surface	without	7.9±3.5	15.2±6.9
complete Gold surface	with	9.1±3.2	17.6±6.2

In all experiments, the nanoisland surface demonstrated reliable binding with relatively little variation from the mean and few outliers, in contradiction to the completely covered gold surface. With the recorded signals the antibody loading was calculated using the phase shifts, in order to compare the binding capacity of the different structures (Figure 22 und 23; Table 9). The calculated amount of bound antibody was between 2.3 - 2.7 times higher on the plain gold surface than on the nanostructured surface. The use of a SAM increased the amount of antibodies by 27% for the nanostructured surface, and by 15% for the plain gold surface. About 5.6 ng/mm² antibody was bound to the nanostructured chip surface, and 15.2 ng/mm² was bound to the completely covered gold surface..

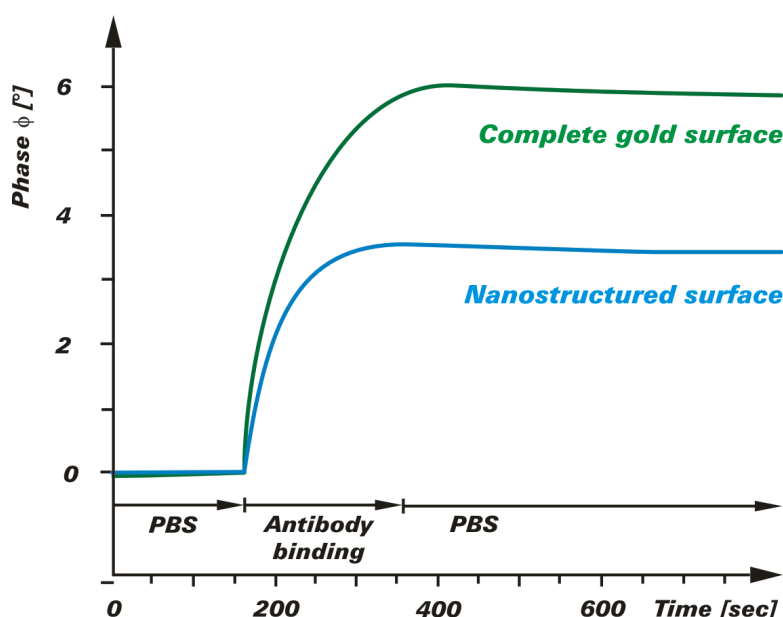


Figure 22 Phase shift documentation of the binding of antibodies by adsorption to Sam@-chip surfaces consisting of a complete gold layer (green line) or gold nano-islands (blue line).

6.1.2 Calculation of the number of antibodies per nanopot

Analyses of nanostructured surfaces revealed that about 8 μg of antibody can be bound to 1 cm² of the surface corresponding to 53 pmol. Based on the Avogadro constant of 6.022×10^{23} molecules per mole the calculated number of antibodies attaching to this area is 2.3×10^{10} . The number of nanoislands obtained by nanosphere lithography with polystyrene beads of a diameter of 440 nm for 1 cm² is 9×10^8 . Thus about 25 antibody molecules bind to each triangular nanoisland of about 20000 nm².

After determining the number of antibodies bound to the nanostructured surface it had to be shown that the antibodies were in a functional orientation and deposited in a density high enough for catching cells.

A model cell line – the human trophoblast line JEG-3 – was used to demonstrate that these requirements for binding cells to the surface by these antibodies were met. The nanostructured surface of a Sam® 5 chip was charged with anti-CD4 antibodies which detect a 59 kDa glycoprotein expressed on the surface of the JEG-3-cells but not on control cells, e.g. osteoblasts. Binding experiments with the chip were performed with 50, 500 and 5000 cells per ml. With an injection volume of 150 μ l only 7 – 8 cells were actually coming into contact with the antibody modified nanostructured surface of the chip at a concentration of 50 cells per ml (Figure 24).

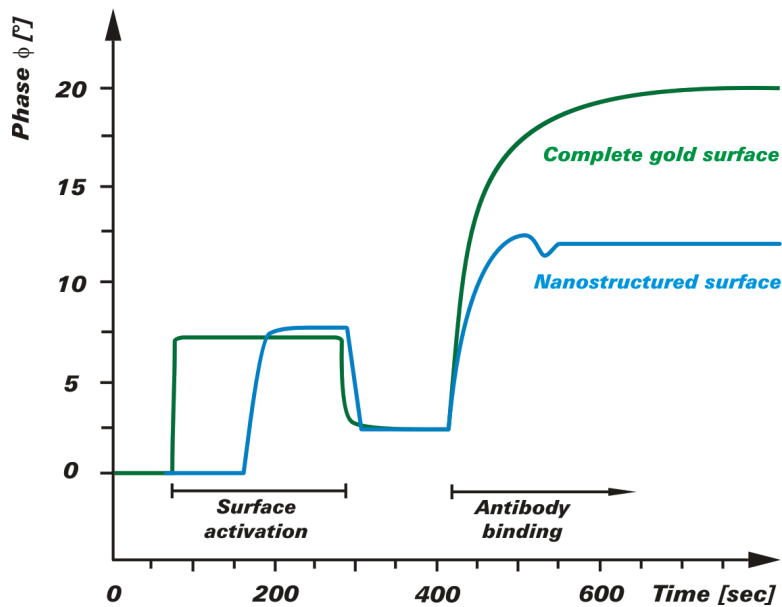


Figure 23 Phase shift documentation of the binding of antibodies by carbodiimide chemistry to Sam®-chip surfaces consisting of a complete gold layer (green line) or gold nano-islands (blue line).

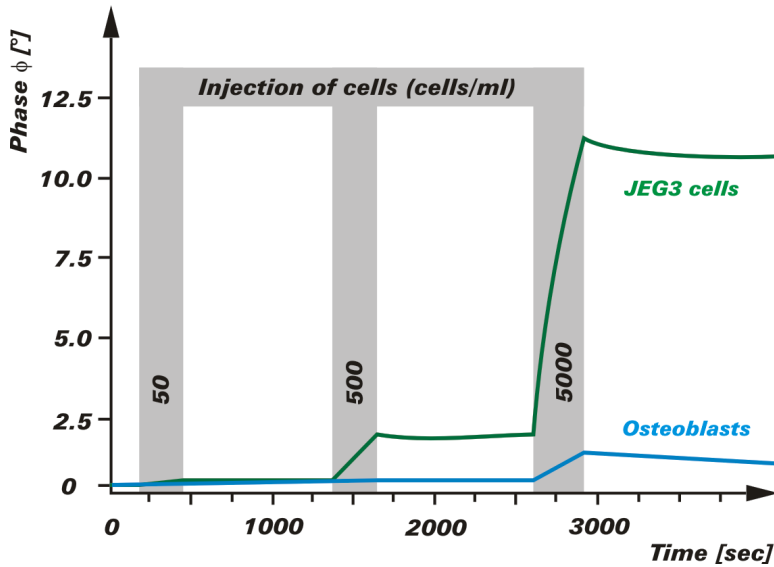


Figure 24 A nanostructured Sam® 5 sensor chip functionalized with anti-CD4 antibodies is selectively binding cells of the human JEG-3 cell line (green line) expressing the CD4 target antigen on their surface but not CD4-negative osteoblasts (blue line). The injection of antibodies resulted in a phase shift of 1.3° ($\sim 16.8 \text{ fmol/cm}^2$) while subsequent injections of 50, 500 or 5000 cells/ml gave additional phase shifts of 0.22° , 1.74° and 11.47° when JEG-3 cells were used and only 0.065° , 0.101° and 0.913° for osteoblast control cells.

In another set of cell binding experiments anti-HLA-G antibodies of two different designs were attached to the nanostructured chip to bind JEG-3 cells which express HLA-G on their plasma membrane. One of the antibodies – MEM/G9 – was a mouse monoclonal antibody while the other antibody was a recombinant human antibody fragment of the F(ab) type. Cell binding on chips functionalized by these two antibodies was compared with chips which carried a mixture of undefined IgG as reference. With low numbers of JEG-3 cells no significant differences in cell binding were observed between the two HLA-G-antibodies. At 5000 cells/ml the MEM/G9 loaded chip bound 43% more cells. One possible explanation is that MEM/G9 is a complete antibody with two binding sites and that due to its structure it is protruding from the chip surface while the F(ab) fragment is lying flat on the surface. Chips with the reference antibodies showed almost no cell binding. Results are shown in Figure 25.

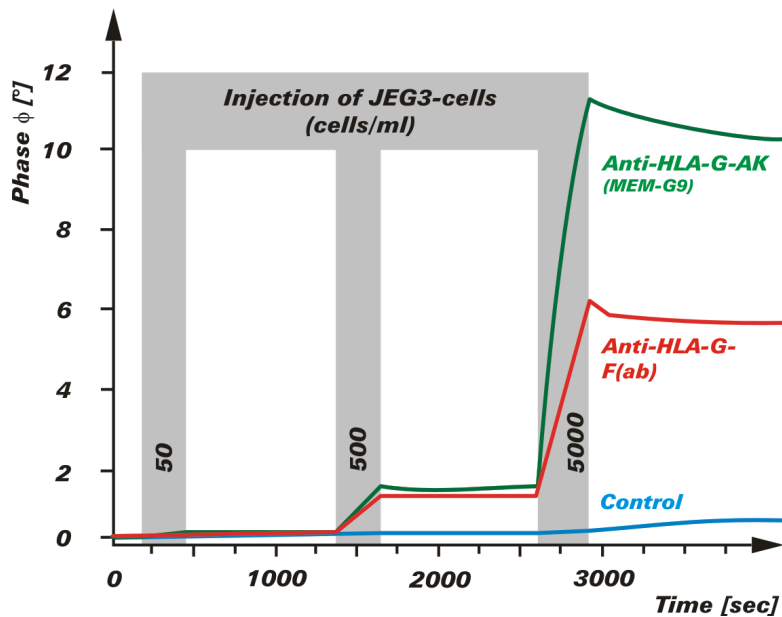


Figure 25 Binding of JEG-3 cells to nanostructured Sam® 5 sensor chips functionalized either with the complete mouse monoclonal anti-HLA-G antibody MEM/G9 (black line) or recombinant human anti-HLA-G antibody fragments of the F(ab) type (red line). The reference chips were covered with an undefined mixture of human IgG. The plots represent the average of five sensor experiments with a standard deviation of < 5%. The injections of 50, 500 or 5000 cells/ml resulted in additional cell binding related phase shifts of 0.18°, 1.69° and 11.47° when MEM/G9 was on the chips and of 0.15°, 1.84° and 6.53° in the case of the F(ab). With the reference chips phase shifts of only 0.05°, -0.14° and 0.07° (blue line) were recorded.

6.2 Vertical approach with different hydrogels adsorbed onto gold surface

Experiments were made to test the efficiency for cell capture of different hydrogels. In the first tests a hydrogel layer was passively adsorbed on polystyrene (PS) surfaces.

6.2.1 Hydrogels based on agarose and polyacrylic acid (PAA)

The carboxyl groups provided by the PAA were activated via EDC/NHS and then further functionalized with the MEMG/9 antibody. The capture of K562-G cells was tested in different media: PBS, 50% serum and blood. K562-A2 cells were included as a control cell line. Each one of the samples was incubated with a total concentration of K562-G cells equivalent to 5×10^5 cells while for the K562-A2 cells was the equivalent to $2,5 \times 10^5$ cells. The incubation with the cells was performed under static conditions (light shaking) for 30 min. The results of the first experiments are shown in Figure 26. From Figure 26 it can be observed that the number of K562-G cells captured in a PBS medium was high (~ 60 cells/mm²), however a comparable number of cells was also present on the sample with no antibody (sample 3—control). On the other hand, in blood and 50% serum the number of cells captured was negligible. Therefore this approach was further considered.

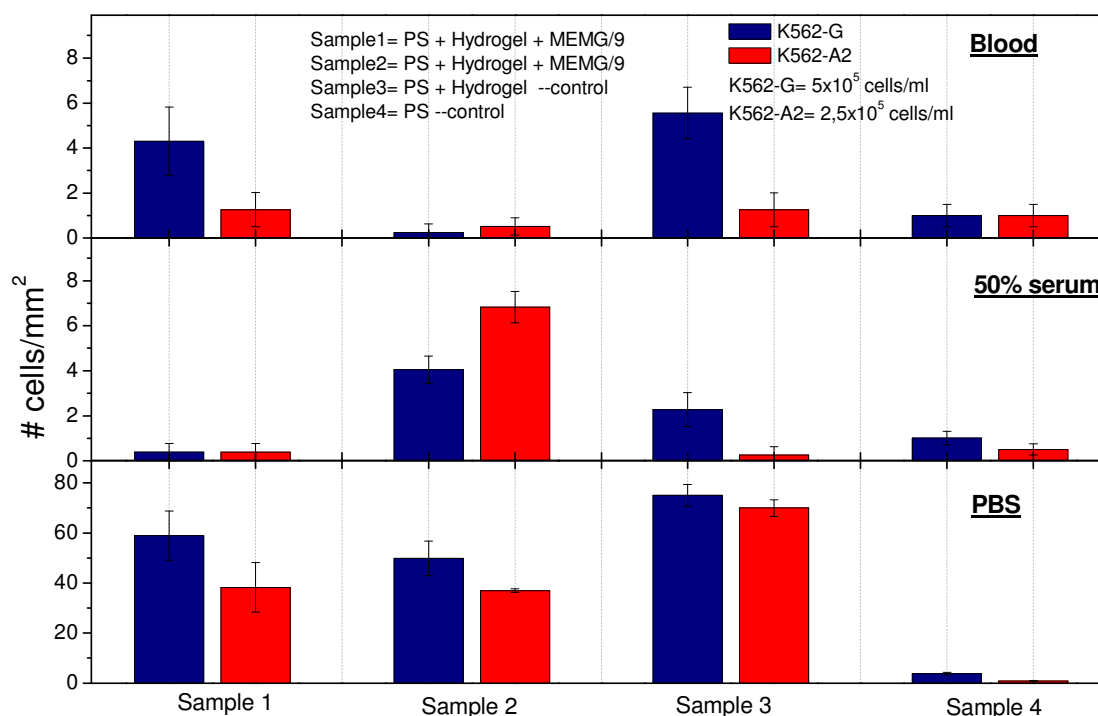


Figure 26 Number of cells captured on hydrogels based in agarose and PAA. A description of the samples is given in the upper inset. The media for the capture of cells were PBS, 50% serum and whole blood. The antibody MEMG/9 specific against HLA-G exposed on K562-G cells was employed while the K562-A2 cell line was used as a control.

6.2.2 Hydrogels based on polyethylene imine (PEI) and polyacrylic acid (PAA)

The principle for employing PEI is based on experiments with fibroblasts, where the gels based on PEI demonstrated to avoid non-specific adsorption. The PAA is employed for providing carboxyl groups. The interaction between PEI and PAA is mediated by hydrogen bonds. The hydrogel layer is passively adsorbed on polystyrene (PS) surfaces.

The following protocol is employed for the further functionalization of the hydrogels:

- COOH groups activated via EDC/NHS (400/100 mM),
- Test antibody anti-EpCAM (buffer: 5mM Na-acetate, pH 5) concentration 50 μ g/ml, incubation time 1h at room temperature.
- Blocking step: 1M ethanolamine, pH 8.5; 30 min at room temperature.
- Incubation in blood spiked with SKBr-3 and MDAMB cells; cell concentrations equivalent to 3×10^5 and $1,5 \times 10^5$ cells/ml, respectively. Incubation time 30 min.

Results in Figure 27 show that on average 17 SKBr-3 cells/mm² can be captured employing these hydrogels. On the reference sample (hydrogel with no antibody) a lower quantity of cells was obtained, 8 cells/mm². It is worth to notice that the number of non-specific cells adsorbed is insignificant even on the sample with no hydrogel.

It has also to be noticed that here the number of captured cells was increased at least 3 times in comparison with the results obtained employing agarose based hydrogels.

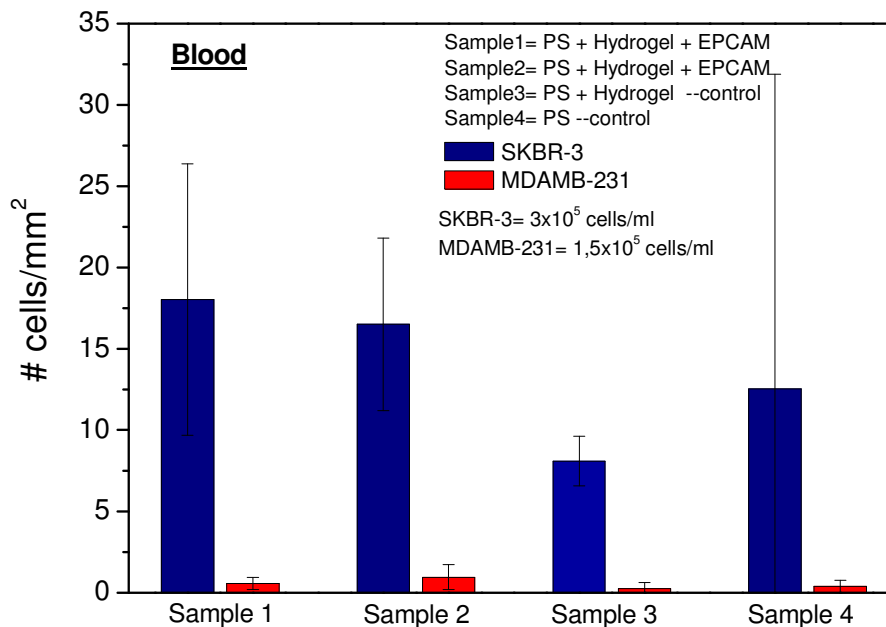


Figure 27 Results of the cell capture with hydrogels based on polyethylene imine and PAA. Incubation with the cells was performed in spiked blood. The hydrogels were functionalized with the anti-EpCAM antibody for capturing SKBr-3 cells, the cell line MDAMB-231 was used as control. The concentration of SKBr-3 cells was the equivalent to 3×10^5 cells/ml.

6.2.3 Concentration of carboxyl groups

The number of carboxyl groups present in the hydrogel was determined by reaction of the samples with the dye Basic Blue 12 (Nile Blue). The polystyrene surfaces with the hydrogel layers were immersed into a solution of 0.3 mg/ml basic blue dissolved in 100 mM MES, pH 6.0. The samples were rinsed in H₂O to get rid of the unbound dye molecules. Then, the bound Basic Blue on the hydrogel film was desorbed by incubation in 0.5 ml 30% acetic acid for 5 min. Absorption spectra were taken from the solution with acetic acid employed to remove the dye, for this purpose 3 samples were considered: a polystyrene sample covered with hydrogel, a bare polystyrene sample (reference) and the pure 30% acetic acid solution (to disregard any absorption in this spectral range). The absorption spectra are shown in Figure 28. The Basic Blue dye has a strong absorption peak at 638 nm. According to Beer's law an equivalent to $2,13 \times 10^{18}$ carboxyl groups/cm² is presented in these hydrogel layers.

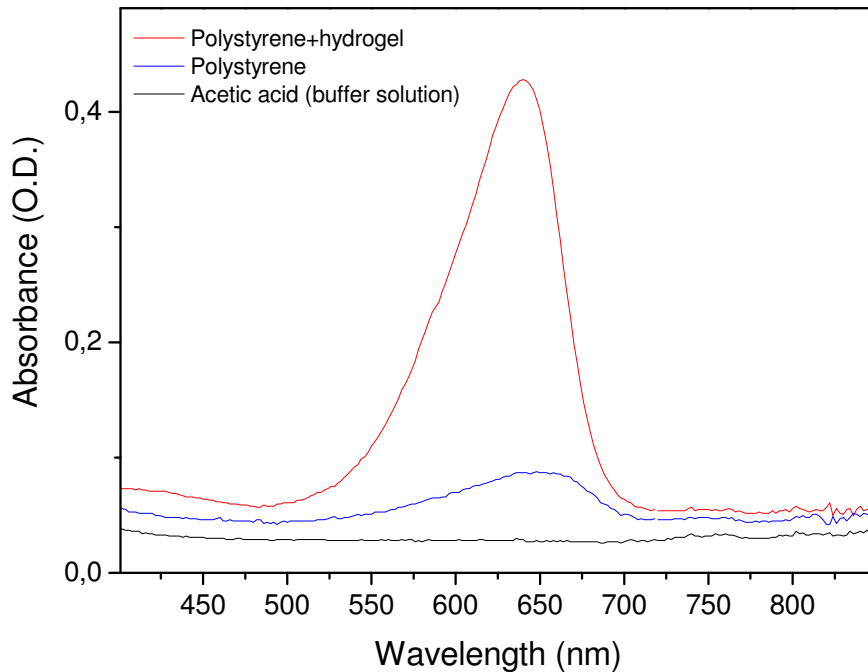


Figure 28 Absorbance spectra obtained from the samples incubated with the dye Basic Blue 12.

6.2.3.1 Implementing of the HC Hydrogel surface from Xantec

Due to problems of cell binding in blood with several kinds of self assembled monolayers (SAM), including lipoic acid, polyethylene imine and agarose a new coating of the surface for nanodetector was necessary. The coating had to be both protein repelling and able to bind high amounts of antibody. For this purpose the Company Xantec provides a surface of a hydrogel consistent of polycarboxylates.

The results with the SAM consisting of lipoic acid as linker were very poor in blood. Usually there were 1 or 2 cells on the whole wire or at the gold-chip after incubating it in blood with spiked target cells (see Figure 29).

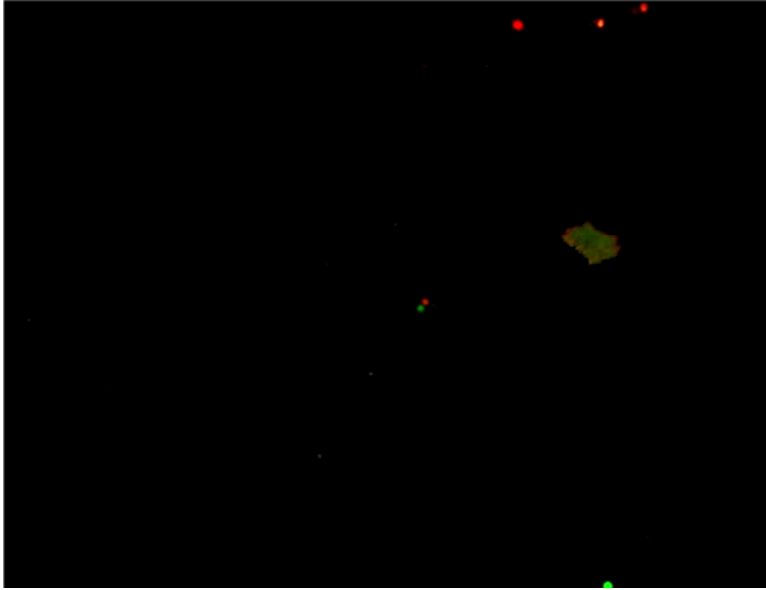


Figure 29 Cell binding to a chip with a SAM consisting of lipoic acid. The antibody AbD 10521 was immobilized to the surface to catch HLA-G-positive cells from blood. HLA-G-positive target cells are stained in red. Control cells are stained in green.

To check if the hydrogel covers the nanodetector the wire is incubated with BSA coupled with the fluorescence tag Oyster 656. The BSA bound reversibly to the hydrogel and can be washed out after analysing under the fluorescence microscope with a buffer of a high salt concentration. The wires were incubated for 10 min in 1.5 mg/ml BSA-Oyster656 dissolved in immobilisation buffer, pH 4.5. Afterwards the wires were washed twice in water to remove the salt. The wires were then analysed under the fluorescence microscope (see Figure 30).

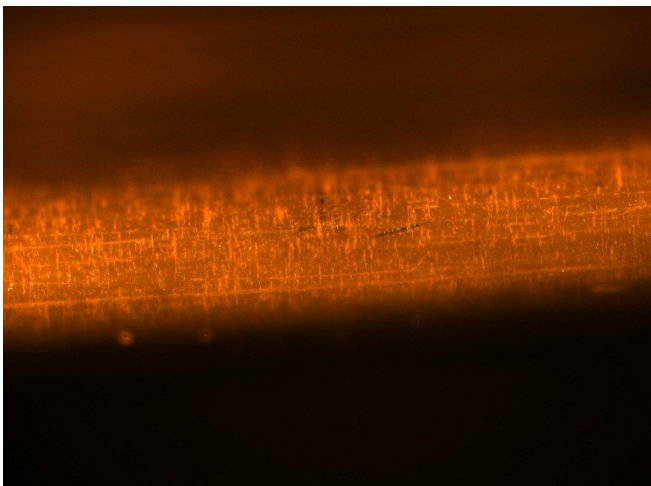


Figure 30 Staining with BSA-Oyster 656 of the wire covered with hydrogel. The wire is glowing orange.

6.2.3.2 Activation of the surface and antibody immobilization

Antibodies were immobilized onto the hydrogel by activating the carboxyl groups on the surface with EDC/NHS. Activation takes place in MES buffer at pH 5.3 (see 6.2.3.3). Therefore, 100 mM of NHS and 0.5 % (w/v) EDC are solved in 50 mM MES pH 5.3. Due to rapid hydrolyzation the hydrogel surface needs to be immediately incubated in the activation buffer. To check the activation of the surface the amount of bound antibody was measured

by ELISA (enzyme linked immunosorbent assay). Therefore, the antibody is bound to the surface, the surface is washed and a secondary antibody is applied to it. This secondary antibody is labelled with horse radish peroxidase (HRP) and added TMB results in a time dependent colour reaction. The colour switches into yellow after stopping the reaction with sulphuric acid. The absorbance was measured at 450 nm in an ELISA-reader.

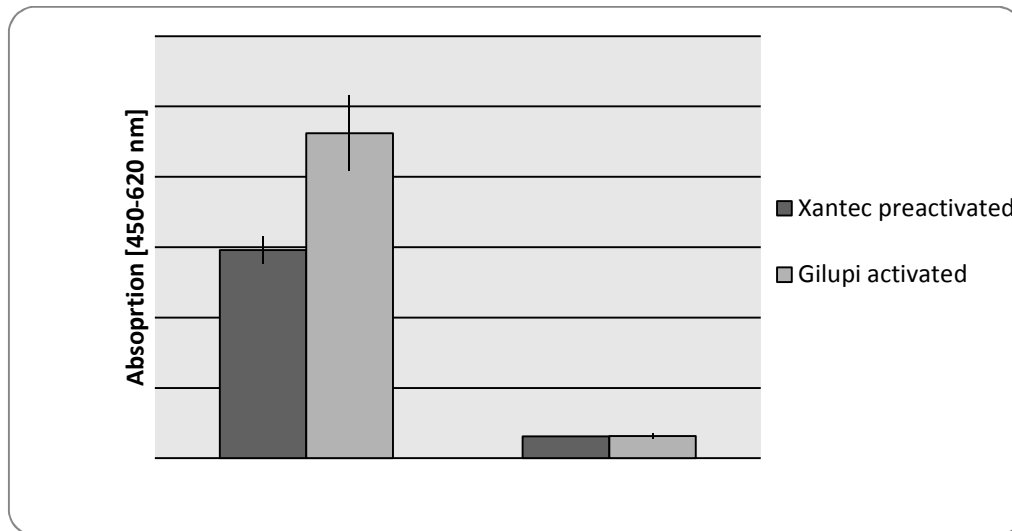


Figure 31 ELISA at Xantec's HC hydrogel coated surfaces. Pre-activated and self activated surfaces were tested. For reference surfaces without antibody were used. Own surface activation was able to bind more antibody than pre-activated surfaces.

In Figure 31 the binding of model antibody MEM-G/9 onto preactivated HC surfaces by Xantec and HC surfaces activated immediately before use is shown. It has been shown that the binding of the antibody after the activation of the surface is slightly higher than the binding onto pre-activated surfaces of Xantec.

6.2.3.3 Analysis of the optimal pH-value for the coupling of the antibodies onto the surface

A very important point of the immobilization of the antibody is the choice of the suitable buffer and the right pH value. To get a high efficiency of coupling the antibody should be used in a high concentration. Over ionic interactions a concentrating of the antibody on the surface can be achieved. The used surface is negatively charged because of the modification of carboxyl groups. Therefore, the antibody should be positively charged to concentrate on the surface over electrostatic interactions. For that reason the pH value of the buffer for immobilizations should be low and of weak ionic strength. The right pH values for the optimal coupling of the antibodies were determined with the surface plasmon resonance (SPR) technique on hydrogel chips. Therefore, the antibody was given over a non-activated surface to analyse the process of concentrating of the antibody in dependency of the pH-value.

The optimal binding pH value for the antibody AbD10521 is pH 5.5 (sodium acetate buffer). The results of the measurements are shown in Figure 32 and Table 10.

Under binding conditions only 10 % of the carboxyl groups of the hydrogel were activated with EDC/NHS so that the pre-concentrating conditions still existed.

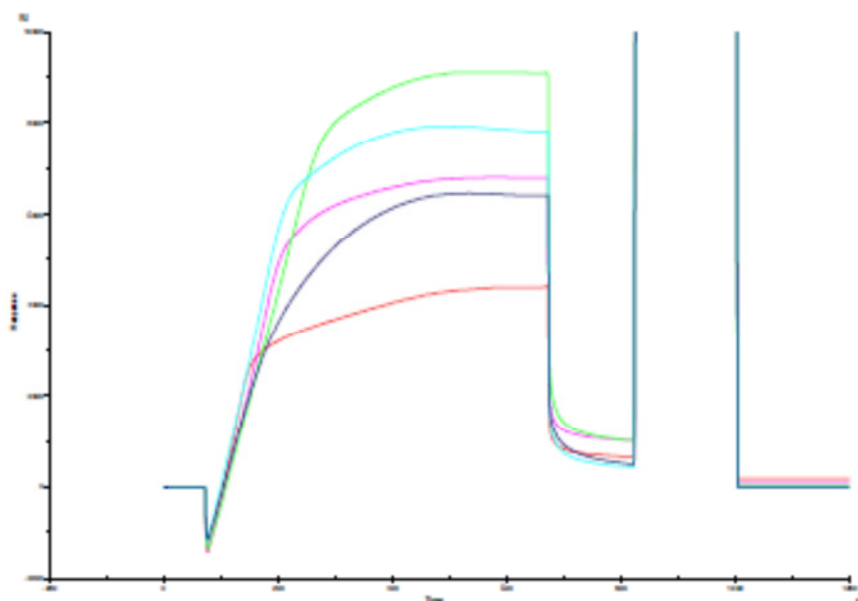


Figure 32 Pre-concentration kinetics of the antibody AbD10521 at different pH-values.

Table 10 Resonance units (RU) of the pre-concentrating kinetics of the antibody AbD10521 at different pH-values

pH	RU	colour
4,5	4400	Red
5	6800	Magenta
5,5	9100	Green
6	7930	Light blue
6,5	6460	Dark blue

6.2.3.4 Determination of the amount of antibody on the surface with SPR

The amount of antibody present on the nanodetector was analysed with SPR. The hydrogel surface was activated with EDC/NHS and then the antibody was bound to the hydrogel. After blocking the remaining carboxyl groups with ethanolamine the amount of 10204 RUs was determined by SPR measurements. So the amount of antibody on the activated surface was $16,326 \text{ pg/mm}^2$ (see Figure 33). The resulting amount of bound antibody calculated for the total area of the nanodetector was 776 ng (see Figure 34).

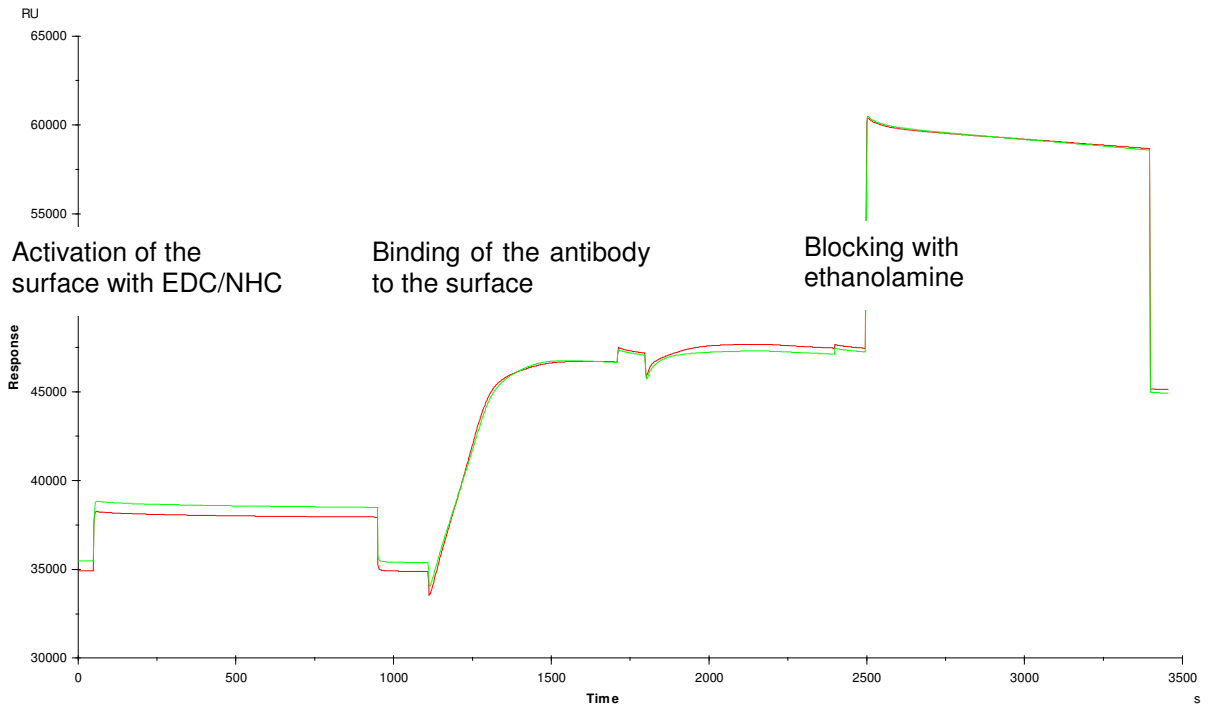
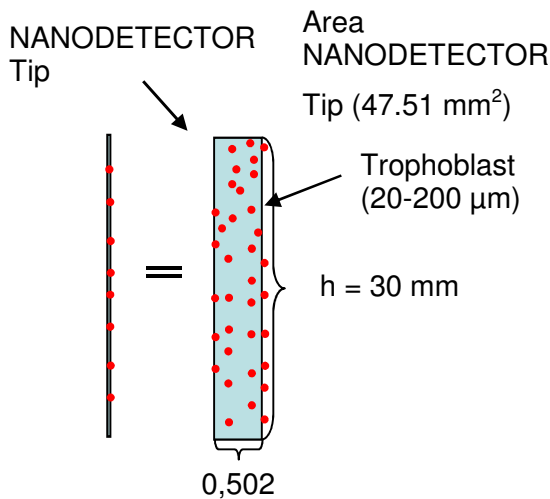


Figure 33 Binding of the antibody AbD10521.3 on the hydrogel surface analysed with SPR. The surface was first activated with EDC/NHS, then the antibody was bound. The remaining activated carboxyl groups were blocked with ethanolamine. The amount of antibody was determined with 1 RU being equal to 1.6 pg/mm^2 .



Calculation of the amount of antibodies theoretically covering the functional wire tip:
 $(r = 0.251 \text{ mm}, h = 30 \text{ mm})$

$$\text{Area of the functional wire tip } A_1 = 2\pi rh + \pi r^2 = 47.51 \text{ mm}^2$$

Amount of antibody determined with SPR:

10204 RUs were measured. 1 RU is equal to 1.6 pg/mm^2

10204 RU are equal to $16326 \text{ pg/mm}^2 = 16.326 \text{ ng/mm}^2$

Figure 34 Wire surface area and theoretical amount of bound antibody. Schematic diagram of the coated tip of the medical wire.

According to the manufacturer XanTec the maximum amount of antibodies which can bind to the surface per mm² is 50 ng. Calculated to the product surface (47.52 mm²) which comes in contact with blood the amount of antibody is about 2350 ng. SPR analysis showed that about 800 ng antibody can bind at the wire. This quantity of the bound antibody can be increased by optimizing the process - such as dipping the wire in the antibody solution. The highest amount on the wire can be estimated to be a maximum of 3 µg.

6.3 Preclinical *in vitro* testing

To test the functionality of the nanodetector a standard procedure was established. The functionality of the antibodies was determined with flow cytometry while the specificity was examined by immunohistochemistry (IHC). The quality and quantity of the antibody binding to the surface were measured by ELISA und SPR experiments.

The cell binding ability was tested by incubating cells in different solutions with the nanodetector. As a model system chips were tested that had the same surface as the nanodetector. To simulate the venous blood flow a dynamic flow system was installed. By this assembling it was possible to alternate the fluid and the flux by which the target cells are transported.

6.3.1 Flow cytometry with the antibody

To test the affinity of the considered antibodies flow cytometry analyses were done with HLA-G positive cells. The following cell lines were used: K562 HLA-G (denatured HLA-G), K562 A2, JEG-3 (native HLA-G) and Jar; and as secondary antibodies goat anti-human-FITC-AK (Jackson Immuno Research) and donkey anti-mouse-FITC-AK (Chemicon).

MorphoSys produced anti-HLA-G Fab-antibodies. One of them is the AbD10521 antibody. The antibodies were tested after removal of endotoxins. The results of the flow cytometry are shown in Figure 35 . The affinity of the antibody AbD10521.3 is 23 fold higher than that of AbD7109.25, which was also considered as a possible antibody in this work.

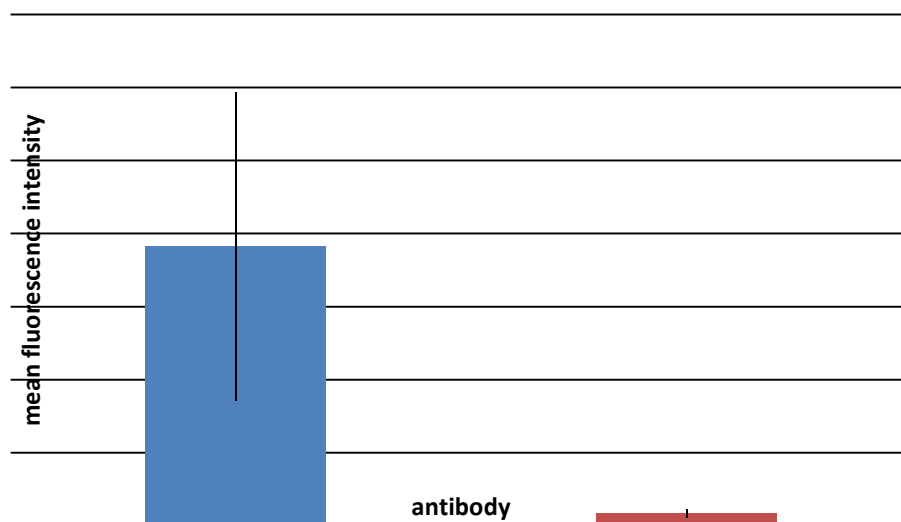


Figure 35 Flow cytometry analysis of antibodies with HLA-G positive cells. K562 HLA-G cells were incubated with the antibodies followed by the incubation with a secondary anti-human Fab-antibody. Data show the mean fluorescence intensity of 2 independent experiments with standard deviation.

A comparison between the MEM-G/9 and different human antibodies is shown in Figure 36. The MEM- G/9 shows a stronger affinity towards the native HLA-G and doesn't show a high cross reactivity as the human F(ab) antibodies.

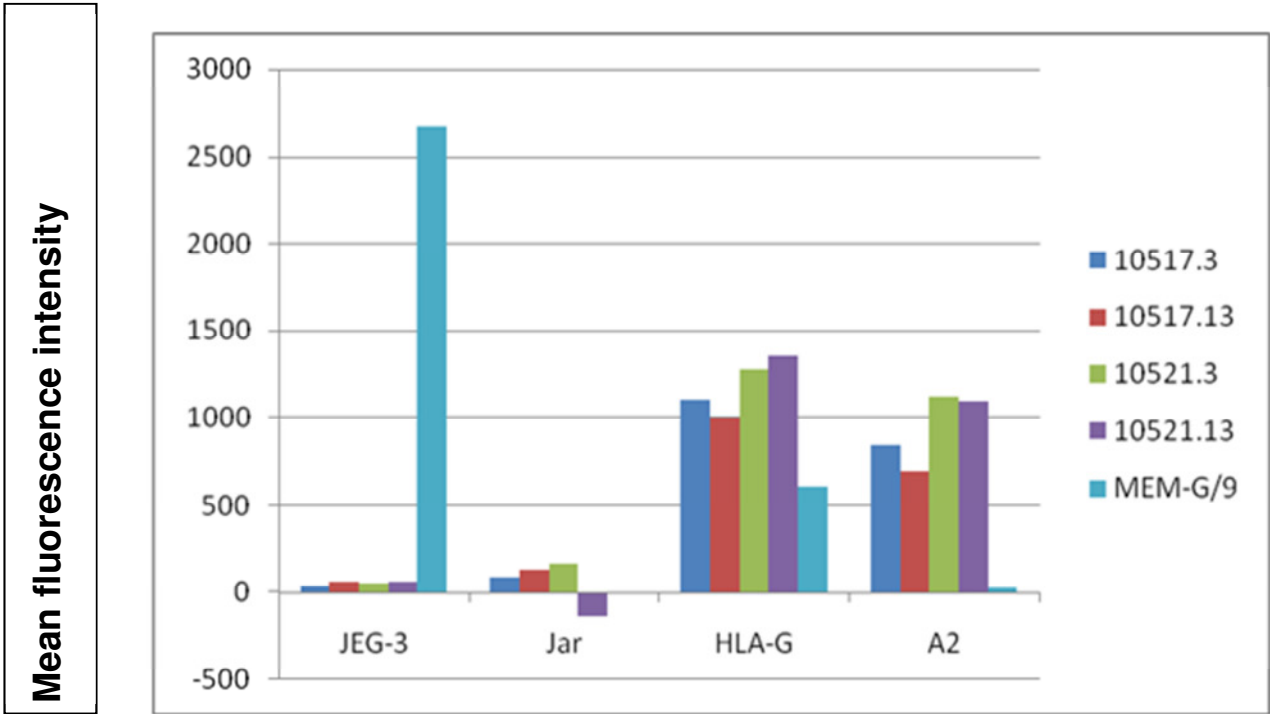


Figure 36 Flow cytometry analysis of antibodies with HLA-G positive and negative cells

6.3.2 Immunohistochemistry (IHC)

IHC was performed with placenta sections in order to determine the specificity of the antibodies which were chosen for application on the nanodetector (Figure 37). The placental villi have a histological structure which allows a clear microscopic distinction between the different cells of which they are composed - among them cytotrophoblasts and syncytiotrophoblasts which find their way into the maternal circulation where they are the target of the nanodetector bound antibodies.

Mouse monoclonal anti-HLA-G antibody MEM/G9 specifically detected trophoblasts lining the villus surface without cross-reacting with any other cell type.

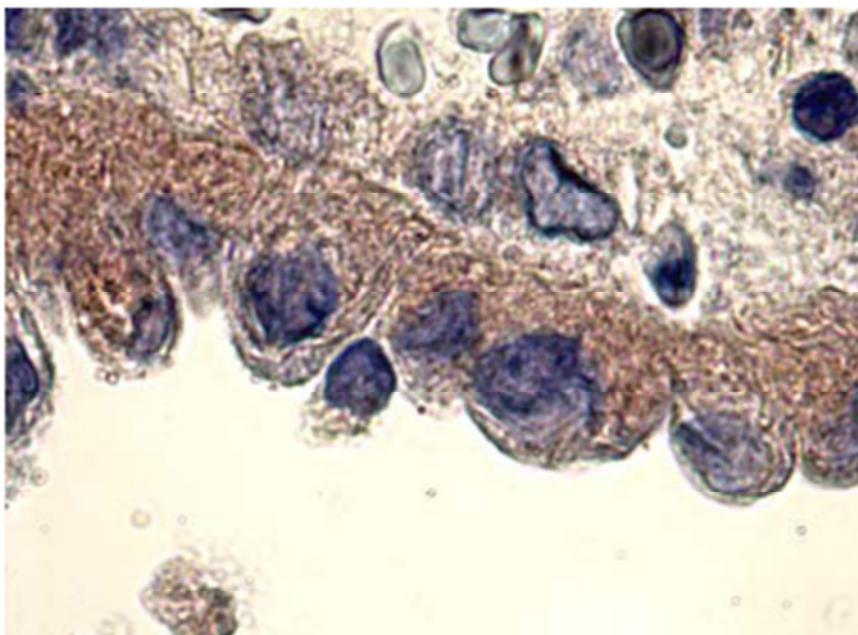


Figure 37 Immunohistochemical staining of trophoblasts in a paraffin section of an anchoring villus of a first trimester placenta with monoclonal anti-HLA-G antibody MEM/G9 (1 : 100; biotinylated, streptavidin-HRP, Allura Red AC is a red azo dye). Second step control was negative.

6.3.3 Cell binding experiments in spiked blood on chips

To prove that the antibodies are able to catch cells the quality of the antibody immobilization on the surfaces of chips was measured by cell binding experiments. Chips were used, because they are easier to analyse under the microscope. In the experiments the surfaces of chips and wires were coated with antibody and incubated in blood of control volunteers with spiked target cells. For these kinds of experiments a dynamic flow system was established to simulate the venous blood flow.

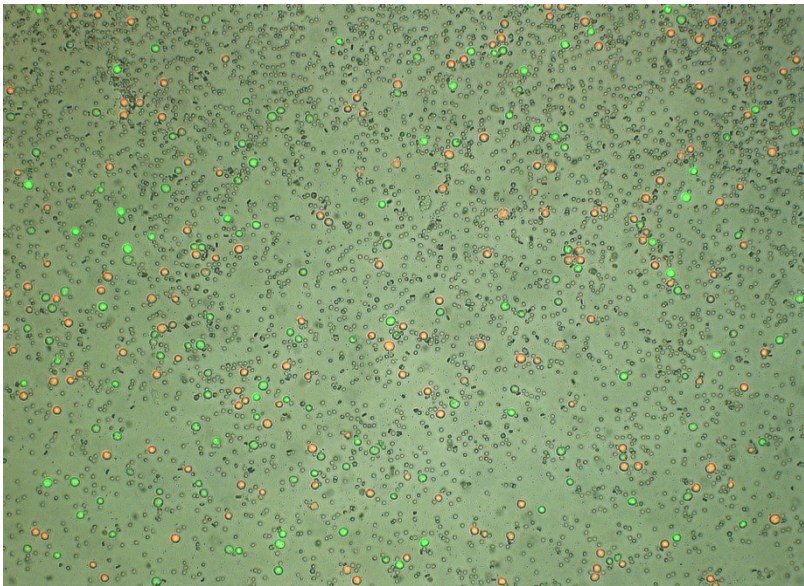


Figure 38 Cell binding to a chip with HC hydrogel coating by Xantec. The antibody AbD 10521 was immobilized to the surface to catch HLA-G-positive cells from blood. The HLA-G target cells are stained in red. A reasonable binding of green stained control cells also was measured.

To measure the cell binding quantitatively we applied a model system by spiking a certain amount of HLA-G-positive cells in human blood. By this approach we were able to compare the functionality of different surfaces. In most cases 50,000 to 100,000 cells/ml blood were used.

In Figure 38 the cell binding is shown on a chip with HC hydrogel coating by Xantec. The cell binding is considerably higher on the HC hydrogel surface. In comparison to Figure 29 there is a much higher amount of bound cells. In general we detected a mean quantity of 50 cells per mm^2 at the HC hydrogel surfaces and 2 – 5 cells when using SAM's of lipoic acid.

6.3.3.1 Cell binding experiments in spiked blood with the nanodetector

With HC hydrogel (XanTec) coated nanodetector were coated with anti-HLA-G antibodies and tested with spiked JEG-3 cells in peripheral blood. Here, the flow system Figure 15 was used. The incubation conditions in the flow system were maintained constant. The flow rate was 1 ml / min and the incubation period 30 min. The temperature was maintained at 37 °C. In cell binding experiments with spiked 100,000 JEG-3 cells / ml, cells could be detected on the nanodetector (see Figure 39).

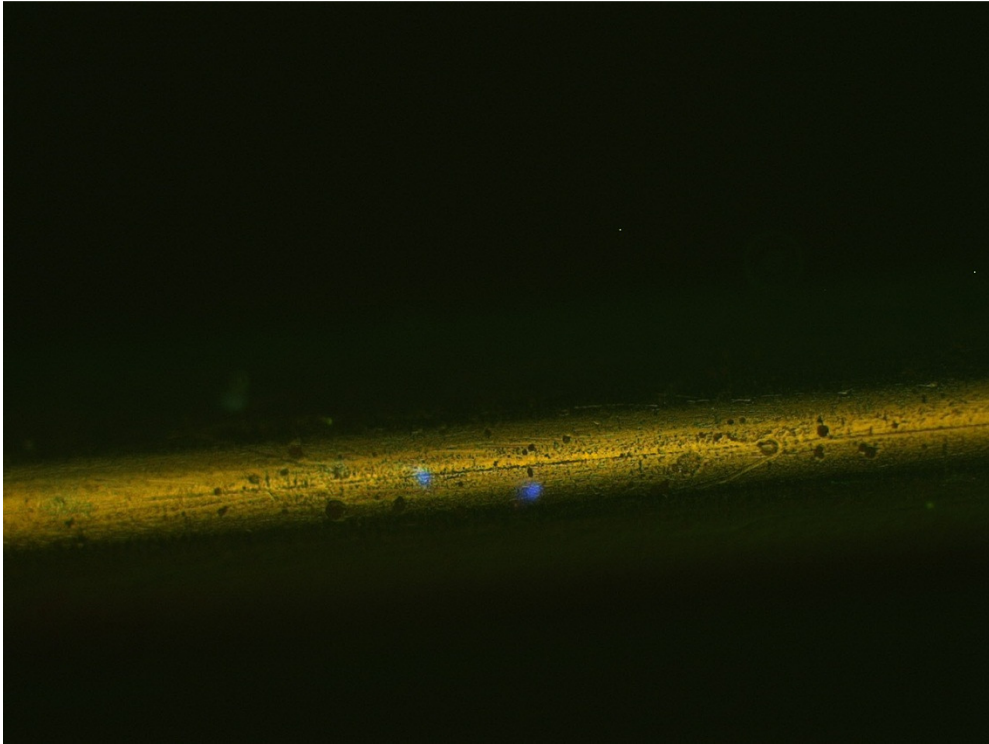


Figure 39 Trophoblast cells detected on the Nanodetector from spiked blood. non-specific connection was hardly recognizable

6.3.4 Cell binding experiments in peripheral blood of pregnant women

To assess the probability of the nanodetector to catch cells in the human body blood of pregnant women was used in the dynamic flow system. In these experiments we were also able to detect fetal cells. After incubating the wires in blood they were stained by fluorescence labeled antibodies against trophoblast antigens.

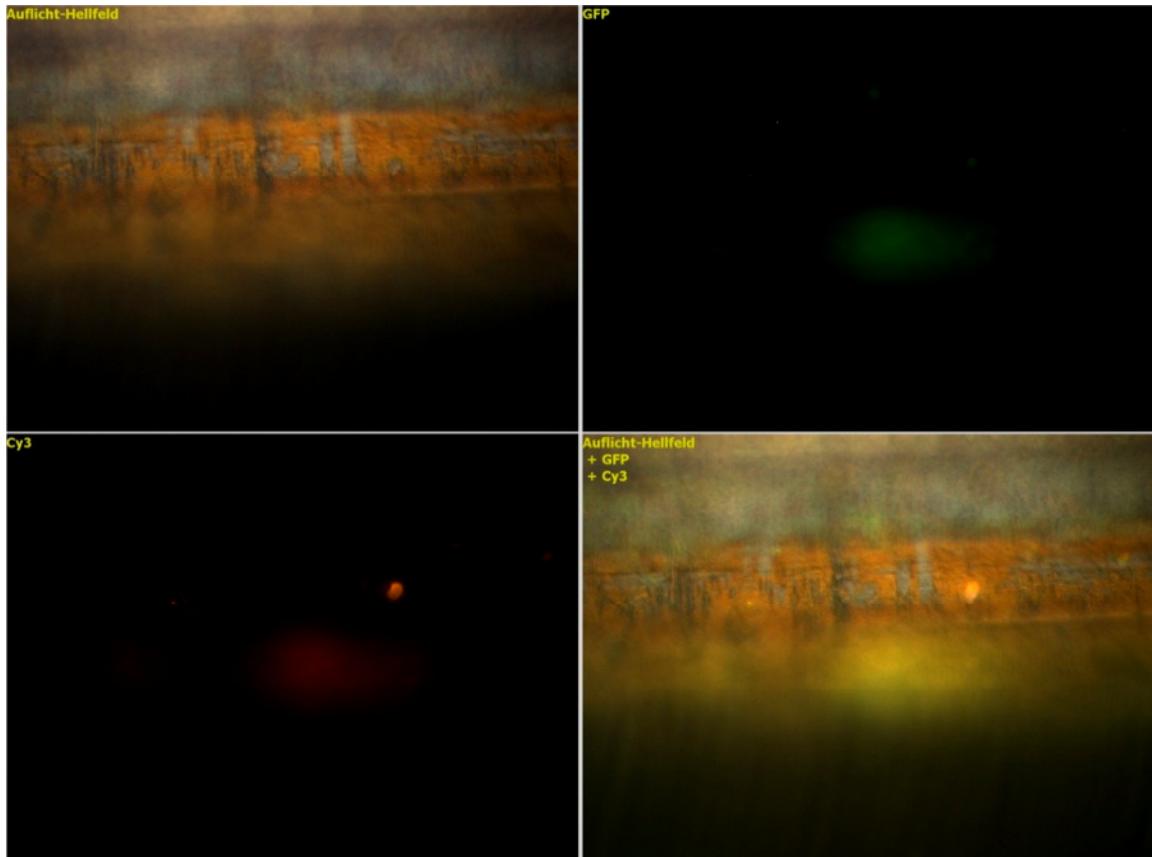


Figure 40 Detected cell at the nanodetector from peripheral blood of a pregnant woman. The red staining is a marker for HLA-G, the green staining is a marker for macrophages which sometimes also carry the HLA-G antigen.

6.4 Cytotoxicity tests

6.4.1 Cytotoxicity of the nanodetector with and without PEG

In general the test cells showed the typical morphology of a proliferating cell line, as it is found even under normal culture conditions. The cell layer showed high confluence with fine branched filopodia (cell processes) of the fibroblasts (e.g. Figure 41). Even cells in the immediate vicinity of the wire were unchanged, and thus apparently not affected by potentially cytotoxic components dissolved from the wire. Some mitotic round cells were also brightly colored. The formation of branched filopodia is a morphological characteristic of high cell viability. Under stress, e.g. under the influence of cytotoxic substances the cells will round up.

The fact that the cells have taken up the vital dye CFSE showed that the cells were intact and vital. There were no morphological differences in the human fibroblasts between treated with passivated and non-passivated wires.(Figure 41+Figure 42) A trend towards fewer cells was observed on the antibody-coated wires in comparison to wires without antibodies (Figure 41-Figure 44). The cells growing on the wires also showed no changes in cell morphology, which is characterized by the presence of branched processes (right).

There was no cytotoxic effect of the wires used in these tests on the human fibroblast cell line NHDF-c.

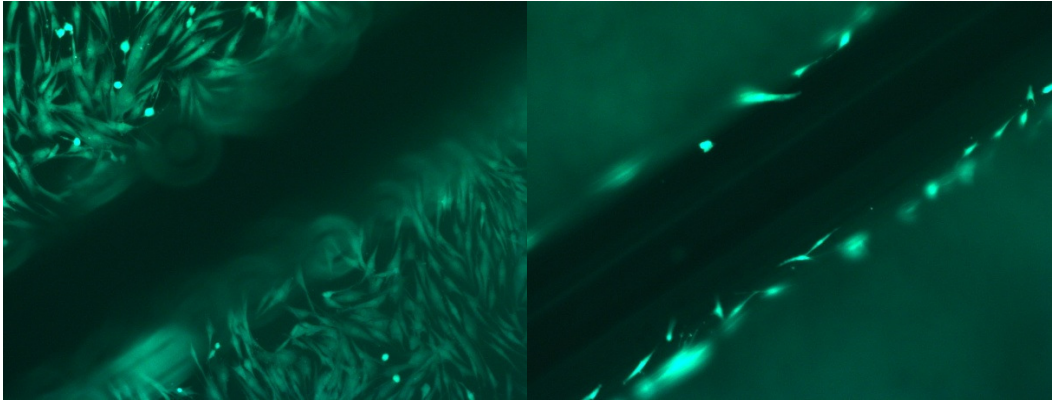


Figure 41 NHDF cell culture on (right) and next to the nanodetector (left) with PEG-passivation and without antibody coating

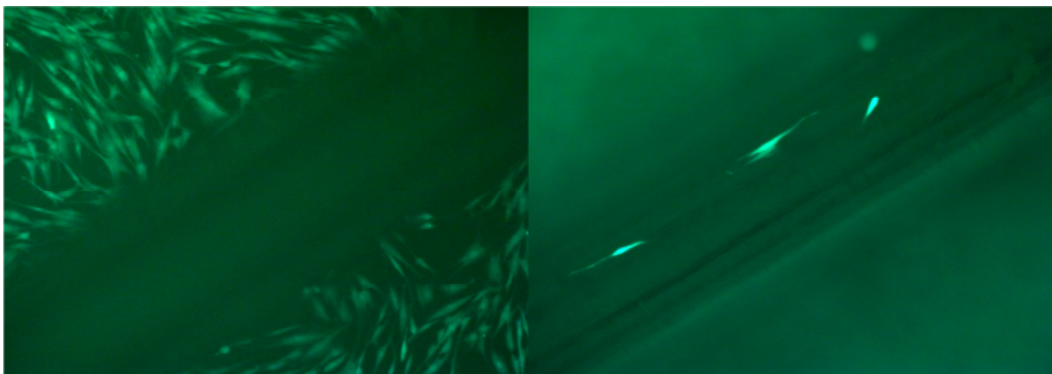


Figure 42 NHDF cell culture on (right) and next to the nanodetector (left) with PEG-passivation and coating with antibody

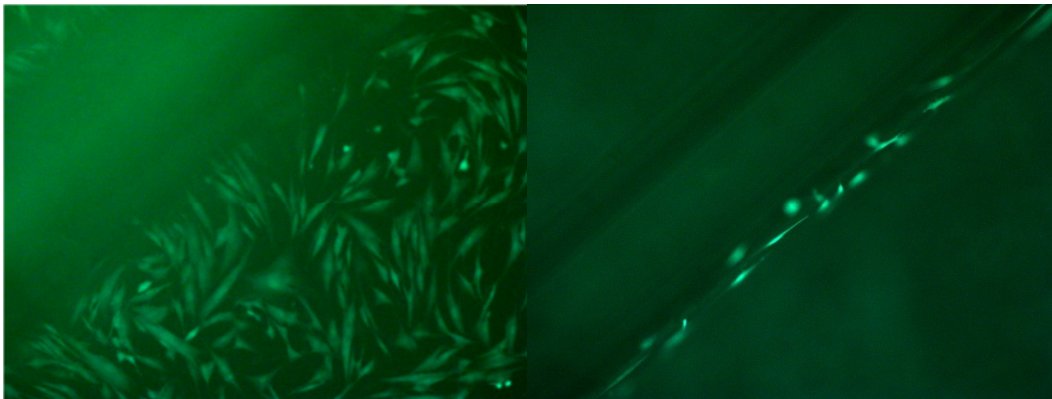


Figure 43 NHDF cell culture on (right) and next to the nanodetector (left) without PEG-passivation and without antibody coating

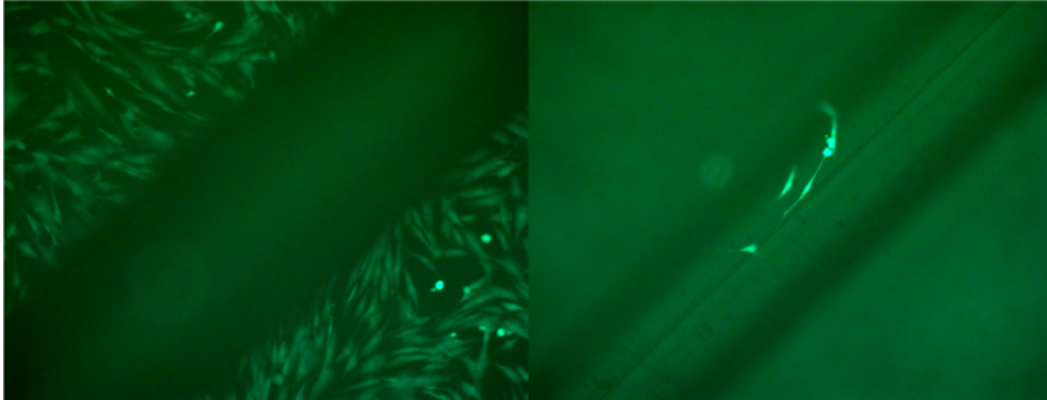


Figure 44 NHDF cell culture on (right) and next to the nanodetector (left) without PEG passivation but coating with antibody

6.4.2 Investigation of the cytotoxicity of antibody solutions

The aim was to validate the cell viability of human NHDF-c cells after treatment with different antibody solutions. The concentration of antibodies (anti-human HLA-G: human Fab 7109.13 C; MorphoSys AbD and murine MEM-G / 9; Exbio) was 500 ng per sample and thus more than 10 times the amount of antibodies which is fixed on the whole wire. This cytotoxicity test is based on a colour change of the XTT reagent (tetrazolium salt). Differently treated cells were incubated with the yellowish colour reagent XTT, which is converted metabolically by active cells to the orange-coloured formazan. The intensity of the orange color correlates with the amount of living cells. 10% ethanol, which acts as a cell poison is used in the experimental approach as a positive control while untreated cells and medium are used as negative controls in the test.

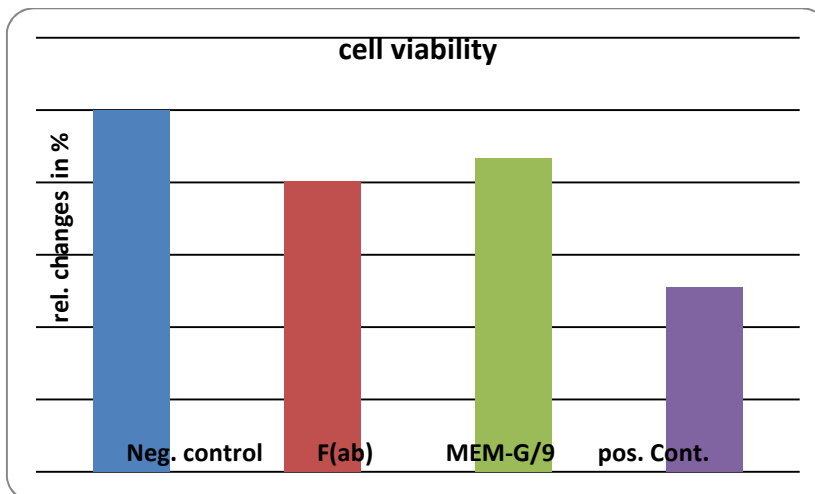


Figure 45 Diagram showing the viability of fibroblasts treated with antibodies compared with the viability of cells of the negative and positive control

The results in Figure 45 show that the treatment of human fibroblast cell line NHDF-c with antibodies leads to a cell viability of 80% (Fab) and 87% (MEM-G / 9). According to the classification of reactivity (see table Table 5 Reactivity Grades for the Elution Test) those values demonstrate a slight reactivity of the cells (grade 1) to the antibody treatment. This was confirmed by another attempt. If the treatment of the cells is showing a maximum reactivity of grade 2 (mild reactivity), the test is passed. In general, if the positive control

achieves at least a reaction of grade 3 (moderate reactivity), the experiment can be accepted. Both conditions were met in the experiments conducted with the nanodetector.

In conclusion, the cytotoxicity test show, that the tested antibodies (Fab and MEM-G / 9) showed only a slight reactivity and thus passed the test.

6.4.3 Study of the cytotoxicity of the nanodetector with an elution test

The cultures of the negative control were assessed with an average of reactivity of 0 and were compared to the untreated elution medium control: no evidence of a cytotoxic effect. In contrast, in cultures of the positive control, a clear cytotoxic effect was observed, which was valued at an average reactivity of 4. For the eluate from the nanodetector under the experimental conditions no significant cytotoxic effect was detected.

Microscopically, the cells appeared adherent and spindle-shaped. Proliferation was the basis of increasing cell density and confluence, but seemed in comparison to the negative control somewhat less pronounced. Based on the elution medium for the negative control with a percentage of vitality of 110% the nanodetector reached 98% to 99%. This represents an average ranking of the reactivity with grade 0 (no reactivity). The undiluted eluate of the catheter showed a reactivity of grade 0 (no reactivity; see Figure 46). The cells did not show morphological changes, they were adherent and typically spindle shaped like the controls. In contrast well-defined, cytotoxic effects were observed in the positive control, which was evaluated with an average score of 4 (severe reactivity).

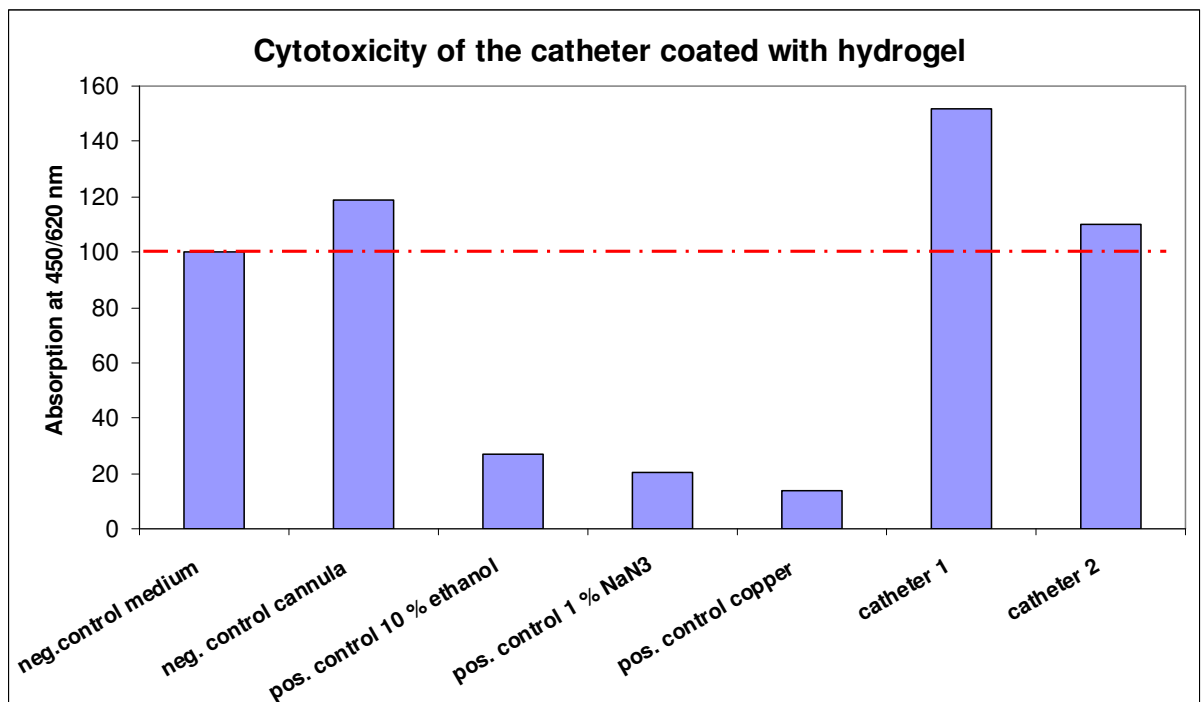


Figure 46 Results of the cytotoxicity test with the hydrogel. The absorbance correlates with the cell-activity. In contrast to the positive control the negative control showed a 100 % cell vitality. Catheter eluates did not influence the viability and showed a cell-vitality of round about 100 %.

The results show that the fibroblast cells respond to the eluates with a viability of over 100%. This is in line with the reactivity grading (table) of no reactivity of the cells. The cell morphology showed no damage, the cell processes were clearly marked and the cells were not rounded.

The conclusion from this part is that the leachate test to check the cytotoxicity showed no reactivity of the cells to the eluate and therefore, all tested wires passed the test.

6.5 Animal tests

In the groups of pregnant rats the condition of fetuses were evaluated [65]. The appearance of fetuses from experimental groups did not differ from the ones belonging to the control groups (control group, control /catheter /catheter gold group, catheter group, catheter gold group). During the autopsy, the selected organs (kidney, lung, liver, spleen) were collected, and after drying them in the filter paper, they were weighed. Additionally, in the case of the pregnant rats the placentas and fetuses were weighed. The mean values of placentas and fetuses from all the studied groups are shown in Table 11.

Table 11 The mean weight of placenta and foetus in pregnant rats

Group symbol	Body weight [g]	
	Non-pregnant	Pregnant
	Mean \pm SD (<i>n</i>)	Mean \pm SD (<i>n</i>)
Control	251.0 \pm 3.6 (12)	286.5 \pm 12.5 (11)
Catheter	252.8 \pm 3.7 (11)	280.0 \pm 5.7 (6)
Catheter Gold	248.8 \pm 4.5 (15)	288.2 \pm 6.1 (6)
Control/Catheter/ Catheter Gold	249.5 \pm 6.3 (6)	302.8 \pm 16.8 (6)
Catheter + Anti-HLA-G	243.2 \pm 3.1 (5)	298.8 \pm 23.6 (6)
Catheter Gold + Anti-HLA-G	253.7 \pm 7.2 (7)	279.0 \pm 16.3 (6)
Anti-HLA-G 0.05 ng/2 hours	249.5 \pm 4.2 (6)	290.2 \pm 10.4 (6)
Anti-HLA-G 0.10 ng/2 hours	247.7 \pm 6.4 (6)	286.8 \pm 13.9 (6)
Anti-HLA-G 0.25 ng/2 hours	248.0 \pm 4.8 (6)	272.8 \pm 9.9 (6)
Anti-HLA-G 0.05 ng/24 hours	244.8 \pm 4.6 (6)	288.3 \pm 8.9 (6)
Anti-HLA-G 0.10 ng/24 hours	242.8 \pm 4.1 (6)	289.2 \pm 6.2 (6)
Anti-HLA-G 0.25 ng/24 hours	242.3 \pm 0.4 (6)	282.5 \pm 7.1 (6)
Anti-HLA-G 0.05 ng/6 weeks*	241.7 \pm 3.6 (6)	255.7 \pm 6.9 (6)
Anti-HLA-G 0.10 ng/6 weeks*	241.5 \pm 1.5 (6)	254.8 \pm 8.3 (5)
Anti-HLA-G 0.25 ng/6 weeks*	244.7 \pm 4.9 (6)	252.2 \pm 3.8 (5)

* In pregnant rats time was 3 weeks

The biochemical tests were performed using blood samples collected from all animals. The concentration of interleukin 6 (IL-6), and interleukin 10 (IL-10) as well as the tumour necrosis factor alpha (TNF-alpha) were measured. In Figure 47, Figure 48 and Figure 49 the results are shown, the assumption is that one nanodetector was not sterile, all other values are in the range. In both non-pregnant and pregnant groups of rats, after the introduction of the catheter/catheter gold with the antibody and after the injection of the antibody, the concentration of IL-6 dropped below the limit of detection. In the case of non-pregnant rats, no other statistically significant differences in the level of IL-6, IL-10 or TNF-alpha have been observed. In the case of pregnant rats, the level of IL-10 was significantly higher in the groups which went through the introduction of the catheter (Pregnant-catheter and Pregnant catheter gold) in comparison with the rats that underwent only surgery (Pregnant-control/catheter/catheter gold).

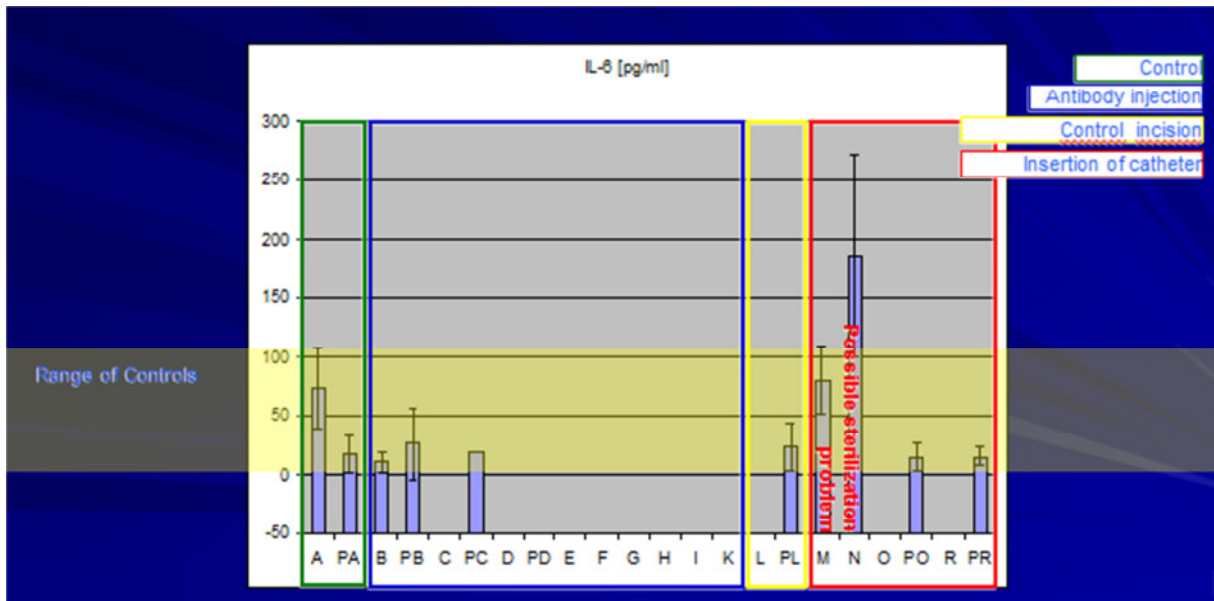


Figure 47 Interleukin-6

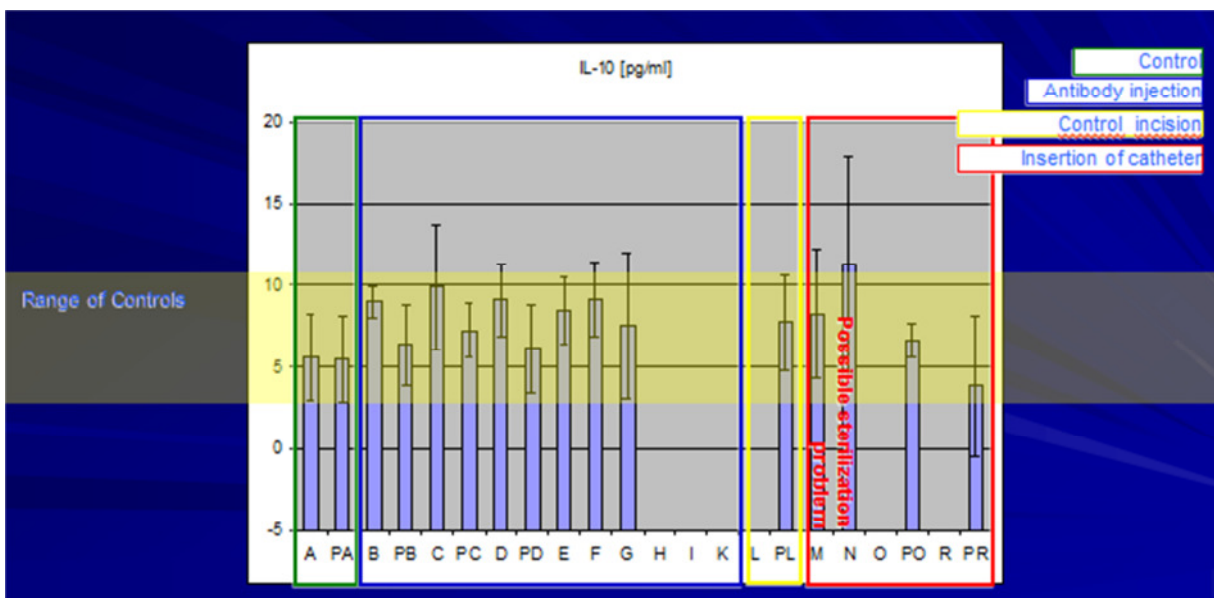


Figure 48 Interleukin 10

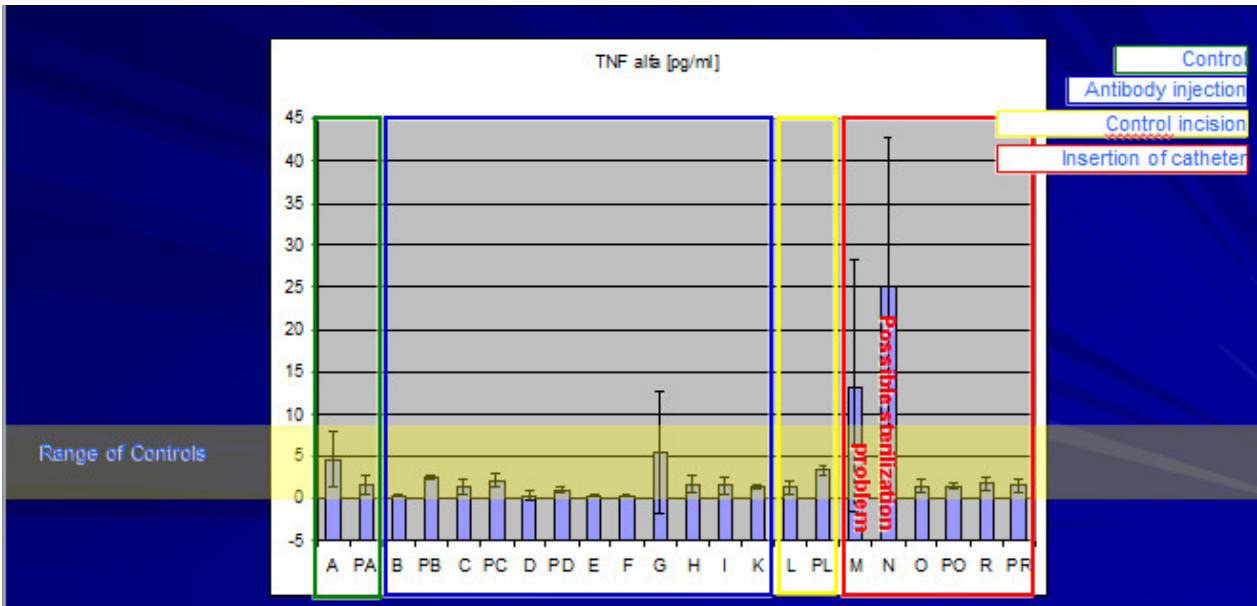


Figure 49 Tumor necrosis factor- α

The mean values of hematological parameters for non-pregnant and pregnant rats are shown in Figure 50, Figure 51 and Figure 52.

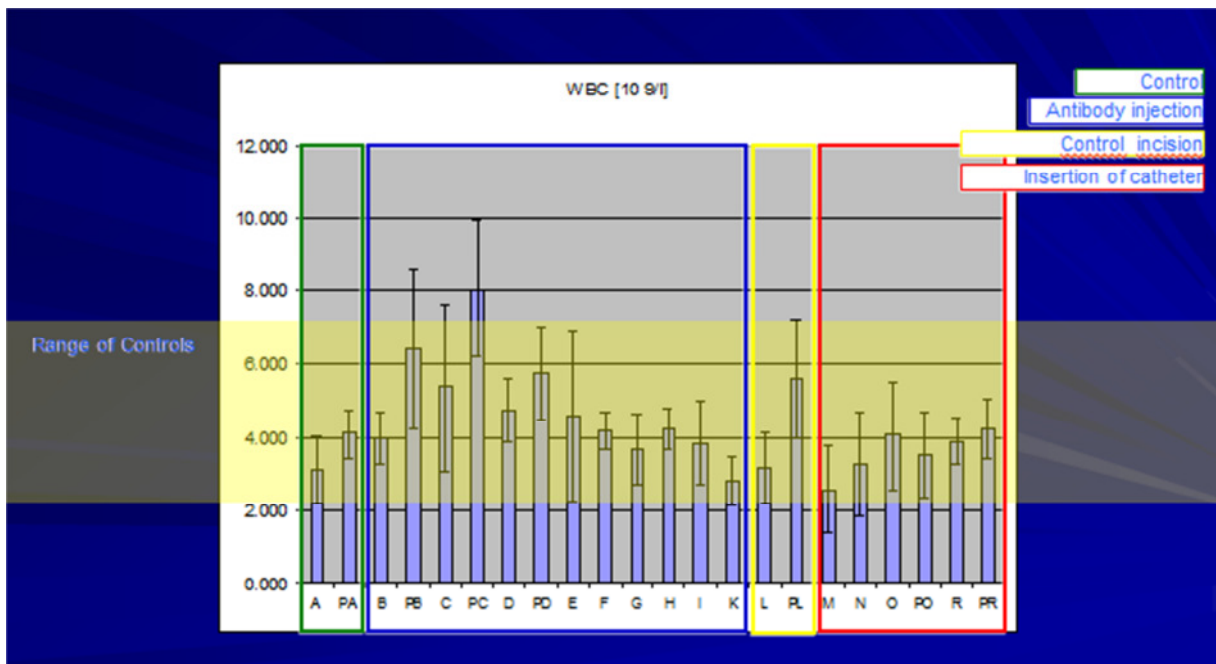


Figure 50 White Blood count

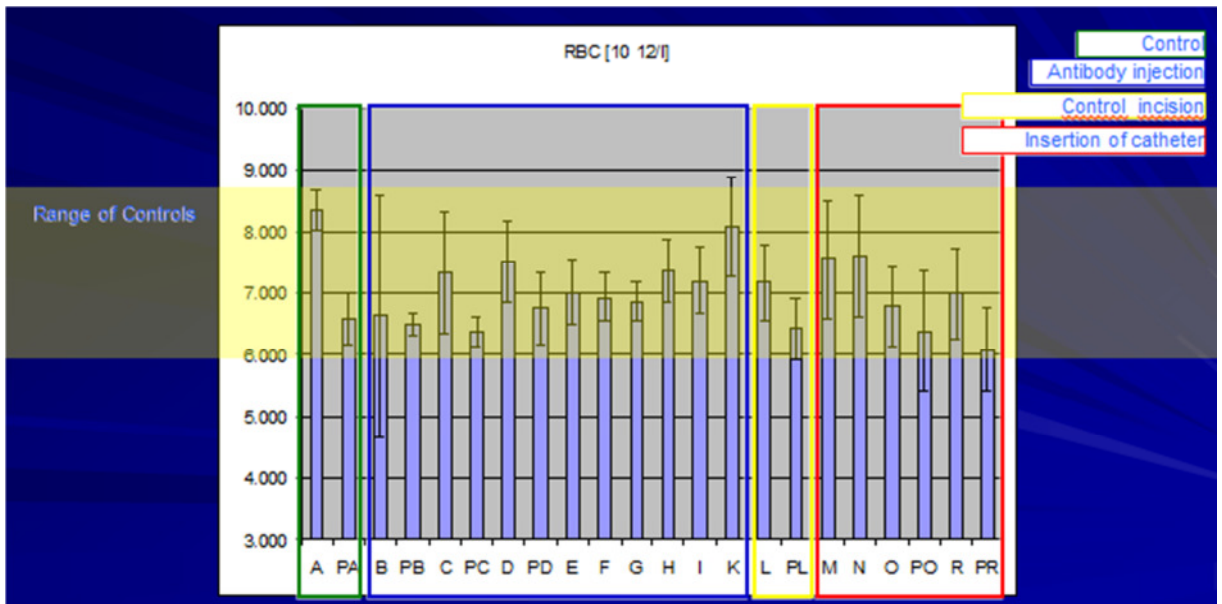


Figure 51 The mean values of the red blood count for non-pregnant and pregnant rats

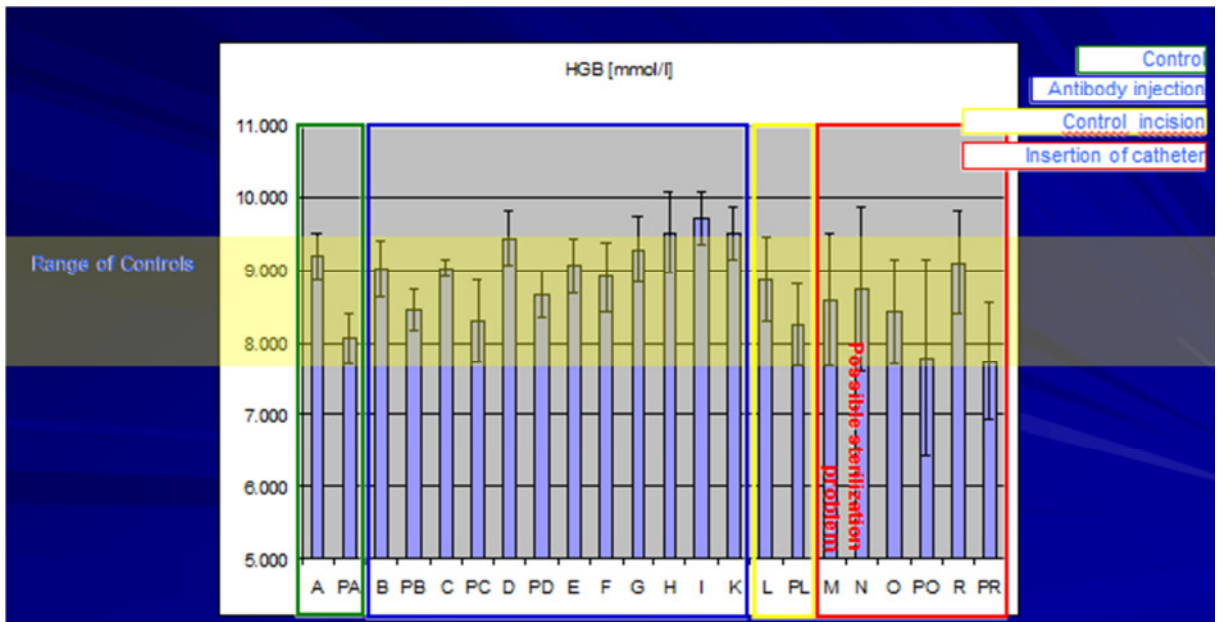


Figure 52 The mean values of hemoglobin for non-pregnant and pregnant rats

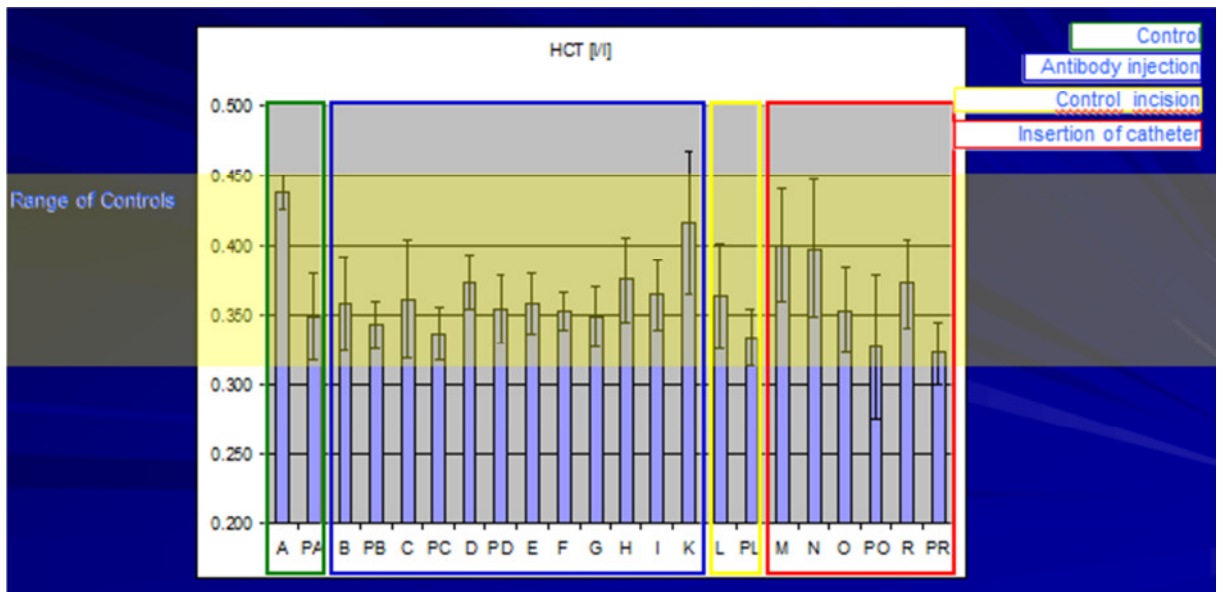


Figure 53 The mean values of hematocrit for non-pregnant and pregnant rats

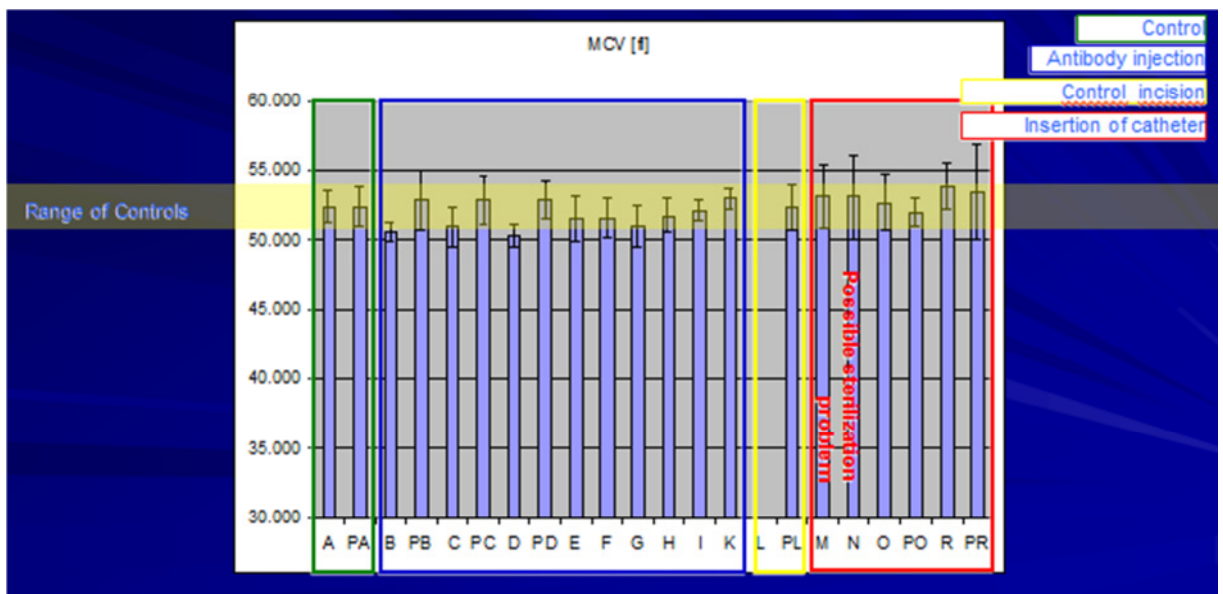


Figure 54 The mean values of mean corpuscular volume for non-pregnant and pregnant rats

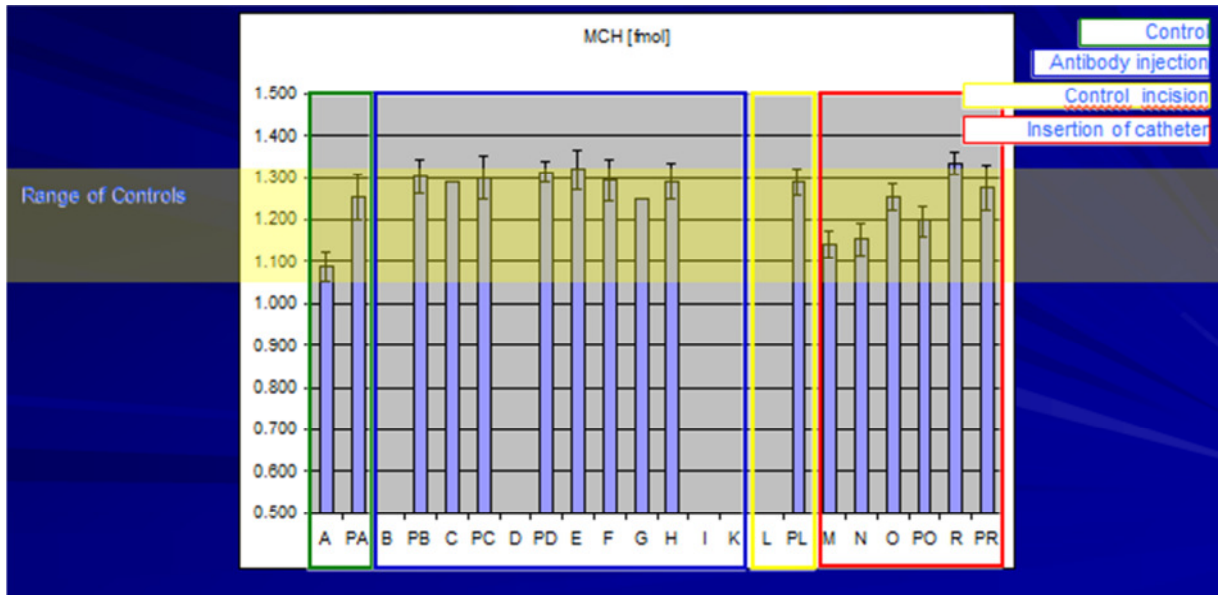


Figure 55 The mean values of mean corpuscular hemoglobin for non-pregnant and pregnant rats

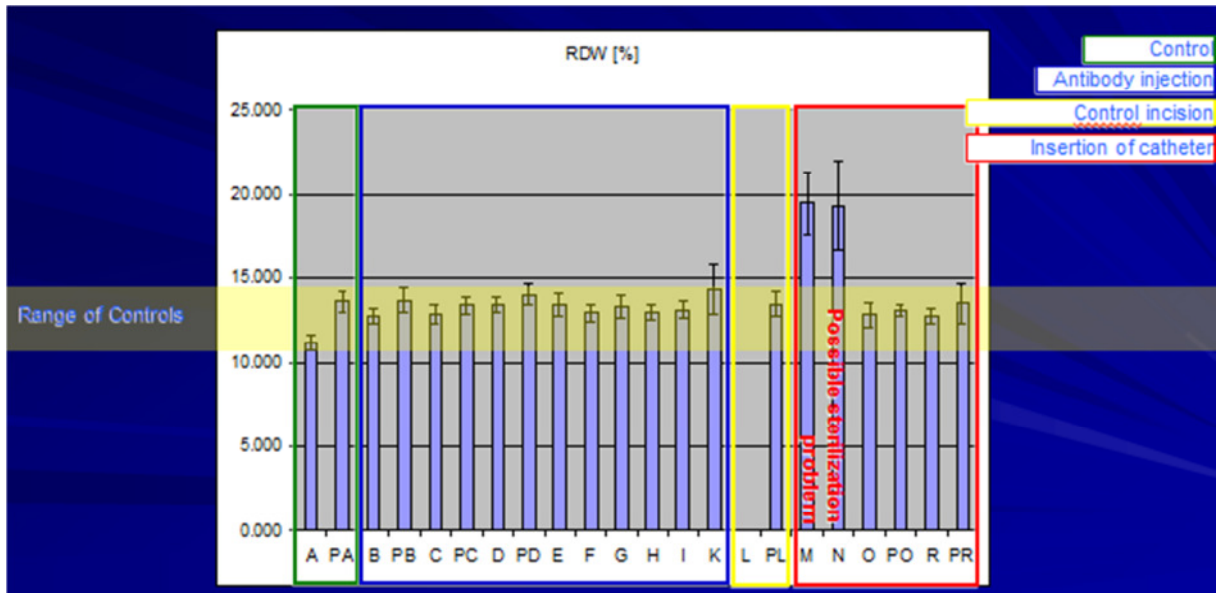


Figure 56 The mean values of red blood cell distribution width for non-pregnant and pregnant rats

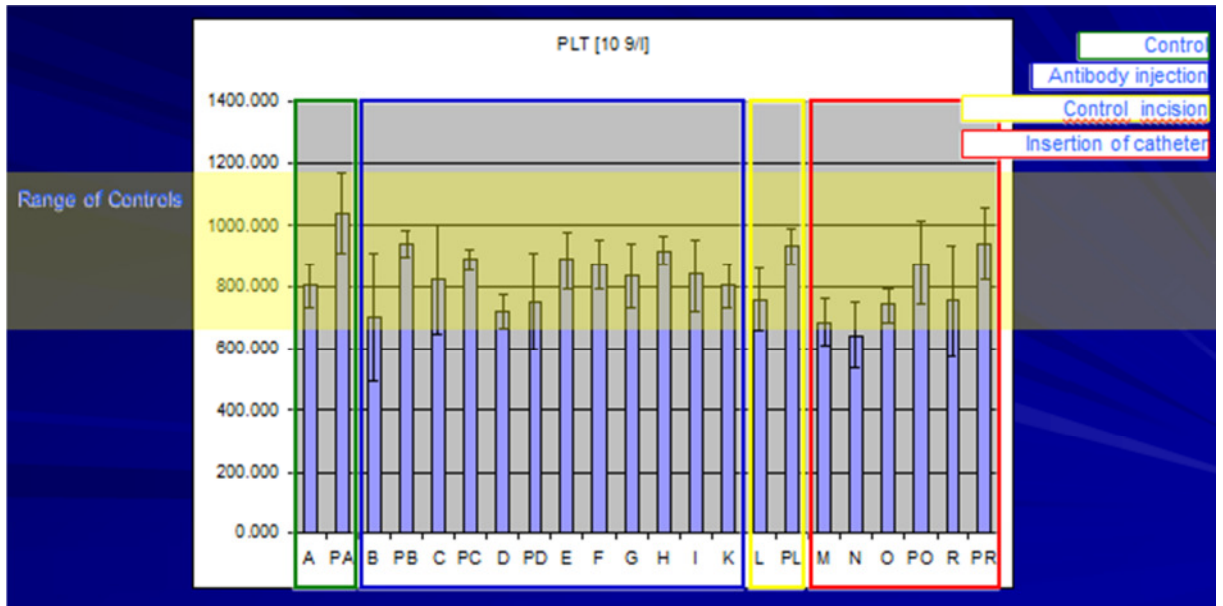


Figure 57 The mean values of the platelets count for non-pregnant and pregnant rats.

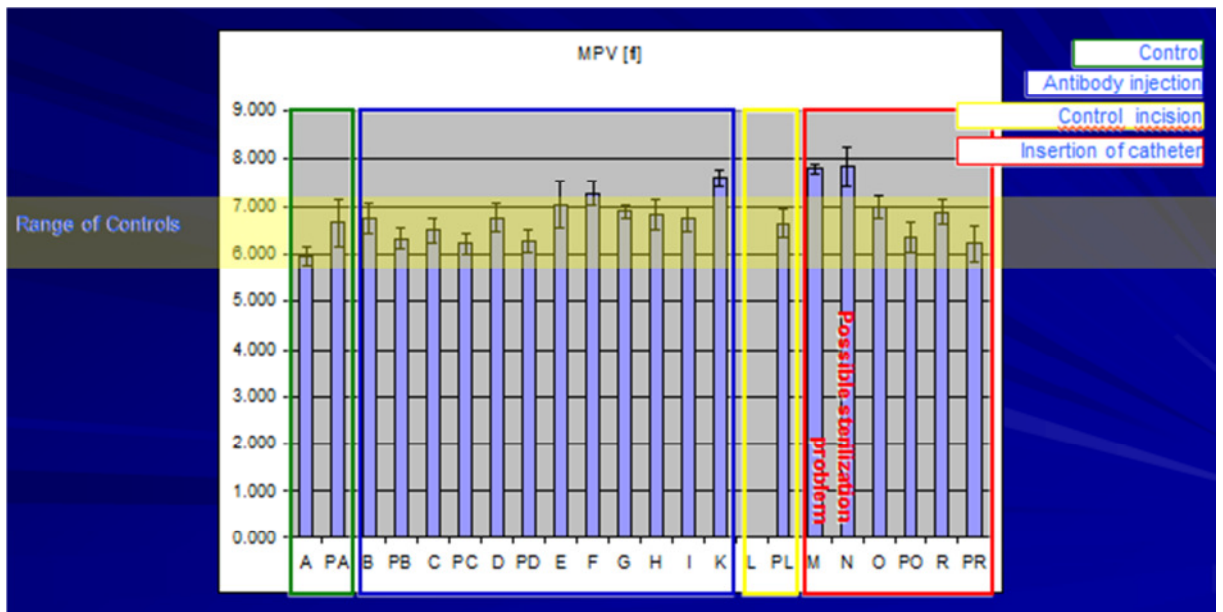


Figure 58 The mean values of mean platelet volume for non-pregnant and pregnant rats.

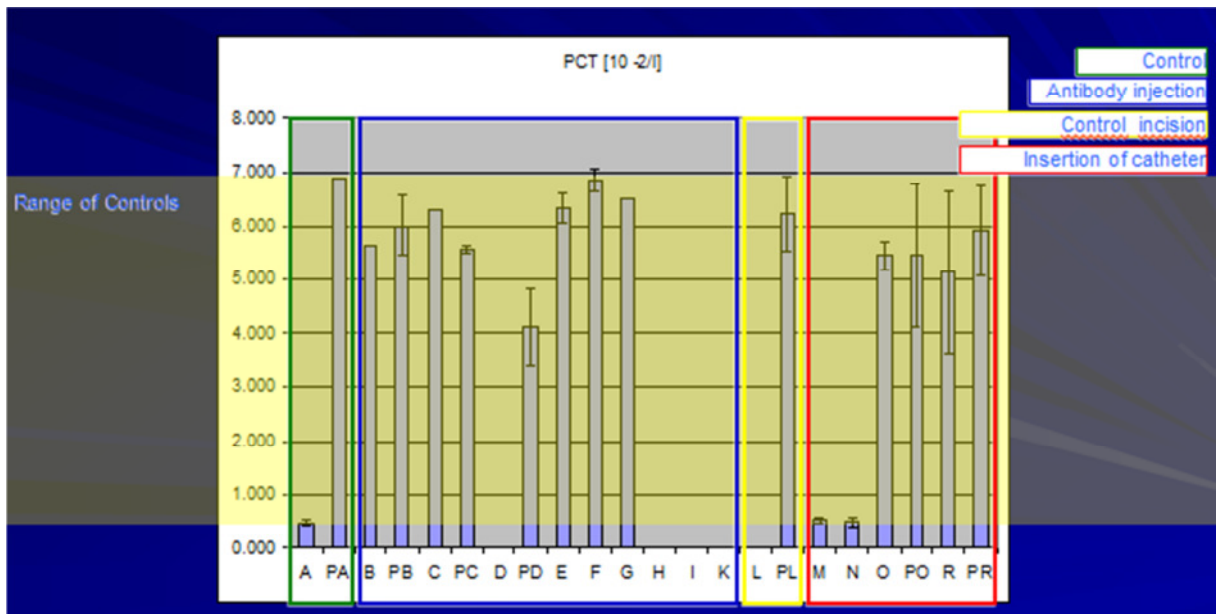


Figure 59 The mean values of platelet hematocrit for non-pregnant and pregnant rats.

In the group of non-pregnant rats, the values of mean corpuscular volume (Figure 54), mean corpuscular hemoglobin concentration (Figure 55), red blood cell distribution width (Figure 56) and mean platelet volume (Figure 58) were higher after the introduction of catheter and catheter gold coated with the antibody than after the introduction of these devices into the vein without antibodies. Although, the differences were statistically significant, from the biological point of view an increase of less than 20% has no importance.

The observed decreases in hematocrit (Figure 53) after the injection of antibodies were relatively small and are of no biological importance. The statistically significant differences were caused by high stability of this parameter in the control group (very low standard deviation).

Small individual differences after the administration of the antibody were noticed in the case of mean corpuscular volume, mean corpuscular hemoglobin concentration, red blood cell distribution width and mean platelet volume.

There were much less differences in the studied parameters among different experimental groups with regard to the pregnant rats. Individual statistical differences were observed in the number of white blood cells (2 hours after the injection of antibody in a dose of 0.1 ng/rat) and concentration of hemoglobin (24 hours after the injection of the antibody in a dose of 0.1 ng/rat). The introduction of the catheter coated with antibodies decreased the mean platelet volume by about 10%. Also these changes did not have any biological importance.

For technical (no possibility to collect enough urine after two hours) and factual reasons (no justification for collection of urine after 3 or 6 weeks after the introduction of the catheter or administration of antibodies), the analysis of the urine was performed only in animals, which had been subjected to autopsy after 24h and in the control group. The obtained results do not indicate an impact of pregnancy on the specific weight of urine. Within the non-pregnant group of rats, it ranged from 1.01 to 1.03 g/ml, and within the group of the pregnant ones - 1.02-1.03 gl. A similar lack of differences concerned the pH of urine, which amounted to 6.0-6.58 in the group of pregnant females, and 6.0-7.0 in the group of non-pregnant rats. The values of these parameters did not depend on the earlier administration of antibodies.

In the case of the remaining determined parameters (bilirubin, glucose, ketone, nitrate, protein, red blood cells, specific gravity, urobilinogen and white blood cells), neither

an impact of the administration of antibodies nor of a pregnancy on their size was observed. Only in the case of the pregnant rats, the increased concentration of protein and number of white blood cells was observed in 50% of the animals. These changes concerned both the animals from the control group and the animals to which antibodies were administered, and the deviations from the normal values were not significant.

In general, the main part of the results regarding the urine analysis were within the range of the reference values. The observed values above the recommended values did not point to any important disturbances in homeostasis caused by the antibodies or the catheters.

With the nanodetector no compound related mortalities and no other signs of toxicity were recorded within 72 hours post-dose for any of the animals. Therefore, according to ISO 10993-11 (and cross referencing ASTM F 750-87 and USP), a sufficient estimation of the acute toxicity of the test item is provided. Under the conditions of the present study it can be stated that the test item nanodetector-human Fab antibody showed no acute toxic characteristics.

In general, the main part of the results regarding the urine analysis were within the range of the reference values. The observed values above the recommended values did not point to any important disturbances in homeostasis caused by the antibodies or the catheters.

6.5.1.1 Histology tests for systemic toxicity

Material from four organs (lungs, liver, spleen and kidneys) was fixed in formalin for around 24 hours, washed in water, dehydrated in a row of alcohol and embedded in paraffin. Sections of around 5 µm in thickness were classically stained with hematoxylin and eosin. Table 12 shows for which study group the analysis was performed

Table 12 *Outline of the data obtained during the animal trial. Listed is the study group together with the numbering of animals included in this group.*

Test	No.	Histology
A	1-12	-
PA	501-512	+
B	61-66	+
PB	581-586	+
C	81-86	+
PC	601-606	+
D	101-106	+
PD	621-626	+
E	181-186	+
PE	641-646	+
F	201-206	+
PF	661-666	+

Test	No.	Histology
G	221-226	+
PG	681-686	+
H	121-126	+
PH	701-706	-
I	141-146	+
PI	721-726	-
K	161-166	+
PK	741-746	-
L	241-246	+
PL	561-566	+
M	21-31	-
N	41-55	-
O	261-267	+
PO	521-526	+
R	281-285	+
PR	541-546	+

The organs prepared during autopsy (kidney, liver, lung, spleen) were evaluated macroscopically. No visible changes were observed. In the groups of pregnant rats the condition of fetuses were evaluated. The appearance of fetuses from experimental groups did not differ from the ones belonging to the control groups (control group, control/catheter/catheter gold group, catheter group, catheter gold group).

In animals of all groups of control and experimental (see Table 12), the following results were obtained:

Lungs – showed a normal histological structure of the organ. Bronchi demonstrated a normal structure, epithelium and the remaining parietal elements demonstrated no lesions. Close to bronchi or at the periphery of their walls small but evident infiltrates of lymphocytes were noted. Structure of bronchioli and of accompanying blood vessels was normal. Inter-alveolar septa showed no pathology. Occasionally seen slight thickening resulted from erythrocytes which filled the capillaries. No pathological lesions were detected (see Figure 60).

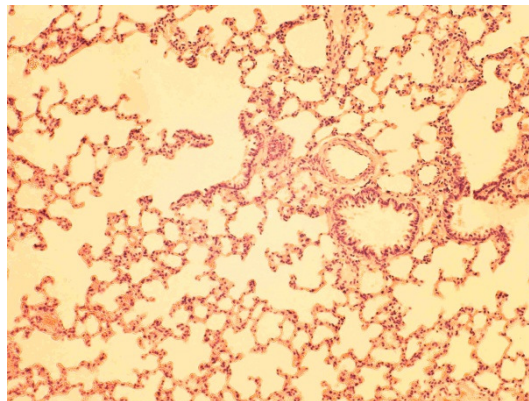
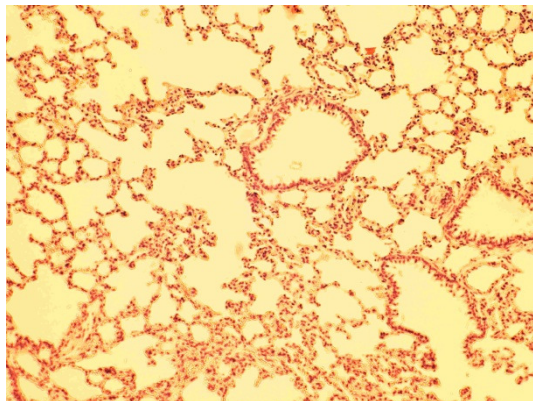


Figure 60 Lungs, a fragment of lung parenchyma. Note normal structure of parenchyma, interalveolar septa and of the bronchiole. Staining with hematoxylin and eosin. Rat No 512 (1- control) and 163 (2 - experimental). Objective magnification: x 10.

Liver – showed normal histological structure of the organ. Evident portal spaces contained normal system of blood vessels and biliary ducts. The lobular structure was preserved. The system of hepatic lamellae and hepatic sinuses was normal. Cytology of liver cells was normal. No pathological lesions were detected (Figure 61).

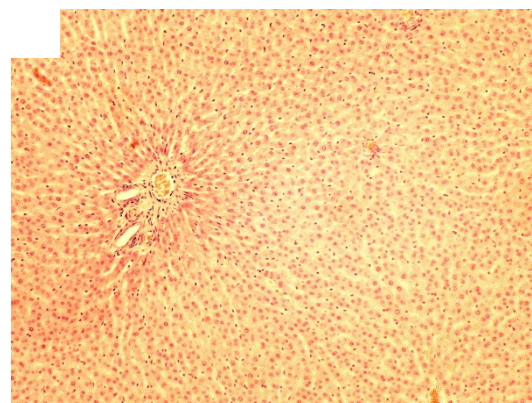
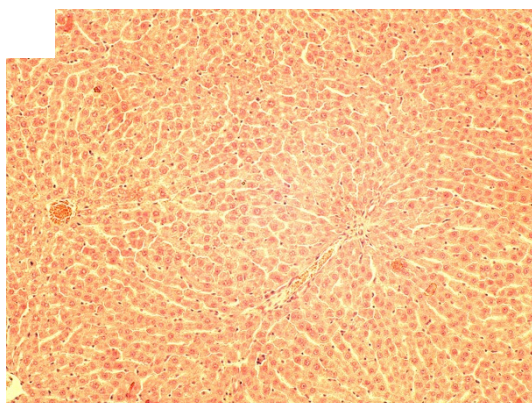


Figure 61 **Liver** Note normal structure of the organ with portal spaces and a normal pattern of trabecules and sinuses, normal structure of hepatocytes. Staining with hematoxylin and eosin. Rat No 509 (3 - control) and 164 (4 - experimental). Objective magnification: x 10.

Kidney – normal histological structure of the organ. The clear division of the organ into cortex and medulla was preserved. In the cortical part numerous renal glomeruli were present, manifesting normal structure. Individual vascular glomeruli manifested traits of cell crowding. Proximal and distal tubuli demonstrated no structural abnormalities. In the medulla the parallel system of collecting tubules and loops of Henle of a normal histological structure was noted. Medulla manifested a system of arcuate vessels and of vasa recta. No pathological lesions were detected (Figure 62).

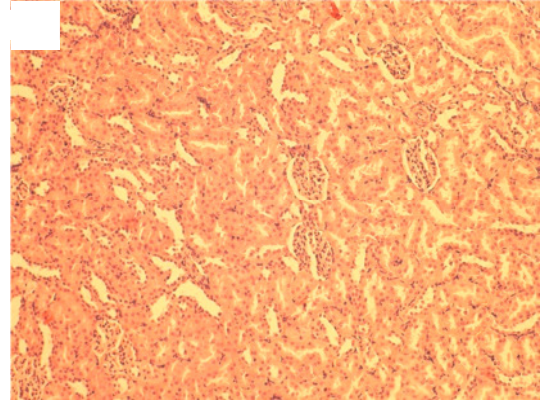
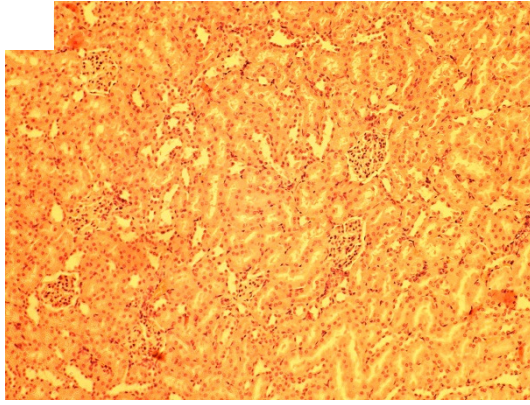


Figure 62 Kidney, cortical portion. Note normal structure of cortex, glomeruli and renal tubuli. Staining with hematoxylin and eosin. Rat No 504 (5 - control) and 162 (6 - experimental). Objective magnification: x 10.

Spleen – the organ manifested a normal histological structure. The capsule and trabecule system and the system of blood vessels showed no abnormalities. A clear division into red and white pulp was noted. The white pulp was well developed, with evident PALS and marginal zones. The red pulp contained spaces filled with erythrocytes. No pathological lesions were detected (Figure 63).

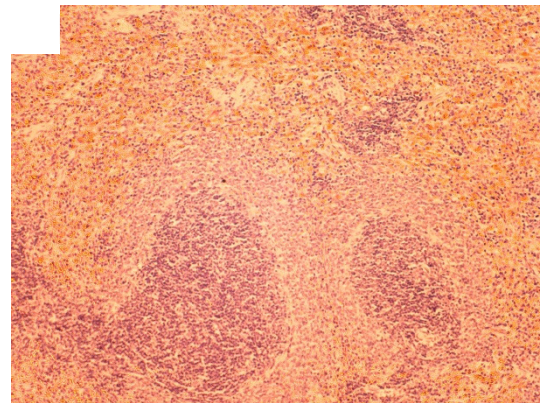
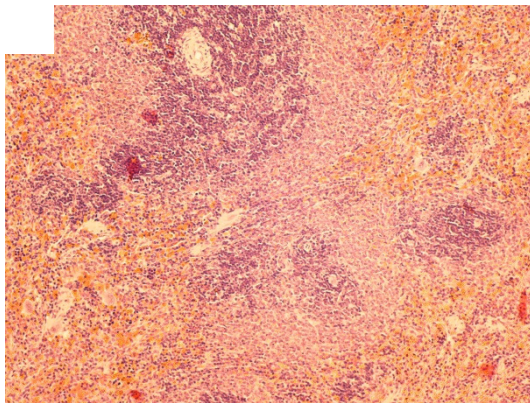


Figure 63 Spleen, a fragment of parenchyma. Note evident division into red pulp and white pulp, the wide belt of PALS and large groups of erythrocytes in the red pulp, corresponding to splenic sinuses. Staining with hematoxylin and eosin. Rat No 504 (7 - control) and 163 (8 - experimental). Objective magnification: x 10.

6.6 Hemocompatibility test

6.6.1 Thrombosis

6.6.1.1 Scanning Electron Microscopy

Figure 64 show SEM images from the *in vitro* protein adsorption tests on the hydrogel covered surfaces. No adsorption of blood components (e.g. erythrocytes, leukocytes, platelets, etc.) on the hydrogel surfaces exposed to the blood flow could be detected. What was seen was a strong modification of the hydrogel surface due to lacking of a proper freeze-drying method before the SEM characterization. When the hydrogel was dried its morphology changed completely forming clumps which could be shown by SEM on the control sample and on the surface of the hydrogel immersed in blood. On the contrary, on the gold covered

stainless steel wires some organic remnants were present; they could be possibly associated with blood stuff.

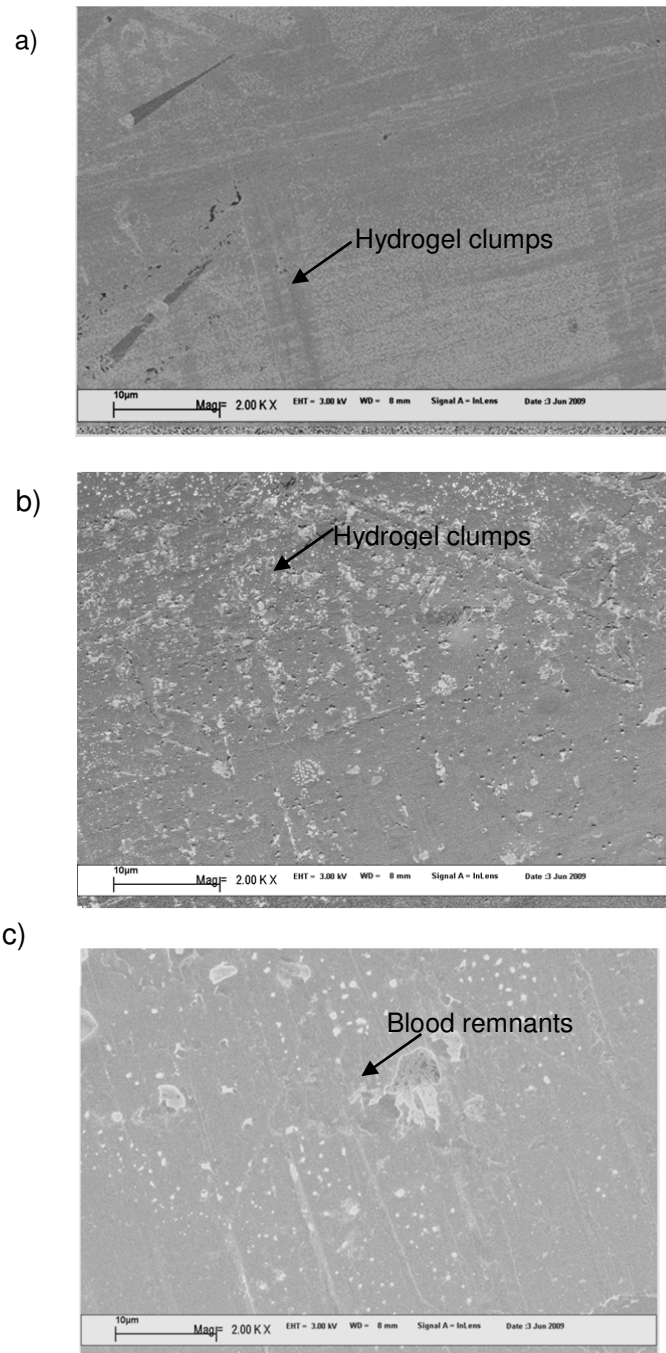


Figure 64 SEM images from the different surfaces considered for the experiment a) hydrogel covered stainless steel, b) hydrogel covered stainless steel immersed in blood, c) gold covered stainless steel immersed in blood.

All the samples were coated with a thin layer of gold before the SEM characterization performed at an accelerating voltage of 3kV using a LEO 32 microscope. The analysis consisted of three different regions that were randomly chosen on every sample. Representative images are shown in Figure 65 for the normal wires.

On the surface of the negative control we observed only features associated with the air-dried hydrogel layer as well as a high roughness characteristic of the stainless steel

wires. For Samples 2 and 3 the adsorption of organic stuff possibly associated with blood debris was found only on very few places; dominating the features associated with the hydrogel.

On the other hand, the surface of the positive control exhibited blood remnants on most of the areas that were analyzed corresponding to the black features that appear in Figure 65 (d). These results indicate the hydrophilic properties of the hydrogel are repelling efficiently the non-specific adsorption of blood components on the device.

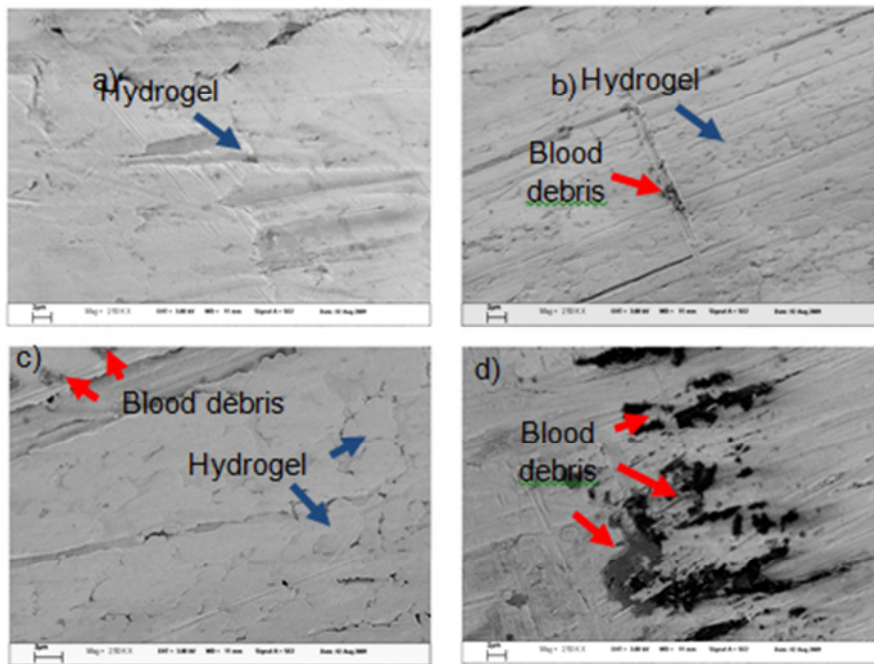


Figure 65 SEM images of the different surfaces included in the experiment functionalized with the MEMG/9 antibody: a) Negative control; b) and c) hydrogel incubated with blood; d) Positive control.

Table 13 Summary of the results of the two experiments from the SEM

Sample	Test device	Description of the sample	Category
1	Negative control	Nanodetector in no blood	without debris
2	Test device 1	Nanodetector in blood	1
3	Test device 2	Nanodetector in blood	1
4	Positive control	Au wire+LA+MEM G/9+blood	3

The hydrogel layer has a passivation effect. It reduced the unspecific blood cell or blood component binding to the wire covered with hydrogel. It can be concluded that the nanodetector did show a slight adhesion of blood cells or blood remnants under the experimental conditions of this *in vitro* study. The microscopic images (Figure 66) show no or only a few platelets adhering to the surface of wires covered with hydrogel. The control wires were undistinguishable from tested wires.

6.6.1.2 Staining for fibrin

The microscopic qualitative assessment of the deposition of fibrin and platelets on the nanodetector there is a quantitative assessment by measuring the quantity of labeled antibody, which are specific for fibrin or platelet membrane receptors. For this purpose, the nanodetector after contact with blood was washed, so that not-adhering blood components were removed prior to the binding of the labeled antibody. Under a fluorescence microscope no stained fibrin could be detected on the wire nanodetector. So one can conclude that no platelets were activated and no fibrin was bound.

6.6.1.3 Platelet adhesion

Microscopic pictures Figure 66 show the surface of wires covered with hydrogel and antibody. Probably present dots are only scratches characteristic for wire's surface. Surface of both types of wires looked uneven, probably because of the structure of hydrogel and stainless steel. There were cuts and scratches caused by gold aggregation.

The platelet adhesion studies performed in the presented experiments are not indicative of the conditions that would be observed *in vivo* because of the missing shear forces. Under static conditions it was observed that using surfaces covered with hydrogel show no platelet adhesion. There were neither activated platelets with the characteristics of spreading, aggregation and pseudopodia.

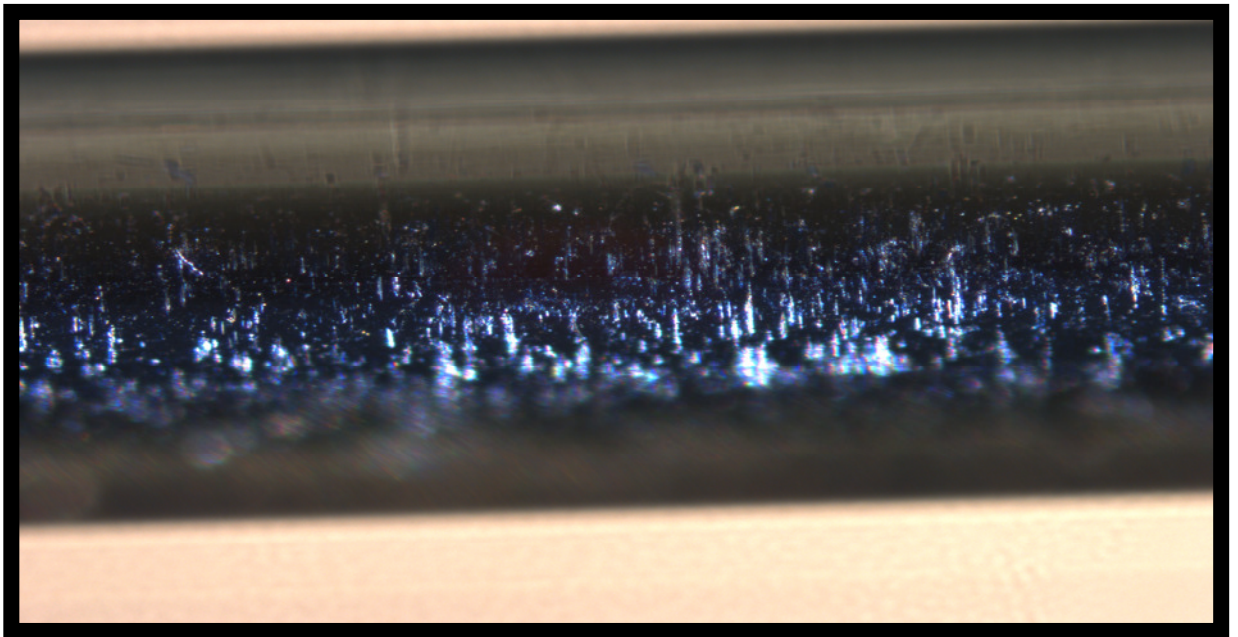
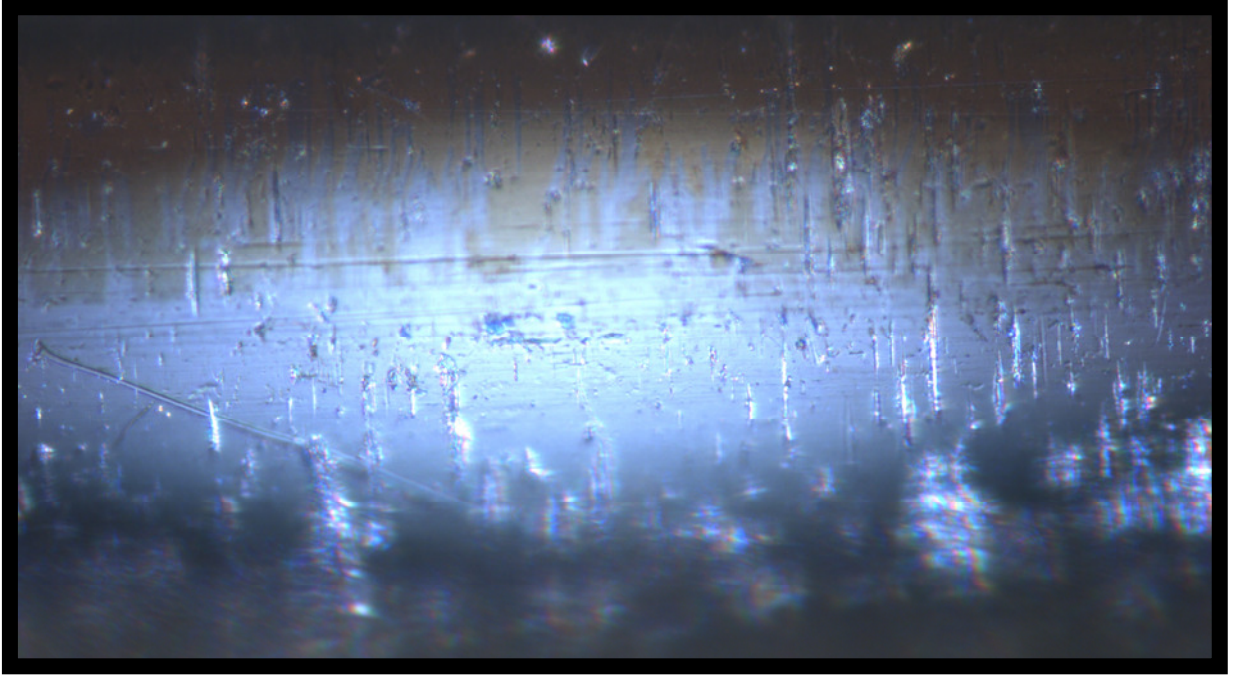


Figure 66 Pictures from light microscopy with different magnification from platelet adhesion experiments. No platelets could be seen.

6.6.2 Coagulation

Table 14 Summary of the results of the experiments from the recalcification time with different materials. PPP was mixed with CaCl_2 as long as the first fibrin threads could be detected.

	Stainless steel	Glass	Plastic	Nano-wire PEG	Wire with Hydrogel
Scratched glass	2-3 min				
Plain glass	2 min 30 s	3 min 10sec			
Plastic	11 min.; 10 min 30 s		> 12 min	11 min 20 s.	9 min; 8 min; 10 min 25 s.

The normal reaction of blood contacting a foreign surface is coagulation, leading to thrombogenesis and foreign body response. For a healthy human being this time is estimated to be 44 s. The experiment is based on adding Ca^{2+} (factor IV) in a form of CaCl_2 to platelet-poor plasma which provokes activation of prothrombin (factor II), later thrombin (TB) and finally the formation of insoluble fibrin from soluble fibrin. Performing this experiment enables us to evaluate the influence of foreign body contact (wire covered with hydrogel) to the human blood. The duration of this process is called plasma recalcification time (PRT). Combinations of glass and plastics were checked to choose the most suitable surface for performing the experiments. As we didn't observe any coagulation in the combination plastic / plastic until 12 min. after mixing this surface was chosen as the least influencing for measurements. The rest of the experiments was conducted on plastic surfaces. We tested 3 types of wires: stainless steel wires, nanostructured + PEG wires and hydrogel-covered wires. The longest time of recalcification had the nanostructured +PEG wire, longer than the stainless steel wires and as the last hydrogel wire.

The range of 8-10.5 minutes for plasma recalcification is safe for humans and the conclusion is that the wires covered with hydrogel can be used in clinical trials.

6.6.3 Specific coagulation factors

Although some values (Table 15) are out of range, one could see no significant difference between the blood sample not used in flow system and the blood sample exposed to the medical product and the flow system. All differences are within the interassay variability. The influence of the nanodetector is very low. Consequently, we can conclude that the the it is safe.

Table 15 Summary of two independent tests for specific coagulation factors.

Parameter	With flow system	With flow system, with nanodetector	Normal Range
D-Dimer	< 0,156 mg/ml 0,200 mg/ml	0,110 mg/ml < 0,156	0 – 0,278 mg/ml
Quick (TRZ)	101 % > 130 %	101 % 129 %	70 – 130 %
INR (Int. Normal. Ratio)	0,99 0,8	0,99 0,87	0,85 – 1,15
PTT	33,5 s 32,5	33,3 s 31,8 s	21 – 33,0 s

6.6.4 Hemolysis

Table 16 Hemolysis. Free hemoglobin under different conditions

	w/o flow system, w/o nanodetector	With flow system	With flow system, with nanodetector
Free Hemoglobin	25,1 $\mu\text{mol/l}$	35,5	67,4

There is free hemoglobin after filling the blood into the flow system (see Table 16) and additional hemolysis then occurs which is apparently caused by the nanodetector - presumably due to mechanically damaged erythrocyte membranes and the subsequent release of free hemoglobin. But free hemoglobin will be rapidly removed by the spleen and liver phagocyte systems. The slightly increased level is not toxic and is not dangerous for the kidney. Additionally, the blood has to pass several times through the flow system under the used experimental design. So the turnover rate of the same blood is much higher than that under *in vivo* conditions. In summary one can conclude that the nanodetector with hydrogel and antibody is safe and biocompatible.

6.7 Abrasion tests on the nanodetector

High abrasion resistance is very important for a medical device like the nanodetector. Therefore several different abrasion experiments were carried out to test whether the hydrogel or the gold can be scratched off during the application of the product.

In the abrasion experiments wires coated with gold or with gold and hydrogel were tested by single- and double-pass sliding through an 18G Vasofix Safety IV Catheter (BBraun). If pulled through the catheter carefully none or virtually none abrasion could be observed. On the contrary if the wire was tilted against the metal sleeve of the catheter the gold along with the hydrogel got scraped off. Since the bonding between gold and hydrogel proved to be stronger than between gold and wire a solid gold surface is essential for the product. A comparison test between different gold coatings confirmed galvanized wires as the best. Additionally, to minimize abrasion a catheter without a metal sleeve inside (BD Venflon) should be used for the clinical study.

As a result some rules can be deduced:

- surfaces must be rendered hydrophilic and non-charged
- coatings comprising oligomers or polymers seemed to be best suitable
- an effective barrier between the original surface and the biocompatible layer seems to be helpful not only for noble metal substrates

7 Discussion

The first version of the newly developed nanodetector was designed for isolating circulating trophoblasts from maternal blood. The predominant type of trophoblasts which circulate in maternal blood is the HLA-G-positive uninuclear endovascular trophoblast. According to recent findings about 1 cell per mL can be expected between gestational weeks 9 and 18 in the maternal blood. In contrast to current *in vitro* methods of enrichment of trophoblasts from blood samples the nanodetector is coming into contact with about 500 times more trophoblast cells during its time of application in the arm vein of a pregnant woman.

The achieved positive results of the *in vitro* functional tests of the nanodetector justify future clinical *in vivo* studies. The immunocytochemical identification of nanodetector bound cells as trophoblasts was done with anti-HLA-G specific F(ab) fragments and mAb MEM-G/9. The horizontal nanostructure approach with the hydrogel indicated a better performance of the detector because the unspecific attachment of blood cells or blood components could be prevented.

This innovative technique can be combined with FISH or PCR analyses for demonstrating the presence of genetic disorders and aberrations in the caught trophoblasts and thus has the potential to enable a less risk prone detection of trisomies such as the Down syndrome.

7.1 Functionality of the nanodetector

Nanostructured and plain gold SAW sensor surfaces were generated and compared by defining the isolation efficiencies for trophoblast cells by surface-specific antibodies. JEG-3 cells were successfully detected. Compared with a complete gold surface, sensitivity was increased.

First experiments with highly sensitive antibodies have been performed. The technology was applied to a nanostructured wire and tested in an *ex vivo* artificial blood flow-system. The major problem with the horizontal approach is the passivation of the stainless steel area between the nanospots. Different approaches to suppress the adsorption of plasma proteins, which can activate clotting factors and trigger platelet adhesion, leading to thrombosis, were applied with little success. It is the device surface that first comes into contact with blood. Thus, it is of great importance to modify the device surface with a functional hydrogel to suppress protein adsorption, and to prevent thrombogenesis and other adverse body responses. In the vertical approach the passivation problem is solved by the hydrogel. Hydrogel coated gold wires and chips were coated with anti-HLA-G antibodies and tested with spiked JEG-3 cells in blood or peripheral blood of pregnant women. Here, the flow system was also used. The flow system conditions were maintained constant. The flow rate was 1 ml / min and the incubation period was 30 minutes. The temperature was maintained at 37 ° C. The Fab and the murine antibody were used. In cell binding experiments in the flow system with 100,000 JEG-3 cells/ ml enough cells can be detected on the nanodetector for a PCR analysis. With the developed nanodetector a sensitivity in the single cell range was achieved similar to the most sensitive current methods.

In Figure 67 a single trophoblast cell isolated out of peripheral blood of a pregnant woman is shown on a nanodetector.

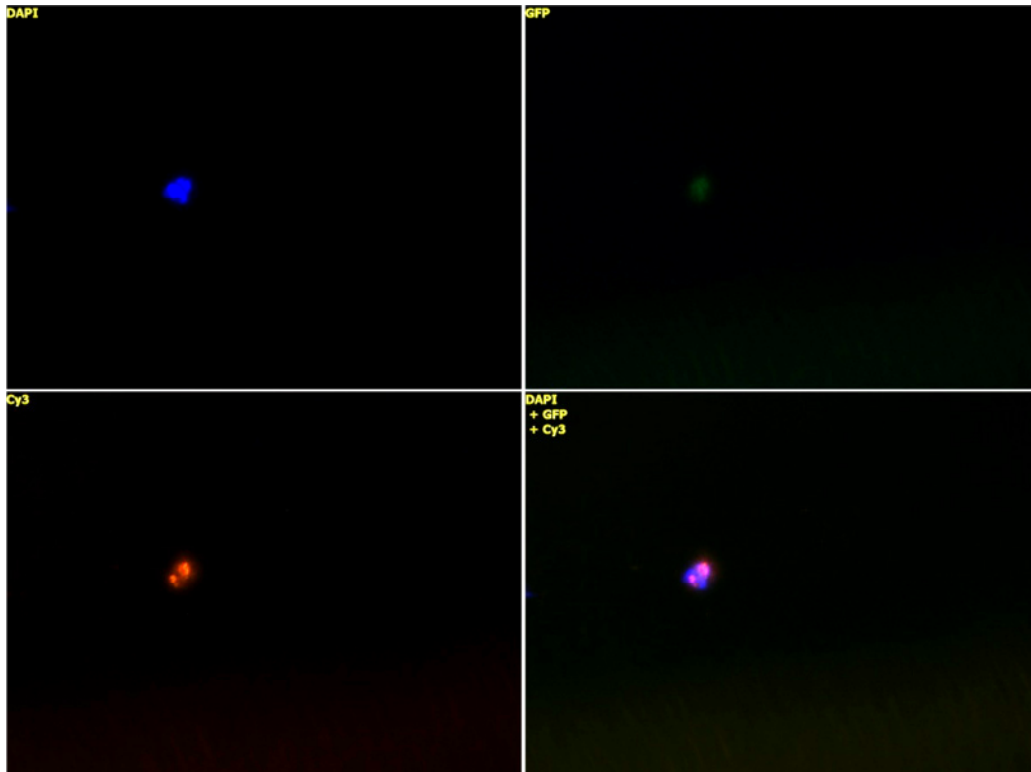


Figure 67 A trophoblast cell from peripheral blood of a pregnant woman was detected on the nanodetector. The illustrated cell is HLA-G positive (red, bottom left), has a nucleus (blue, upper left) and is CD14-negative (upper right), indicating that the cell contains HLA-G antigen, but is not a macrophage.

Experiments detecting cells from blood, serum and PBS have successfully been performed. In this set of experiments, antibody binding was based on self assembly to the nanostructures, sufficient to achieve a simple procedure avoiding toxic components from entering the surrounding fluid. Possibly, a functional orientation of the antibodies might result in even higher cell binding.

7.2 Amount of antibody on the nanodetector

To determine the amount of bound antibody the Surface Plasmon Resonance (SPR) technology was applied, a nanostructured chip was used as a model for the nanodetector. The carboxyl groups of the hydrogel surface were activated with EDC / NHS and coupled to the antibodies. To block still free binding sites, a final incubation step with ethanolamine was added. The antibody AbD10521.3 resulted in a mass increase of 10 204 RUs (see Figure 68). 1 RU corresponds to 1.6 pg/mm^2 . Accordingly, an amount of 16 ng/mm^2 is on the chip. If this quantity is used for calculating the amount of antibodies bound to the surface of the wire a theoretical amount of 775 ng antibodies could bind to the wire. Simultaneously the time was determined for the antibody incubation and a time of 30 min was found to be sufficient to achieve saturation of the surface of the wire. These results correspond with a mass loading of $7,5 \text{ ng/mm}^2$ with the Love-wave sensor. The mass loading on the BIAcore chip is generally higher than on the Love-wave sensor, which was also measured by Schlensoeg et al. [79]. They explain this difference by the lower dead volume in the flow-through cell of the BIAcore system ($0.6 \mu\text{l}$) compared with the Love-wave system ($14.5 \mu\text{l}$).

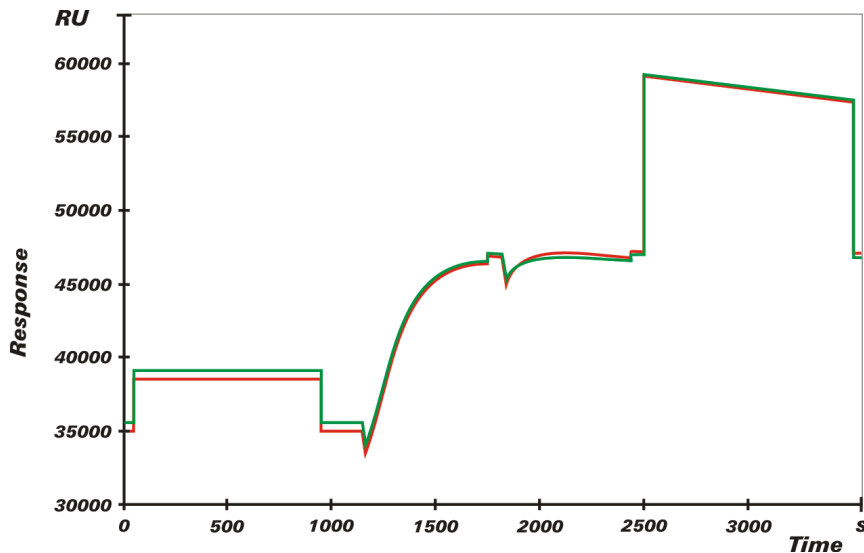


Figure 68 SPR Analysis

7.3 Device risk analysis and risk assessment (EN ISO 14971)

7.3.1 Introduction

The nanodetector should be used as a medical product, which is functionalized with immobilized human antibody fragments or the murine antibodies which are bound to carboxyl groups on top of the hydrogel in order to isolate rare cells from venous blood. The antibodies are specific against defined antigens which are located on the surface of the cells to be isolated.

7.3.2 Wire, gold and hydrogel

The antibody carrying probe is a stainless steel wire, which is already a certified medical product.

The whole wire is covered with nanostructured or complete gold. Gold is already used in the therapy of rheumatoid arthritis (RA), where its therapeutic effect is based on the reaction of sulphur containing amino acids of serum proteins with gold. However, the investigations showed that the gold contained on the nanodetector remains bound to the wire and is not set free. The only effect may be the binding of serum proteins to the gold nanostructures on the wire that are not coated with hydrogel. Stainless steel and gold are used to ensure tolerance by the human biological system.

The functional tip of the wire is covered with a hydrogel based on carboxylates. In the already performed animal trial the nanodetector without the hydrogel no side effects were detected. Many blood parameters were tested animal showed any increased value. It is known from other polymers like heparin coupled polyethylene glycol [81] that polymers exhibit good anti-fouling properties and provide a practically non-clotting surface. This was also supported by the performed biocompatibility tests in which a plasma recalcification time of 10 min was measured. Additionally, with the positive results from acute systemic toxicity and cytotoxicity tests the introduction of the hydrogel will improve the safety and the performance of the nanodetector.

7.3.3 Application time

The antibody covered nanodetectors are applied intravenously via a cannula and remain in the venous blood for selected time of 30 min.

The specificity of the antibodies bound to the probe determines the area of application of the nanodetector. Primary fields of application are prenatal diagnostics (early detection of possible genetic aberrations of the fetus) and cancer diagnostics.

7.3.4 Safety

Toxicological and biocompatibility studies of the nanodetector were carried out on the basis of observations of animals which came into contact with the detector or its components, the macroscopic evaluation of selected organs of those animals, and biochemical and haematological tests and urine analyses.

None of the performed tests revealed effects of the examined device on physiological processes or the health conditions of the animals subjected to the tests. Observed deviations of some individual parameters from reference values are not considered to have biological significance.

The histological structure of organs of the controls animals and of the animals in any experimental group did not differ and no pathological changes could be observed in the experimental groups.

Hemocompatibility and cytotoxicity tests of the nanodetector or its components were performed according to international norms and standards and did not reveal any serious disturbances. The nanodetector only caused a detectable but very low level of hemolysis.

The general conclusion based on the results of all performed tests is that the nanodetector can be expected to be well tolerated under *in vivo* conditions and in the milieu of the blood. It does not pose risks such as serious hemolysis or triggering thrombus formation and thus creating the danger of embolism for the subject.

7.4 Evaluation of the potential effects which might originate from nanodetector-bound antibodies

Structure of the used antibodies

Human Fab-fragments will be used to functionalize the nanodetector. Fab-fragments are in principal derived from antibodies by cleaving off their Fc-part, but the antibodies for the nanodetector are produced as Fab-fragments. They are still able to bind their specific antigen and are thus ensuring the intended functionality of the nanodetector but lack the domain of the antibody which is responsible for numerous other functions and interactions of a complete antibody.

Assessment of purity of the used antibodies

The final Fab preparations are checked for their endotoxin contents and their protein composition. They mainly contain Di-Fab fragments as the basic functional fraction and high molecular weight aggregates which – according to their immunoblot reactivity - are composed of human antibody fragments – apparently fragments of the two chains which make up the antibody but which are not linked together to a functional unit. They are not of microbial origin.

Amount of antibodies immobilized on the nanodetector

The total amount of antibodies or antibody fragments which will be covalently bound to the nanodetector is far below the amount of 30 nmol which is considered to be safe for

proteins which are applied intravenously – lower by a factor of 10^3 - and is in the range of 3 micrograms.

In addition to this the production of human anti-human or human anti-mouse antibodies may prove to be a risk factor [84], but the extremely small amount of antibodies totally bound to the nanodetector is below the scientifically accepted amount known to trigger such a reaction. Due to the fact that fully human antibodies are used the risk of reaction against the antibody is extremely low.

Therapeutic effects of the antibodies fixed onto the nanodetector are extremely unlikely or can be completely ruled out for the following reasons:

- The antibodies used for the nanodetector are immobilized on the nanodetector in extremely small amounts.
- The antibodies are bound to the hydrogel on the nanodetector via covalently bonds, which cannot easily be broken.
- The antibodies on the nanodetector stay in the organism for half an hour and are then completely removed from the system together with the nanodetector.
- Even if all antibodies bound to the nanodetector would get lost and would be set free a therapeutic effect of these antibodies could be ruled out because the total amount fixed to the nanodetector is extremely small and in the microgram range.
- Scientific investigations prove that there is a certain dose limit for every substance below which there is no pharmacological effect caused by a substance in a test person. Information can be found on the Emea homepage. [85]
- For proteins, antibodies are proteins, there is an accepted limit amount of 30 nmol—more than a thousand times the amount on the nanodetector. Even though antibodies have specific effects the absolute amount of antibody bound onto the surface of the nanodetector is far below the limit amount which is necessary for triggering its specific effects.
- For decades therapeutic antibodies are an integral part of modern medicine in the treatment of various diseases – especially of cancers. They are used in gram amounts to achieve therapeutic effects - amounts which exceed those used on the probes by a factor of at least 10^6 . Even the treatment of pregnant women suffering from cancer with high amounts of therapeutic antibodies did not cause any effects or damage in mother and child [86-89].
- Recently, [90, 91] have applied Fab-fragments intravenously for diagnostic and therapeutic purposes in milligram amounts and have seen no side effects endangering the health of their patients.
- In the much smaller mouse organism [92, 93] were able to show that anti-HLA-G-antibodies, similar to those used on the nanodetector - but in doses as high as 100 μg - are unable to elicit detectable cellular reactions after binding to their target. For the same reasons a chain of reactions with negative effects cannot be expected after an antibody molecule which is lost from the nanodetector has bound to its target.
- It is the intention to use Fab-fragments of specific antibodies. They are lacking the Fc-part of complete antibodies which is essential for mediating therapeutic effects. Since this domain is responsible for the detection of antigen-antibody complexes by phagocytes Fab fragments are generally not able to trigger any substantial systemic effect.
- Other relevant effects caused by antibodies released from the nanodetector – like early or late reactions mediated by different branches of the innate or adaptive immune system – are also unlikely. The amount of antibodies is too small to trigger such reactions.

7.4.1 The use of fully human antibodies is preferred to murine, humanized or chimeric antibodies

In general, monoclonal antibodies are generated in mice. However, mouse antibodies have a very restricted use in *in vivo* applications, because mouse antibodies (murine antibodies, ending -omab) may be recognized in the human organism as a foreign antigen and could eventually elicit an immunological response resulting in the production of so called HAMA (human-anti-mouse-antibodies). This immune response can be reduced if the mouse antibodies are chimeric or humanized so that their immunogenicity is lowered.

Recently it has become possible to create fully human antibodies. Immunogenicity of these antibodies is not expected according to current data. However due to the fact that antibodies are proteins these antibodies may still cause an immune response.

In the present form of the nanodetector a maximum amount of 3 µg of the human antibody is exposed to the human circulatory system. From that amount not more than 10 % are estimated to be released into the circulation. This amount is at least 10⁵ times lower than the dosage of common therapeutic antibodies.

7.5 Therapeutic monoclonal antibodies

A number of antibodies have been successfully introduced into therapy (see Table 17). These are either mouse (-omab), chimeric (-ximab), humanized (-zumab) or human (-umab) antibodies. Chimeric antibodies contain the constant part of the immunoglobulin as a human amino acid sequence. Only the variable regions (Fab) are obtained from mouse antibodies.

Monoclonal antibodies have been used in therapy for many years. The areas of implementation apart from cancer therapy are immunological diseases e.g. rheumatoid arthritis (RA), Alzheimer's disease, transplant rejection, viral infections and allergic reactions, to name but a few.

Table 17 **Therapeutic** antibodies, which are fully human or at least chimeric and which have partially been applied in pregnant women.

Name Medicine (original name)	Type	Target structure /Antigen	Scope of implementation for a specific disease	Application according to professional information
Panitumumab Vectibix®	Human	EGF- receptor	EGF-receptor expressing tumors, colorectal cancer	6 mg/kg body weight every 2 weeks
Rituximab MabThera®	Chimeric	CD20	NHL (non-Hodgkin Lymphoma)	375 mg/m ² /week for 4 weeks
Adalimumab Humira®	Phage display, human library	Tumor necrosis factor α (TNF-α)	RA (Rheumatoid arthritis), psoriasis-arthritis, Morbus Bechterew, Morbus Chron	40 mg every 2 weeks
Ranibizumab (rhuFab V2) Lucentis	Humanised Fab	VEGF	Wet age-related macular degeneration (AMD)	0,5 mg/eye in 4 weeks interval
Muromonab (OKT3)	Murine	CD3 (T cells)	Transplantation, rheumatoid arthritis	

Orthoclone				
Igovomab (OC125) Indimacis-125	Murine F(ab') ₂ fragment	CA125	Gastrointestinal, ovarian cancer	

Panitumumab (Vectibix, Amgen Inc, FDA approval in 2006 for metastatic colorectal cancer when other therapies fail) is a human monoclonal antibody against EGFR. It is applied at a dosage of 6 mg/ kg body weight given within 60 min every 2 weeks. Severe infusion reactions were observed in 1 % of clinical study patients. These reactions included anaphylactic reactions, bronchospasm, fever, chills, and hypotension. Fatal infusion reactions did not occur (http://www.amgen.com/pdfs/products/vectibix_pi.pdf).

Rituximab has been used in pregnant women [88]. They treated a pregnant woman of week 16 in her pregnancy with four weekly infusions of rituximab (375 mg/m²), because she developed a Burkitt lymphoma during pregnancy. At the time of birth, both mother and child had very high serum levels of rituximab with a complete absence of B-cells. The concentration of rituximab in the cord blood (32 µg/ml) exceeded that in the mother's serum three times. Due to an active transport involving specific Fc-receptors at the placental barrier fetal concentrations of different physiological IgG types usually exceed maternal concentrations at full term. As rituximab has a human IgG/k constant region, this mechanism might be involved in this case. Up to the age of 26-months the girl was repeatedly seen by her paediatrician, who reported completely normal growth and developmental status.

A similar case was reported by [94], in which a woman treated for a non-Hodgkin lymphoma (NHL) became pregnant between the first and second treatment infusion with rituximab. Pregnancy was diagnosed one week after the final infusion with rituximab. Early pregnancy was without complications and had no serious side effects on the fetus.

Adalimumab (Humira, Abbott, EU approval for Morbus Bechterew in 2006) [95] is a human monoclonal antibody against TNF-α, which is applied at a dosage of 40 mg/ adult by subcutaneous injection every two weeks. Adverse effects were found to be mild to moderate [96].

Antibodies have been used in medicine for several purposes and fields of application for more than a century. Today the number of antibodies for therapy and diagnostics is steadily increasing. Many of these antibodies are used for fighting cancers or other chronic illnesses – like rheumatoid arthritis. In contrast to antibodies for diagnostic purposes the antibodies for a prospected therapeutic application are given in large amounts. In the past there were several reports documenting possible complications related to the use of therapeutic antibodies. Apparently these problems could be attributed to the specific effects of the administered antibody or to the large amount given and not to the structure of the antibodies – human or murine.

All conceivable consequences and effects of antibodies which might be applied to a living human being require a minimal amount of antibody which is not even reached if all the antibodies which are bound to the nanodetector would get lost from it during its application.

Based on the scientific literature the following statement can be made: antibodies neither those fixed on the nanodetector nor those antibodies sheared off from the probe – even if they were totally set free - would be expected to have therapeutic or pharmacological effects.

The risk of hematogenic reactions during the application is going to be investigated in the first phase of the clinical investigation with healthy women. This risk may include the unspecific binding of proteins, resulting in a blood clot or in local inflammation. In addition the insertion of the nanodetector may result in a hematoma at the site of puncture, catheter-

caused sepsis, arterial injuries due to incorrect punctures, catheter induced thrombosis, thrombophlebitis and thromboembolism or other generalized reactions.

7.6 Risk analysis and assessment including a description of the risk graph

The objective of a risk analysis is protect the patient. Here a first risk assessment based, for the nanodetector in the definition of a Risk graph is implemented. Three areas have been defined as "largely acceptable", "ALARP (as low as reasonable possible) " and " unacceptable ". The result of the risk assessment by the product to the patient should be in the "acceptable" or at least after taken measurements in the "ALARP" region. The product is not suitable for clinical use, when the risk analysis included "not acceptable" fields. The following risk graph which was created with the Quare Risk Manager in accordance to DIN EN ISO 14 791, [97] it also contains all possible partely purely theoretical risks, before and after taken effective risk reduction techniques. The different fields (green = acceptable range, yellow = ALARP region, red = Not acceptable range) contained statistics reflect the number of risks equal probability and the same level of damage.

frequent	yellow	red	red	red
probable	yellow	red	red	red
occasionally	yellow	yellow	1	2
imaginable	green	yellow	yellow	red
improbable	green	green	yellow	yellow
unimaginable	green	green	green	green
	unimportant	low	serious	catastrophic

Amnioncentesis: 1 means : Health risk for the pregnant women
 2 means: lesion of the child

frequent	yellow	red	red	red
probable	yellow	red	red	red
occasionally	yellow	yellow	red	red
imaginable	green	yellow	yellow	red
improbable	green	green	yellow	yellow
unimaginable	green	green	green	green
	unimportant	low	serious	catastrophic

NANODETECTOR 1 means: Insertion of Nanodetector for 30 mins

In order to avoid potential risks of lesion of the vein only well trained persons should perform the vein puncture.

To avoid the risk of thrombosis hemocompatibility tests for platelet aggregation, fibrin formation and protein absorption were performed. The results showed full biocompatibility of the catheter in respect to the risks mentioned above.

A risk comparison between amnioncentesis and the usage of the nanodetector is shown in

7.7 Claims and intended performance of the device that are to be verified in a clinical study

To protect the safety of the subjects, a study should be divided into two parts, because in the study the nanodetector of this design will be used in humans for the first time. The proposed study will assess the safety (part I) as well as the functionality (part II) of the antibody-coated medical wire:

The first phase should be performed with healthy women with the intention of assessing a potential risk. After this study, pregnant women should be exposed for 30 min to assess the functionality after the safety has been shown in part I.

Primary objective: to catch trophoblast cells in pregnant women in the 10th till 14th week of gestation. The gender and chromosomal aberrations of the fetus should be analysed with PCR or FISH. To prove the result of the gender analysis of the fetus women have to go for a further ultrasound examination in week 10-20 of gestation.

7.8 Possible other applications

The basic concept and the design of the developed nanodetector provide a promising platform for other fields of medical applications. In prenatal diagnostics fetal nucleated erythroid cells or even DNA fragments could be possible targets to be bound by the detector. Employing different binding molecules extends the opportunities of the detector further. In cancer diagnostics circulating tumor cells (CTC) are of major interest. They could also be isolated for diagnostics by this technique and even the isolation of special cell types for their

transient *in vitro* cultivation and propagation for treatment of certain diseases may be an option for the detector.

7.9 Can enough cells be caught ?

The main goal of the application of the nanodetector under the scope of this work is to capture a sufficient number of defined fetal cells out of the circulating blood. These cells are to be used for subsequent analyses which require a minimum number of such cells to get a reliable description of the genetic status of the fetus. On the basis of the sensitivity of the present diagnostic methods a number of 10 such cells should be sufficient for this purpose – a number which the nanodetector is expected to bind under *in vivo* conditions.

In addition, the concept of isolating rare cells under *in vivo* conditions with a detector on the basis of the developed device offers the opportunity for further improvements of the method:

The efficacy of the wire could be enhanced

- by prolonging the functional tip of the wire,
- by introducing improved structural elements in the functional area,
- by increasing the application time and
- by employing antibodies against more than just one target on the cells in focus or against several different cell types.

8 Conclusions

1. A common medical guide wire can provide the base for a functional effective nanodetector, a tool able to detect and isolate minimal residual unique cells population out of the peripheral blood.
2. It was shown that nanodetector is efficient, safe and easy tool can be applied in medical procedures aiming *in vivo* cell isolation from peripheral blood.
3. Covered with hydrogel and specific antibodies (humanized specific F(ab) fragments and mAb MEM-G/9) against HLA-G antigens nanodetector can be used for *in vivo* isolation of trophoblast cells with high specificity. It has full hemocompatibility, is not cytotoxic and immunogenetic.
4. *In vivo* usage of the nanodetector can be considered as an alternative method for obtaining fetal derived biological material for prenatal diagnostics minimal invasive for mother and non-invasive for a child.

9 Summary

The current prenatal diagnostic which is based mainly on invasive procedures carries out both for a child and a mother any significant risk. There are any non-invasive methods for access fetal tissue derived diagnostic material suitable for further evaluation. It is known that from the earliest stages of pregnancy (approximately 10 weeks of gestational) there are circulating trophoblasts in the peripheral blood. The goal of this study was to isolate these cells. In order to achieve the goal a common medical guide wire was used as a base for developing a nanodetector, a device covered by specific antibodies targeting trophoblast cells. During the development of a nanodetector different optimized nanostructure surface (horizontal or vertical approach) were tested. With the help of flow cytometry and SPR the antibody specificity and avidity was characterized as well as antibody amount on the nanodetector surface was determined. Determination of nanodetector cell binding efficiency in *in vitro* and *in vivo* settings were preceded by evaluation of nanodetector cytotoxicity, hemocompatibility and immunogenicity.

For isolating trophoblast cells the recognition of the HLA-G antigen present on their plasma membrane by a specific antibody was essential. HLA-G has an important role in reproduction because its restricted expression to extravillous trophoblasts protects fetus from destruction by mother's immune system.

Different technologies were used to bind antibodies specific for HLA-G onto the novel nanodetector device. Besides integration of a hydrogel component allowed the reduction of unspecific binding of blood components. In *in-vitro* experiments performed on an *ex vivo* flow system which mimics peripheral blood flow, showed that nanodetector was able to isolate trophoblast cells from blood environment. The device has been optimized for maximal isolation efficiencies.

The conclusion of the study are:

1. A common medical guide wire can provide the base for a functional effective nanodetector, a tool able to detect and isolate minimal residual unique cells population out of the peripheral blood.
2. It was shown that nanodetector is efficient, safe and easy tool can be applied in medical procedures aiming *in vivo* cell isolation from peripheral blood.
3. Covered with hydrogel and specific antibodies (humanized specific F(ab) fragments and mAb MEM-G/9) against HLA-G antigens nanodetector can be used for *in vivo* isolation of trophoblast cells with high specificity. It has full hemocompatibility, is not cytotoxic and immunogenic.
4. *In vivo* usage of the nanodetector can be considered as an alternative method for obtaining fetal derived biological material for prenatal diagnostics minimal invasive for mother and non-invasive for a child.

10 References

1. Cunniff, C., *Prenatal Screening and Diagnosis for Pediatricians*. Pediatrics, 2004. 114: p. 889-894.
2. Papp, C., Papp, Z., *Chorionic villus sampling and amniocentesis: what are the risks in current practice?* Curr. Opin. Obstet. Gynecol., 2003. 15: p. 159-165.
3. Evans, M.I., Wapner, R.J., *Invasive Prenatal Diagnostic Procedures 2005, Invasive Prenatal Diagnostic Procedures 2005*. Semin. Perinatology, 2005. 29: p. 215-218.
4. Snijders, R.J., Noble, P., Sebire, N., Souka, A., Nicolaides, K.H., *UK multicentre project on assessment of risk of trisomy 21 by maternal age and fetal nuchal-translucency thickness at 10–14 weeks of gestation*. Lancet, 1998. 352: p. 343–346.
5. Cicero, S., Avgidou, K., Rembouskos, G., Kagan, K.O., Nicolaides, K.H., *Nasal bone in first-trimester screening for trisomy 21*. Am J Obstet Gynecol., 2006. 195: p. 109–114.
6. Tongsong T, W.C., Kunavatikul C, Sirirhotiyakul S, Piyamongkol W, Chanprapaph P., *Fetal loss rate associated with cordocentesis at midgestation*. . Am J Obstet Gynecol. , 2001. 184: p. 719–723.
7. Fan, H.C., Blumenfeld, Y.J., Chitkara, U., Hudgins, L., Quake, S.R., , *Noninvasive diagnosis of fetal aneuploidy by shotgun sequencing DNA from maternal blood*. PNAS, 2008. 105(42): p. 16266-16271.
8. Zimmermann, B.G., et al., *Digital PCR: a powerful new tool for noninvasive prenatal diagnosis?* Prenat Diagn, 2008. 28(12): p. 1087-93.
9. Wilson, R.D., Gagnon, A., Davies, G., Desilets, V., Reld, G.J., Summers, A., Wyatt, P., Allen, V., Langlois, S. , *Cell-free fetal DNA in the maternal circulation and its future uses in obstetrics*. . JOGC, 2005. 152: p. 54-57.
10. Chiu, R.W.K., Ranjit Akolekar, YamaWL Zheng, Tak Y Leung, Hao Sun, K C Allen Chan, Fiona M F Lun, Attie T J I Go, Elizabeth T Lau, WilliamWK To, Wing C Leung, Rebecca Y K Tang, Sidney K C Au-Yeung, Helena Lam, Yu Y Kung, Xiuqing Zhang, John M G van Vugt, Ryoko Minekawa, Mary H Y Tang, Jun Wang, Cees B M Oudejans, Tze K Lau, Kypros H Nicolaides, Y M Dennis Lo, *Non-invasive prenatal assessment of trisomy 21 by multiplexed maternal plasma DNA sequencing: large scale validity study*. BMJ, 2011. 342(7401).
11. Papageorgiou EA, K.A., Tsaliki E, Velissariou V, Carter NP, Patsalis PC. , *Fetal-specific DNA methylation ratio permits noninvasive prenatal diagnosis of trisomy 21*. Nat Med., 2011. 17(4): p. 510-3.
12. Huppertz, B., Kadyrov, M., Kingdom, J. C., *Apoptosis and its role in the trophoblast*. Am. J. Obstet. Gynecol., 2006. 195(1): p. 29-39.
13. Stenqvist, A.-C., Chen, T., Hedlund, M., Dimova, T., Nagaeva, O., Kjellberg, L., Innala, E., Mincheva-Nilsson, L., *An efficient optimized method for isolation of villous trophoblast cells from human early pregnancy placenta suitable for functional and molecular studies*. American Journal of Reproductive Immunology, 2008. 60: p. 33-42.
14. Schmorl, G., *Pathologisch-anatomische Untersuchungen über Puerperal-Eklampsie*. FCW Vogel, 1893.
15. Lapaire, O., et al., *Georg Schmorl on trophoblasts in the maternal circulation*. Placenta, 2007. 28(1): p. 1-5.
16. Hiby, S.E., et al., *Molecular studies of trophoblast HLA-G: polymorphism, isoforms, imprinting and expression in preimplantation embryo*. Tissue Antigens, 1999. 53(1): p. 1-13.

17. Crisa, L., et al., *Identification of a thymic epithelial cell subset sharing expression of the class Ib HLA-G molecule with fetal trophoblasts*. J Exp Med, 1997. 186(2): p. 289-98.
18. Mallet, V., et al., *HLA-G in the human thymus: a subpopulation of medullary epithelial but not CD83(+) dendritic cells expresses HLA-G as a membrane-bound and soluble protein*. Int Immunol, 1999. 11(6): p. 889-98.
19. Carosella, E.D. and J. LeMaout, *HLA-G: a look back, a look forward*. Cell Mol Life Sci, 2011. 68(3): p. 337-40.
20. Rizzo, R., et al., *The importance of HLA-G expression in embryos, trophoblast cells, and embryonic stem cells*. Cell Mol Life Sci, 2011. 68(3): p. 341-52.
21. Bahri, R., et al., *Soluble HLA-G inhibits cell cycle progression in human alloreactive T lymphocytes*. J Immunol, 2006. 176(3): p. 1331-9.
22. Menier, C., et al., *Erythroblasts secrete the nonclassical HLA-G molecule from primitive to definitive hematopoiesis*. Blood, 2004. 104(10): p. 3153-60.
23. Carosella, E.D., et al., *Beyond the increasing complexity of the immunomodulatory HLA-G molecule*. Blood, 2008. 111(10): p. 4862-70.
24. Le Bouteiller, P., C Solier, J Pröll, M Aguerre-Girr, S Fournel, F Lenfant *Mini symposium. The major histocompatibility complex in pregnancy: Part II. Placental HLA-G protein expression in vivo: where and what for?* Hum. Reprod. Update, 1999. 5(3): p. 223-233.
25. Ganshirt, D., H.S. Garritsen, and W. Holzgreve, *Fetal cells in maternal blood*. Curr Opin Obstet Gynecol, 1995. 7(2): p. 103-8.
26. van Wijk, I.J., et al., *Enrichment of fetal trophoblast cells from the maternal peripheral blood followed by detection of fetal deoxyribonucleic acid with a nested X/Y polymerase chain reaction*. Am J Obstet Gynecol, 1996. 174(3): p. 871-8.
27. Bianchi, D.W., *Current knowledge about fetal blood cells in the maternal circulation*. J Perinat Med, 1998. 26(3): p. 175-85.
28. Taniguchi, R., et al., *Trophoblastic cells expressing human chorionic gonadotropin genes in peripheral blood of patients with trophoblastic disease*. Life Sci, 2000. 66(17): p. 1593-601.
29. Knight, M., et al., *Shedding of syncytiotrophoblast microvilli into the maternal circulation in pre-eclamptic pregnancies*. Br J Obstet Gynaecol, 1998. 105(6): p. 632-40.
30. Sargent, I.L., A.M. Borzychowski, and C.W. Redman, *Immunoregulation in normal pregnancy and pre-eclampsia: an overview*. Reprod Biomed Online, 2006. 13(5): p. 680-6.
31. Hawes, C.S., Suskin, H.A., Kalionis, B., Mueller, U.W., Casey, G., Hall, J., Rudzki, Z., *Detection of paternally inherited mutations for beta-thalassemia in trophoblast isolated from peripheral maternal blood*. ANNALS NEW YORK ACADEMY OF SCIENCES 1994. 731: p. 181-5.
32. Mueller, U.W., Hawes, C.S., Wright, A.E., Petropoulos, A., DeBoni, E., Firgaira, F.A., Morley, A.A., Turner, D.R., Jones, W.R., *Isolation of fetal trophoblast cells from peripheral blood of pregnant women*. Lancet, 1990. 336(8709): p. 197-200.
33. Cacheux, V., Milesi-Fluet, C., Tachdjian, G., Druart, L., Bruch, J.F., Hsi, B.L., Uzan, S., Nessmann, C., *Detection of 47, XYY trophoblast fetal cells in maternal blood by fluorescence in situ hybridization after using immunomagnetic lymphocyte depletion and flow cytometry sorting*. Fetal Diagn. Ther. , 1992. 7(3-4): p. 190-4.

34. Sbracia, M., Scarpellini, F., Lalwani, S., Grasso, J.A., Scarpellini, L., *Possible use of an unusual HLA antigen to select trophoblast cells from the maternal circulation to perform early prenatal diagnosis*. Ann. N. Y. Acad. Sci., 1994. 731: p. 170-4.
35. Durrant, L., McDowall, K., Holmes, R., Liu, D., *Non-invasive prenatal diagnosis by isolation of both trophoblasts and fetal nucleated red blood cells from the peripheral blood of pregnant women*. Br. J. Obstet. Gynaecol., 1996. 103(3): p. 219-22.
36. van Wijk, I.J., et al., *HLA-G expression in trophoblast cells circulating in maternal peripheral blood during early pregnancy*. Am J Obstet Gynecol, 2001. 184(5): p. 991-7.
37. Oudejans, C.B., et al., *Circulating trophoblast in maternal blood*. Prenat Diagn, 2003. 23(2): p. 111-6.
38. Lim, T.H., A. Tan, and V.H. Goh, *Enrichment of fetal trophoblasts and nucleated erythrocytes from maternal blood by an immunomagnetic colloid system*. Hum Genet, 1999. 104(5): p. 399-404.
39. Hviid, T.V., S. Sorensen, and N. Morling, *Detection of fetal-specific DNA after enrichment for trophoblasts using the monoclonal antibody LK26 in model systems but failure to demonstrate fetal DNA in maternal peripheral blood*. Prenat Diagn, 1999. 19(3): p. 271-8.
40. Schueler, P.A., et al., *Inconsistency of fetal trophoblast cells in first trimester maternal peripheral blood prevents non-invasive fetal testing using this cell target*. Placenta, 2001. 22(8-9): p. 702-15.
41. Lim, T.H., A.S. Tan, and V.H. Goh, *Relationship between gestational age and frequency of fetal trophoblasts and nucleated erythrocytes in maternal peripheral blood*. Prenat Diagn, 2001. 21(1): p. 14-21.
42. Koumantaki, Y., et al., *Microsatellite analysis provides efficient confirmation of fetal trophoblast isolation from maternal circulation*. Prenat Diagn, 2001. 21(7): p. 566-70.
43. Vona, G., et al., *Enrichment, immunomorphological, and genetic characterization of fetal cells circulating in maternal blood*. Am J Pathol, 2002. 160(1): p. 51-8.
44. Guetta, E., L. Gutstein-Abo, and G. Barkai, *Trophoblasts isolated from the maternal circulation: in vitro expansion and potential application in non-invasive prenatal diagnosis*. J Histochem Cytochem, 2005. 53(3): p. 337-9.
45. Zhang, L., Y. Wang, and A.H. Liao, *Quantitative abnormalities of fetal trophoblast cells in maternal circulation in preeclampsia*. Prenat Diagn, 2008. 28(12): p. 1160-6.
46. Daniel, M.-C.A., D., *Gold Nanoparticles: Assembly, Supramolecular Chemistry, Quantum-Size-Related Properties, and Applications toward Biology, Catalysis, and Nanotechnology*. Chem. Rev., 2004. 104(1): p. 293-346.
47. Eustis, S. and M.A. el-Sayed, *Why gold nanoparticles are more precious than pretty gold: noble metal surface plasmon resonance and its enhancement of the radiative and nonradiative properties of nanocrystals of different shapes*. Chem Soc Rev, 2006. 35(3): p. 209-17.
48. Rotello, V., *Nanoparticles Building Blocks For Nanotechnology*. Nanostructure Science and Technology Series, Ed. D. J. Lockwood., 2004.
49. Schmid, G., *Nanoparticles: From Theory To Application*. 2004.
50. Jennings, T., Strouse, G. , *Past, present, and future of gold nanoparticles*. Adv. Exp. Med. Biol., 2008. 620: p. 34-35.

51. Ghosh, P., et al., *Gold nanoparticles in delivery applications*. Adv Drug Deliv Rev, 2008. 60(11): p. 1307-15.
52. Gil, P.R. and W.J. Parak, *Composite nanoparticles take aim at cancer*. ACS Nano, 2008. 2(11): p. 2200-5.
53. Jain, K.K., *Nanomedicine: application of nanobiotechnology in medical practice*. Med Princ Pract, 2008. 17(2): p. 89-101.
54. Xing, Y. and J. Rao, *Quantum dot bioconjugates for in vitro diagnostics & in vivo imaging*. Cancer Biomark, 2008. 4(6): p. 307-19.
55. Michalet, X., et al., *Quantum dots for live cells, in vivo imaging, and diagnostics*. Science, 2005. 307(5709): p. 538-44.
56. Jain, K.K., *Drug delivery systems - an overview*. Methods Mol Biol, 2008. 437: p. 1-50.
57. Jain, K.K., *Recent advances in nanooncology*. Technol Cancer Res Treat, 2008. 7(1): p. 1-13.
58. Gaumet, M., et al., *Nanoparticles for drug delivery: the need for precision in reporting particle size parameters*. Eur J Pharm Biopharm, 2008. 69(1): p. 1-9.
59. Ozdemir, V., et al., *Shifting emphasis from pharmacogenomics to theragnostics*. Nat Biotechnol, 2006. 24(8): p. 942-6.
60. Firkowska, I., Giannona, S., Rojas-Chapana, J., Lücke, K., Brüstle, O., Giersig M., *Biocompatible Nanomaterials and Nanodevices promising for Biomedical Applications*. Nanomaterials for Application in Medicine and Biology, 2008: p. 1-16.
61. Kosiorek, A., et al., *Fabrication of nanoscale rings, dots, and rods by combining shadow nanosphere lithography and annealed polystyrene nanosphere masks*. Small, 2005. 1(4): p. 439-44.
62. Clements, C.S., et al., *Crystal structure of HLA-G: a nonclassical MHC class I molecule expressed at the fetal-maternal interface*. Proc Natl Acad Sci U S A, 2005. 102(9): p. 3360-5.
63. Kohler, G. and C. Milstein, *Continuous cultures of fused cells secreting antibody of predefined specificity*. Nature, 1975. 256(5517): p. 495-7.
64. Barbas, C.F., Lerner, R.A., *Combinatorial immunoglobulin libraries on the surface of Phage (Phabs): Rapid Selection of antigen-specific Fabs*. Methods: A Comparison of Methods in Enzymol, 1991. 2(2): p. 119-124.
65. Florek, E., Bręborowicz, G.H., Lücke, K., Madejczyk, M., Chuchracki, M., Dworacki, G., Zabel, M., Giersig, M., *The acute systemic toxicity study for normal catheter and cell-select catheter (CSC)*. Archives of Perinatal Medicine, 2008. 14(2): p. 20-31.
66. Gyovary, E., et al., *Formation of nanoparticle arrays on S-layer protein lattices*. J Nanosci Nanotechnol, 2004. 4(1-2): p. 115-20.
67. Heddle, J.G., et al., *Using the ring-shaped protein TRAP to capture and confine gold nanodots on a surface*. Small, 2007. 3(11): p. 1950-6.
68. Armelao, L., et al., *Preparation of gold nanoparticles on silica substrate by radio frequency sputtering*. J Nanosci Nanotechnol, 2005. 5(2): p. 259-65.
69. Hall, J.B., et al., *Characterization of nanoparticles for therapeutics*. Nanomedicine (Lond), 2007. 2(6): p. 789-803.
70. Kempa, K.K., B.; Rybczynski, J.; Huang, Z. P.; Wu, P. F.; Steeves, D.; Sennett, M.; Giersig, M.; Rao, D. V. G. L. N.; Carnahan, D. L.; Wang, D. Z.; Lao, J. Y.; Li, W.

Z.; Ren, Z. F., *Photonic Crystals Based on Periodic Arrays of Aligned Carbon Nanotubes*. Nano Lett., 2003. 3.

71. Koriorek, A.W.K., P. Chudzinski, K. Kempa, M. Giersig, *Shadow Nanosphere Lithography: Simulation and Experiment*. Nanoletters, 2004. 4(7): p. 1359-1363.

72. J. Rybczynski, U.E., M. Giersig, *Large-scale, 2D arrays of magnetic nanoparticles*. Colloids and Surfaces Physicochemical and Engineering Aspects, 2003. 219: p. 1-6.

73. Löfås, S., Johnsson, B. J. , *A Novel Hydrogel Matrix on Gold Surfaces in Surface Plasmon Resonance Sensors for Fast and Efficient Covalent Immobilization of Ligands*. chem. Soc., Chem. Commun, 1990(21): p. 1526–1528.

74. Song, E., et al., *Collagen scaffolds derived from a marine source and their biocompatibility*. Biomaterials, 2006. 27(15): p. 2951-61.

75. Sin A, M.S., Revzin A, Tompkins RG, Toner M. Biotechnology and a. Bioengineering, *Enrichment using antibody-coated microfluidic chambers in shear flow: Model mixtures of human lymphocytes*. Biotechnology and Bioengineering 2005. 91(7): p. 816-826.

76. van Wachem, P.B., et al., *In vivo biocompatibility of carbodiimide-crosslinked collagen matrices: Effects of crosslink density, heparin immobilization, and bFGF loading*. J Biomed Mater Res, 2001. 55(3): p. 368-78.

77. Gronewold, T.M., *Surface acoustic wave sensors in the bioanalytical field: recent trends and challenges*. Anal Chim Acta, 2007. 603(2): p. 119-28.

78. Jung, A., Gronewold, T. M. A., Tewes, M., Quandt, E., Berlin, P., *Biofunctional structural design of SAW sensor chip surfaces in a microfluidic sensor system*. Sens. Actuat. B, 2007. 124: p. 46-52.

79. Schlensog M.D., G.T.M.A., Tewes M., Famulok M., Quandt E. , *A Love-wave biosensor using nucleic acids as ligands*. Sens. Actuator B-Chem, 2004. 101: p. 308-315.

80. Perpeet, M., Glass, S., Gronewold, T., Kiwitz, A., Malavé, A., Stoyanov, I., Tewes, M., Quandt, E., *SAW sensor system for marker-free molecular interaction analysis*. Anal. Lett., 2006. 39(8): p. 1747-1757.

81. Xu, F.J., et al., *Heparin-coupled poly(poly(ethylene glycol) monomethacrylate)-Si(111) hybrids and their blood compatible surfaces*. Biomacromolecules, 2005. 6(3): p. 1759-68.

82. Lampert, R.H. and M.C. Williams, *Effect of surface materials on shear-induced hemolysis*. J Biomed Mater Res, 1972. 6(6): p. 499-532.

83. Paluszkiwicz, A., et al., *Effect of hemolysis and free hemoglobin on optical hematocrit measurements in the extracorporeal circulation*. ASAIO J, 2008. 54(2): p. 181-4.

84. Clark, M., *Antibody humanization: a case of the 'Emperor's new clothes'?* Immunol Today, 2000. 21(8): p. 397-402.

85. EMEA, H., *Summary of Product Characteristics (SPC) Sulesomab (LeukoScan)*.

86. Bader, A.A., et al., *Anhydramnios associated with administration of trastuzumab and paclitaxel for metastatic breast cancer during pregnancy*. Lancet Oncol, 2007. 8(1): p. 79-81.

87. Fanale, M.A., et al., *Treatment of metastatic breast cancer with trastuzumab and vinorelbine during pregnancy*. Clin Breast Cancer, 2005. 6(4): p. 354-6.

88. Friedrichs, B., et al., *The effects of rituximab treatment during pregnancy on a neonate*. Haematologica, 2006. 91(10): p. 1426-7.
89. Williams, L., et al., *Successful treatment of dermatomyositis during pregnancy with intravenous immunoglobulin monotherapy*. Obstet Gynecol, 2007. 109(2 Pt2): p. 561-3.
90. Adair, C.D., et al., *The hemodynamic effects of intravenous digoxin-binding fab immunoglobulin in severe preeclampsia: a double-blind, randomized, clinical trial*. J Perinatol, 2009. 29(4): p. 284-9.
91. Macfarlane, D., et al., *Imaging of deep venous thrombosis in patients using a radiolabelled anti-D-dimer Fab' fragment (99mTc-DI-DD3B6/22-80B3): results of a phase I trial*. Eur J Nucl Med Mol Imaging, 2009. 36(2): p. 250-9.
92. Waldmann, H., et al., *Infectious tolerance and the long-term acceptance of transplanted tissue*. Immunol Rev, 2006. 212: p. 301-13.
93. Waldmann, H. and S. Cobbold, *Exploiting tolerance processes in transplantation*. Science, 2004. 305(5681): p. 209-12.
94. Kimby, E., A. Sverrisdottir, and G. Elinder, *Safety of rituximab therapy during the first trimester of pregnancy: a case history*. Eur J Haematol, 2004. 72(4): p. 292-5.
95. Abbott, *Humira*. EU approval for Morbus Bechterew, 2006.
96. Weinblatt, M.E., et al., *Adalimumab, a fully human anti-tumor necrosis factor alpha monoclonal antibody, for the treatment of rheumatoid arthritis in patients taking concomitant methotrexate: the ARMADA trial*. Arthritis Rheum, 2003. 48(1): p. 35-45.
97. *DIN EN ISO 14791*, I.c. office, Editor 2002: Zürich.

11 Acknowledgement

I would like to express my deep and sincere gratitude to my supervisor, Professor Prof. dr hab. n. med. Grzegorz H. Bręborowicz , Head of the Department of Perinatology and Gynecology, Medical University of Poznan. His wide knowledge and his logical way of thinking have been of great value for me. His understanding, encouraging and personal guidance have provided a good basis for the present thesis.

I am deeply grateful to, Dr hab. med. Grzegorz Dworacki Head of the Department of Clinical Immunology, Medical University of Poznan, for his detailed and constructive comments, and for his important support throughout this work.

I wish to express my warm and sincere thanks to Prof. Dr. hab. med. Ewa Florek Laboratory of Environmental Research, Department of Toxicology, Medical University in Poznań, who introduced me to the field of Toxicology and animal trials y and Professor Dr. hab. med. Maciej Zabel Department of Histology, whose inputs gave me important guidance during my first steps into medical and clinical studies. Their ideals and concepts have had influence on my career in the field of medical device research.

I warmly thank Dr. med. Ekkehard Weber, for his valuable advice and friendly help. His extensive discussions and support around my work have been very helpful for this study.

My warm thanks are due to the GILUPI team, who directed me in biology and biochemistry topics and experiments. Their kind support and guidance have been of great value in this study.